AD-A256 724

NAVAL POSTGRADUATE SCHOOL
Monterey, California

THESIS

DTIC
ELECTE
NOV 06 1992
S E D

STATIC PRESSURE MEASUREMENTS OF THE
SHOCK-BOUNDARY LAYER INTERACTION
IN A SIMULATED FAN PASSAGE

by

William L. Golden, Jr.

March 1992

Thesis Advisor: Raymond P. Shreeve

Approved for public release; distribution is unlimited.

92-29067

UNCLASSIFIED
SECURITY CLASSIFICATION OF THIS PAGE

REPORT DOCUMENTATION PAGE

Form Approved OMB No 0704-0188

1a REPORT SECURITY CLASSIFICATION UNCLASSIFIED	1b RESTRICTIVE MARKINGS
2a SECURITY CLASSIFICATION AUTHORITY Multiple Sources 2b DECLASSIFICATION/DOWNGRADING SCHEDULE	3 DISTRIBUTION/AVAILABILITY OF REPORT Approved for public release; distribution is unlimited.
4 PERFORMING ORGANIZATION REPORT NUMBER(S)	5 MONITORING ORGANIZATION REPORT NUMBER(S)
6a NAME OF PERFORMING ORGANIZATION Naval Postgraduate School 6b OFFICE SYMBOL (If applicable) 39	7a NAME OF MONITORING ORGANIZATION Naval Postgraduate School
6c ADDRESS (City, State, and ZIP Code) Monterey, CA 93943-5000	7b ADDRESS (City, State, and ZIP Code) Monterey, CA 93943-5000
8a NAME OF FUNDING/SPONSORING ORGANIZATION Naval Air Systems Command 8b OFFICE SYMBOL (If applicable) AIR 536 T	9 PROCUREMENT INSTRUMENT IDENTIFICATION NUMBER N0001991WRB743R
8c ADDRESS (City, State, and ZIP Code) Washington, DC 20361	10 SOURCE OF FUNDING NUMBERS PROGRAM ELEMENT NO: WR024 PROJECT NO: 03 TASK NO: 001 WORK UNIT ACCESSION NO:

11 TITLE (Include Security Classification)
STATIC PRESSURE MEASUREMENTS OF THE SHOCK-BOUNDARY LAYER INTERACTION IN A SIMULATED FAN PASSAGE

12 PERSONAL AUTHOR(S)
Golden, William L. Jr.

13a TYPE OF REPORT	13b TIME COVERED	14 DATE OF REPORT (Year, Month, Day)	15 PAGE COUNT
Master's Thesis	FROM _____ TO _____	March 1992	136

16 SUPPLEMENTARY NOTATION
The views expressed in this thesis are those of the author and do not reflect the official policy or position of the Department of Defense or the U. S. Government.

17 COSATI CODES			18 SUBJECT TERMS (Continue on reverse if necessary and identify by block number)
FIELD	GROUP	SUB GROUP	Shock-Boundary Layer Interaction, Transonic Cascade Wind Tunnel, Variable Cascade Back Pressure, Boundary Layer Separation

19 ABSTRACT (Continue on reverse if necessary and identify by block number)

Two-dimensional experimental and numerical simulations of a transonic fan blade passage (M=1.4) were conducted to provide baseline data for the study of the effects of vortex generating devices on shock-boundary layer interaction. A back pressure valve was designed for a transonic cascade blowdown wind tunnel, the test section was instrumented, and time-averaged static pressure distributions across the shock-boundary layer interaction were obtained. A numerical Navier-Stokes solution to the flow was also found. Sensitive and repeatable control of the cascade pressure ratio was demonstrated and the flow was shown to be reasonably two-dimensional across the span.

20 DISTRIBUTION/AVAILABILITY OF ABSTRACT [X] UNCLASSIFIED/UNLIMITED [ ] SAME AS RPT [ ] DTIC USERS	21 ABSTRACT SECURITY CLASSIFICATION UNCLASSIFIED
22a NAME OF RESPONSIBLE INDIVIDUAL Raymond P. Shreeve	22b TELEPHONE (Include Area Code) (408) 646-2593 22c OFFICE SYMBOL AA/SF

DD Form 1473, JUN 86 Previous editions are obsolete SECURITY CLASSIFICATION OF THIS PAGE
S/N 0102-LF-014-6603 UNCLASSIFIED

Approved for public release; distribution is unlimited.

Static Pressure Measurements of the Shock-Boundary Layer Interaction in a Simulated Fan Passage

by

William L. Golden, Jr.
Lieutenant, United States Navy
B.S.E.E., Georgia Institute of Technology

Submitted in partial fulfillment
of the requirements for the degree of

MASTER OF SCIENCE IN ASTRONAUTICAL ENGINEERING

from the

NAVAL POSTGRADUATE SCHOOL
March 1992

Author: _____
William L. Golden, Jr.

Approved by: _____
Raymond P. Shreeve, Thesis Advisor

_____
Garth V. Hobson, Second Reader

_____
Dr. D. J. Collins, Chairman
Department of Aeronautics and Astronautics

ABSTRACT

Two-dimensional experimental and numerical simulations of a transonic fan blade passage (M = 1.4) were conducted to provide baseline data for the study of the effects of vortex generating devices on shock-boundary layer interaction. A back pressure valve was designed for a transonic cascade blowdown wind tunnel, the test section was instrumented, and time-averaged static pressure distributions across the shock-boundary layer interaction were obtained. A numerical Navier-Stokes solution to the flow was also found. Sensitive and repeatable control of the cascade pressure ratio was demonstrated and the flow was shown to be reasonably two-dimensional across the span.

DTIC QUALITY INSPECTED 4

Accesion For	
NTIS CRA&I	☒
DTIC TAB	☐
Unannounced	☐
Justification	
By	
Distribution /	
Availability Codes	
Dist	Avail and / or Special
A-1	

TABLE OF CONTENTS

I. INTRODUCTION 1

A. SHOCK-BOUNDARY LAYER INTERACTION 1

B. VORTEX GENERATING DEVICES 2

C. 2-D FAN PASSAGE SIMULATION 3

II. EXPERIMENTAL SIMULATION 6

A. TRANSONIC CASCADE WIND TUNNEL 6

1. Wind Tunnel Description 6

2. Optical System 7

B. TEST SECTION PRESSURE INSTRUMENTATION 8

1. Test Section Side Plates 8

2. Test Section Window Blanks 9

3. Test Section Lower Blade 9

C. DATA ACQUISITION AND ANALYSIS SYSTEM 9

1. Pressure Measurement System 9

a. Scanivalves and Transducers 10

b. Digital Equipment 10

c. Measurement Accuracy 11

2. Data Acquisition Programs 12

a. CALIBRATION Program 12

b. SCAN Program 12

3. Data Analysis Programs 13

D. EXPERIMENTAL PROGRAM AND TEST RESULTS 14

1. Control of the Cascade Pressure Ratio . . . 14

2. Passage Flow Behavior 14

a. Unsteadiness of the Normal Shock 14

b. Periodicity of the Cascade 15

3. Upstream Pressure Field 15

4. Baseline Measurements 16

a. Determination of Operational Pressure Ratios 16

b. Baseline Data Acquisition 17

5. Boundary Layer Separation 18

III. NUMERICAL SIMULATION 19

A. GRID GENERATION 19

B. COMPUTATIONAL SCHEME 19

1. The Solution Method 19

2. Solution Inputs 20

C. COMPUTATIONAL SOLUTION 21

IV. DISCUSSION OF RESULTS 23

A. EXPERIMENTAL RESULTS 23

1. Cascade Inlet Flow 23

2. Lower Blade Pressure Data 24

3. Side Wall Pressure Data 25

4. Flow Symmetry 26

B. NUMERICAL RESULTS 26

V. CONCLUSIONS AND RECOMMENDATIONS 28

APPENDIX A 71

APPENDIX B 75

APPENDIX C 82

APPENDIX D 90

APPENDIX E 101

APPENDIX F 110

APPENDIX G 116

APPENDIX H 120

LIST OF REFERENCES 121

INITIAL DISTRIBUTION LIST 123

LIST OF TABLES

TABLE I. STATIC PRESSURE TAP DISTRIBUTION 30

TABLE II. TEST PROGRAM SUMMARY 31

TABLE III. DATA FROM RUN 26--OPEN BACK PRESSURE VALVE 32

TABLE IV. DATA FROM RUN 27--LOWER PASSAGE SHOCK POSITIONED 34

TABLE V. DATA FROM RUN 28--UPPER PASSAGE SHOCK POSITIONED 36

LIST OF FIGURES

Figure 1. Shock-Boundary Layer Interaction [Ref. 1] 38

Figure 2. Low-Profile Vortex Generator Operation [Ref. 4] 39

Figure 3. Vortex Generator Jet Operation [Ref. 4] 40

Figure 4. Transonic Cascade Blade Geometry 41

Figure 5. Schematic of Test Facility 42

Figure 6. Schematic of Wind Tunnel 43

Figure 7. Transonic Cascade Wind Tunnel 44

Figure 8. Schematic of Test Section 45

Figure 9. Test Section (with Side-Wall Removed) 46

Figure 10. Test Section And Instrumentation 47

Figure 11. Back Pressure Valve 48

Figure 12. Schematic of Optical System 49

Figure 13. Instrumented Test Section Lower Blade 50

Figure 14. Schematic of Data Acquisition System 51

Figure 15. Data Acquisition System 52

Figure 16. Shock Structure with Open Back Pressure Valve 53

Figure 17. Shock Structure with Lower Shock in Position 54

Figure 18. Shock Structure with Upper Shock in Position 55

Figure 19. Viscous Grid 56

Figure 20. Viscous Grid Leading Edge 57

Figure 21. Viscous Grid Trailing Edge 58

Figure 22. Viscous Solution Mach Number Profile 59

Figure 23. Viscous Solution Velocity Profile 60

Figure 24. Viscous Solution Convergence History 61

Figure 25. Viscous Solution: Cp vs. Chord Length 62

Figure 26. Cascade Inlet Static Pressures--Open Back Pressure Valve 63

Figure 27. Cascade Inlet Static Pressures--Lower Shock in Position 64

Figure 28. Cascade Inlet Static Pressures--Upper Shock in Position 65

Figure 29. Lower Blade Centerline Static Pressures 66

Figure 30. Lower Blade Static Pressures (All Rows) 67

Figure 31. Static Pressure Variation with Back Pressure 68

Figure 32. Wall Static Pressures (Lower Passage, Bottom Row) 69

Figure 33. Comparison of Blade Centerline Results 70

Figure A1. Back Pressure Valve Left Side Plate 71

Figure A2. Back Pressure Valve Right Side Plate 72

Figure A3. Back Pressure Valve Ramp and Base Plates 73

Figure A4. Back Pressure Valve Top Plate 74

Figure B1. Right Side Plate Instrumentation 75

Figure B2. Left Side Plate Instrumentation 76

Figure B3. Right Window Blank Instrumentation 77

Figure B4. Left Window Blank Instrumentation 78

Figure B5. Right and Left Window Blanks 79

Figure B6. Lower Blade Instrumentation (Top View) 80

Figure B7. Lower Blade Instrumentation (Side View) 81

Figure C1. CALIBRATE Program 82

Figure C2. SCAN Program 84

Figure D1. Scanivalve #1 Numbering Scheme 90

Figure D2. Scanivalve #2 Numbering Scheme 91

Figure D3. Scanivalve #3 Numbering Scheme 92

Figure D4. Scanivalve #4 Numbering Scheme 93

Figure D5. Scanivalve #4 Numbering Scheme (Cont.) 94

Figure D6. Scanivalve #5 Numbering Scheme 95

Figure D7. Scanivalve #6 Numbering Scheme 96

Figure D8. Scanivalve #6 Numbering Scheme (Cont.) 97

Figure D9. Scanivalve #7 Numbering Scheme 98

Figure D10. Scanivalve #7 Numbering Scheme (Cont.) 99

Figure D11. Scanivalve #7 Numbering Scheme (Cont.) 100

Figure E1. Wall Static Pressures--Bottom Row 101

Figure E2. Wall Static Pressures--Row 2 102

Figure E3. Wall Static Pressures--Row 3 103

Figure E4. Wall Static Pressures--Row 4 104

Figure E5. Wall Static Pressures--Row 5 105

Figure E6. Wall Static Pressures--Row 6 106

Figure E7. Wall Static Pressures--Row 7 107

Figure E8. Wall Static Pressures--Row 8 108

Figure E9. Wall Static Pressures--Row 9 109

Figure F1. COMPARE Program 110

Figure F2. Run 26 Left/Right Pressure Differences 113

Figure F3. Run 27 Left/Right Pressure Differences 114

Figure F4. Run 28 Left/Right Pressure Differences 115

Figure G1. GRAPE Input Code (Viscous grid) 116

Figure H1. RVCQ3D Input Code (Viscous Solution) 120

ACKNOWLEDGEMENTS

I would like to thank those people whose thoughts and efforts helped me to conduct this study. I am indebted to Professor Raymond Shreeve for helping me to gain insight into the art of scientific experimentation. Dr. Garth Hobson's guidance was crucial to my understanding of numerical methods. I am grateful to Rick Still for his creativity and dexterity with the equipment of the transonic cascade project. Don Harvey's skilled craftsmanship greatly facilitated the instrumentation of the transonic cascade. Finally, I thank my wife, Jan, for her patience and support in enduring the many days and nights that I spent away from my family.

I. INTRODUCTION

A. SHOCK-BOUNDARY LAYER INTERACTION

In modern turbofan designs, the relative Mach number of the flow at outer radii entering the fan and early core compressor stages is in the transonic regime. This, combined with the inherent pressure rise across a compressor stage, causes a shock to form at the inlet to each blade passage. Commonly, a normal shock extends from the leading edge of one blade to the suction surface of the adjacent blade, where it impinges upon the boundary layer on that surface. The shock impingement causes the boundary layer to separate. If the shock is not too strong, the boundary layer will reattach downstream. The resulting shock structure, consisting of the original normal shock meeting two oblique shocks over a boundary layer separation bubble, is called the lambda foot. This shock-boundary layer interaction, which exhibits highly unsteady behavior, is shown in Figure 1.

It is clear that, since the total pressure loss through the lambda foot would be less than that through the normal shock if the flow were steady, suppressing the shock structure itself (and thereby increasing the size of the normal shock and its associated losses) is not necessarily desirable. However, the boundary layer separation produced by the shock

structure is highly unsteady and definitely undesirable; high total pressure losses are associated with the much thicker boundary layer downstream of the shock-boundary layer interaction and the design turning angles are not achieved. If the effects of this interaction could be reduced, a transonic fan or compressor could be designed to have higher relative Mach numbers with lower losses and, subsequently, more engine thrust would result with lower engine weight and reduced fuel consumption.

B. VORTEX GENERATING DEVICES

A number of methods for reducing the effects of shock-boundary layer interaction have been investigated. McCormick at United Technologies Research Center [Refs. 1, 2] examined some of these. Two promising techniques for the fan application are the low-profile vortex generator and the vortex generator jet. Both devices function by introducing axial vortices to transport high momentum flow from the outer boundary layer into the low momentum region of the boundary layer closer to the blade surface. This momentum exchange enables the layer to adjust to the sudden pressure rise across the shock structure without separation [Ref. 2].

Low-profile vortex generators, shown in Figure 2, are an invention of Wheeler [Ref 3.]. These "Wheeler Doublets" are submerged in the boundary layer.upstream of the shock-boundary layer interaction, and shed vortices that exchange momentum

within the flow as described above. Wheeler Doublet and wishbone type low-profile vortex generators were investigated by Lin, et al [Ref. 4]. A drawback of low-profile vortex generators is the need to attach many of them to each blade suction surface. Achieving reliability and geometrical repeatability in the attachment is a challenge.

Vortex generator jets, which were introduced by Johnston and Nishi [Ref. 5] and are shown in Figure 3, consist of passively or actively controlled ducts within the blade structure that inject fluid at an angle skewed to the flow. This again produces axial vortices for the purpose of momentum exchange. The jet vortex generation is easily implemented by drilling small holes through each blade to allow higher pressure air from the pressure side to vent to the suction side. However, vortex generator jets implemented this way will inevitably reduce blade integrity, and this needs to be examined. A thorough description of vortex generators and their operation is presented in a thesis by Collins [Ref. 6].

C. 2-D FAN PASSAGE SIMULATION

The experiment by McCormick [Refs. 1, 2] examined the effects of vortex generating devices (and other techniques) on shock-boundary layer interaction in a round tube. The goal of the present transonic cascade is to confirm McCormick's results and to examine the control of shock-boundary layer interaction in a cascade simulation of a transonic fan

passage. The present study is an extension of the work performed by Collins [Ref. 6], which resulted in a working wind tunnel and cascade test section. The wind tunnel was designed by Demo [Ref. 7], and the original test section geometry was operated first by Hegland [Ref. 8].

The geometry of the present 2-D experiment was a simulation of the relative flow on a stream surface through an advanced fan rotor at approximately 63% of the span. While the 2-D model was based on the stream surface conditions and geometry, the blade profile was approximated (very closely) as a wedge arc for ease of manufacture. This was reasonable since streamline contraction could not be simulated in the experiment [Ref. 6]. The geometry of the 2-D experimental simulation is shown in Figure 4.

In the course of the present study, the back pressure valve of the transonic cascade wind tunnel was redesigned, static pressure taps were installed in the test section side plates, lower blade, and window blanks, a new data acquisition system was assembled, and baseline static pressure distributions throughout the cascade passages were obtained at controlled pressure ratios. In Section II, modifications to the test facility and experimental results are presented. Section III describes a Computational Fluid Dynamics simulation that was performed to investigate the Navier-Stokes solution to the flow within a transonic turbofan blade passage. Section IV expands upon the results of both the

experimental and numerical simulations, and in Section V, conclusions are drawn and recommendations to further the experiment are proposed.

Details of the experiment are given in Appendicies A through F and details of the computational simulation are given in Appendicies G and H.

II. EXPERIMENTAL SIMULATION

A. TRANSONIC CASCADE WIND TUNNEL

1. Wind Tunnel Description

The Transonic Cascade Wind Tunnel is a blowdown device that was designed originally to permit a two-dimensional study of the flow through a particular transonic compressor blading design. The original and present studies in the tunnel are part of a program at the Turbopropulsion Laboratory of the Naval Postgraduate School, which is sponsored by Naval Air Systems Command. The wind tunnel is located in the Gas Dynamics Laboratory (Bldg. 216). Portions of the Laboratory that are relevant to the Transonic Cascade Wind Tunnel are shown in Figure 5. A schematic and photograph of the tunnel are shown in Figures 6 and 7, respectively.

The general layout of the tunnel is as follows: A convergent-divergent nozzle produces a Mach 1.4 flow at the inlet to the test section. Scoops on the four sides of the inlet remove the nozzle wall boundary layers, to present undisturbed air to the test section. The test section, shown in Figures 8, 9, and 10, consists of three sections ("blades") that form two simulated compressor blade passages. The upper and lower blades each constitute half of an actual blade geometry, while the center blade is complete. The upper

(suction) wedge surface of the center blade is inclined at -1.15 degrees to the flow, and the lower (pressure) surface of the center blade is canted at +4.65 degrees. A back pressure valve, shown in Figure 11, is mounted aft of the test section. It consists of a hinged plate which can be adjusted from fully open to closed (against an opposing fixed ramp) using a small hydraulic jack. The valve provides control of the test section outlet pressure in order to produce the pressure ratios required in the simulated compressor blade row. Drawings for the back pressure valve are give in Appendix A. A more detailed description of the Transonic Cascade Wind Tunnel can be found in Ref. 6.

2. Optical System

A schematic of the optical system is shown in Figure 12. A continuous or spark light source could be selected. A filter attenuated the original beam, a parabolic lens directed a parallel light beam through the test section, and a parabolic mirror reflected the beam to the camera. Shutter speeds of one five-hundredth and one thousandth of a second were used with the continuous source. Shadowgraphs were made by photographing the test section slightly out of focus, thereby emphasizing the density gradients of the shock system. Again, a more detailed description is found in Ref. 6.

During selected runs of the Transonic Cascade, an 8 mm video camera was focused on the ground glass viewing screen

with the Polaroid film holder removed and the shutter open. A video shutter speed of one thousandth of a second was set to record the unsteady shock behavior for viewing later in slow motion.

B. TEST SECTION PRESSURE INSTRUMENTATION

Static pressure taps were drilled in three areas of the test section; namely, the side plates, window replacement blanks, and the lower blade. The right side of the cascade (looking downstream) was chosen as the primary source of data, using the left as a check of the two-dimensionality of the simulation. Pressure taps were distributed accordingly and are listed in Table I. Drawings of the instrumented components are given in Appendix B. Tap size and location were based on guidelines from Volluz [Ref. 9].

1. Test Section Side Plates

Each test section side plate contains the flow forward of the boundary layer scoops. Pressure taps were placed in the test section side plates with three goals in mind. First, a vertical line of taps at the inlet to the test section would verify that the inlet air flow was uniform. Second, seven rows of taps placed just forward of the side plate boundary layer scoop would capture expansion or compression disturbances from the blade leading edges. And third, these same taps would determine whether the four boundary layer scoops were operating properly.

2. Test Section Window Blanks

Aluminum blanks were manufactured to the dimensions of the Plexiglas windows of the test section. This allowed static pressure taps to be placed in the walls of each cascade passage. These taps would provide a map of the time-averaged wall static pressures across the shock-boundary layer interaction and would quantify any differences between the cascade passages.

3. Test Section Lower Blade

The lower blade is pictured in Figure 13. Taps were closely spaced along the centerline of the blade to determine in detail the shock-boundary layer interaction as indicated by the static pressure distribution. Four additional rows of taps were drilled to examine cascade two-dimensionality. Fifty-thousandths inch diameter stainless steel tubing was gathered from the hollow underside of the lower blade into a bundle and routed through the lower surface of the test section. Plastic tubing was used to connect to the data acquisition system.

C. DATA ACQUISITION AND ANALYSIS SYSTEM

1. Pressure Measurement System

The equipment required to measure and record the static pressure distribution over the cascade test section included 305 pressure taps with associated steel and plastic tubing, nine differential pressure transducers, seven

Scanivalve pneumatic selectors, two Scanivalve controllers, two scanners, two digital voltmeters, and a digital computer. A schematic of the data acquisition system is shown in Figure 14 and a photograph is shown in Figure 15.

a. Scanivalves and Transducers

A Scanivalve pneumatic selector is a rotary device that allows 48 pressure taps to be sequentially read by a single differential pressure transducer. Seven Scanivalves and transducers were used, providing the capability to read up to 336 static pressures. One port of each Scanivalve was assigned to ambient air pressure and one port was assigned to a controlled 25 psi calibration pressure. In addition to the Scanivalves, two pressure transducers were mounted individually to provide continuous monitoring of the inlet and exit pressures of the test section, P1 and P2, respectively.

b. Digital Equipment

An HP 9000/300 digital computer, utilizing the HP BASIC 5.1 operating system, controlled the data acquisition process. Two HG-78K Scanivalve Controllers, two HP 3495A Scanners, and two HP 3455A Voltmeters were used to control the Scanivalves and digitize the data.

The HG-78K Scanivalve Controllers, designed by Geopfarth [Ref. 10], allowed up to five Scanivalves to be operated through one controller. The first controller was

connected to five Scanivalves, while the second controller was connected to two Scanivalves and two individual transducers.

The scanners were set up to close relays that, when the appropriate channel was selected by programming, 1) homed the Scanivalves to port number one, 2) stepped the Scanivalves to the next port, or 3) connected the selected transducer output voltage to the digital voltmeter. Scanner connections were in accordance with the address matrix found in Reference 10.

The voltmeters read transducer voltages provided by the controllers and supplied them to the digital computer for manipulation and storage. All instruments were connected via the HP-IB parallel interface bus.

c. Measurement Accuracy

There were three possible types of measurement error in using the multiple Scanivalve system; namely, 1) inconsistency between measurements of different ports on the same Scanivalve (when connected to the same air pressure), 2) inconsistency between measurements from different Scanivalves (when connected to the same air pressure), and 3) drift in calibration over time for each Scanivalve transducer. The first error would result from improper sealing of the tubing or selector valves between the pressure taps and the transducers, and the second and third errors would be due to the transducers alone. A program was written to quantify

these errors by examining sets of collected measurements. The maximum source of error was found to be of the second type listed above. The error was found to give a maximum uncertainty in measurement of 0.1 PSI.

2. Data Acquisition Programs

a. CALIBRATION Program

A program, entitled "CALIBRATE," was written to facilitate the calibration of the Scanivalve transducers prior to a cascade run. The program could also be used to read transducer pressures while setting up and verifying connections. To calibrate a transducer, the Scanivalve number was entered at the computer keyboard. The desired port was selected by operating either the Reset (Home) or Step pushbuttons located on the controller faceplate. (The controller was designed to permit computer or manual operation.) Port number one vented to atmosphere and was used to zero the differential transducer, whose reference side was also open to atmosphere. Port number two was connected to a regulated 25 PSI air supply and was used as a set point to adjust the range of the transducer output. The CALIBRATE program is listed in Figure C1.

b. SCAN Program

After the calibration was completed, the wind tunnel could be operated and pressure data taken. A program, entitled "SCAN," was written to record data with a minimum of

user inputs during tunnel operation. SCAN was menu-driven so that an operator needed only to select (from left to right on "hot keys") the actions required for a successful acquisition, storage, and print-out of data. During a run, and after tunnel transients had settled, one hot key was pushed that started a sequence to read all port pressures, create a storage file, and store the acquired data. An important feature was a continuous readout on the CRT of the test section static pressure ratio, which was used by the back pressure valve operator to quickly bring the cascade to the required operating condition. This allowed the normal shock to be positioned repeatably from test to test without a visual reference. The SCAN program is listed in Figure C2.

3. Data Analysis Programs

A series of programs were written to present the acquired data visually in a format which allowed a quick, qualitative evaluation of the results. Programs that each produced a contour plot with three-dimensional perspective from a stored pressure distribution array were SIDEPLOT, BLADEPLOT, and WINDOWPLOT. GRAPH_ROWS and INLET_PLOT drew graphs of normalized pressure distributions from the lower blade and test section inlet, respectively. In the interest of brevity, listings have not been included in this document.

D. EXPERIMENTAL PROGRAM AND TEST RESULTS

The experimental program involved a total of 29 wind tunnel tests. A summary of the test program is given in Table II and an account is given in the following paragraphs.

1. Control of the Cascade Pressure Ratio

After installation of the new back pressure valve, Run 1 confirmed that the design static pressure ratio could be achieved without difficulty. Normal shocks could be pushed forward through the test section cascade passages by increasing the back pressure at will, and the position of the shocks was finely controllable. Runs 1 through 14 were performed to optimize the optical system with adjustments to focal lengths, substitutions of filters, use of spark and continuous light sources, and to experiment with various camera shutter speeds.

2. Passage Flow Behavior

a. Unsteadiness of the Normal Shock

Runs 1 and 2 immediately demonstrated the highly unsteady behavior of the shock-boundary layer interaction. Run 3 was used to videotape the shadowgraph image to allow closer study of both the test section starting process and normal shock behavior. This videotape resulted in observations given below.

b. Periodicity of the Cascade

Runs 1 through 3 revealed that the upper and lower passages of the cascade did not unstart at the same cascade pressure ratio. The lower passage unstarted first (with increasing back pressure), and the upper passage unstarted after the normal shock in the lower passage had been moved somewhat further forward. Also, the lower shock appeared to be not as strong as the upper shock. Consequently, the flow through the two passages of the cascade was not strictly periodic at pressure ratios close to the design value.

3. **Upstream Pressure Field**

One of the reasons for instrumenting the test section side plates was to determine whether the boundary layer scoops had actually started--that they were swallowing the oncoming boundary layer without creating upstream shocks and allowing spillover into the blade test section. During Runs 15 through 17, the first pressure data were acquired with the right instrumented side plate. Contour plots of the data were generated to allow a qualitative examination. If the boundary layer scoops had been functioning correctly, there should have been a slight drop in static pressure prior to the blade passages due to expansion fans emanating from the lower and center blade leading edges. This was not the case. A rise in static pressure prior to the upper passage and a relatively constant static pressure prior to the lower passage indicated

that the lower scoop was probably working correctly and that the upper scoop was possibly not. The higher pressures at the inlet to the upper passage could explain the aperiodicity of the cascade.

4. Baseline Measurements

a. Determination of Operational Pressure Ratios

Runs 18, 19, and 20 were conducted with the side plates instrumented and the instrumented lower blade installed. The Plexiglas windows were mounted in the test section to allow visual placement of the shocks. The goals of the runs were to 1) determine if the modifications to the test section had changed the behavior of the flow, 2) obtain measured baseline pressure ratios with the normal shocks in the lower and upper cascade passages, and 3) determine the degree of two-dimensionality of the flow.

During Run 18, the back pressure valve was left in the fully open position. After the flow had steadied, the acquisition program was initiated and shadowgraphs were taken. The data acquired provided control data with which to compare later runs. The pressure ratio for a fully open back pressure valve was determined to be 1.34. A shadowgraph of this condition is shown in Figure 16.

During Run 19, the back pressure was raised and the normal shock was visually placed at its design position in the lower passage--centered over the static pressure ports of the

lower blade and below the leading edge of the middle blade. Pressure data and shadowgraphs were obtained. A static pressure ratio of 2.02 was required to place the normal shock in this position. The tunnel and back pressure valve behaved exactly as before, indicating that no noticeable change had occurred as a result of the modification and reassembly of the test section. A shadowgraph showing the normal shock positioned in the lower passage is shown in Figure 17.

Run 20 was similar to Run 19 above, except that the pressure ratio was raised to 2.15 to place the normal shock in the upper passage. A shadowgraph is shown in Figure 18. After completion of this run, exact pressure ratios were known so that shocks could be positioned without the aid of windows. The aluminum window blanks and associated pressure taps could then be installed, and a full map of the static pressure distribution obtained.

b. Baseline Data Acquisition

Runs 26, 27, and 28, corresponding to a fully open back pressure valve, lower shock in place, and upper shock in place, respectively, were conducted with all instrumentation installed, including the instrumented aluminum window blanks. Complete pressure distributions were obtained and are presented in Tables III, IV, and V. A map of pressure tap locations is given in Appendix D. Attaining the proper pressure ratio without the benefit of the optical system to

see the shocks was not difficult. With care, the pressure ratio could be set to within 0.01 of the desired value by monitoring the computer screen while operating the back pressure valve.

5. **Boundary Layer Separation**

For Run 29, the Plexiglas windows were reinstalled. The normal shock was positioned in the lower passage, and an alcohol and fluorescein dye solution was injected onto the lower blade surface from one of the off-centerline taps under the shock-boundary layer interaction. The solution spread out across the span of the blade before being swept downstream, indicating that the boundary layer was separated in this region. Subsequently, a video camera was used to record the surface flow behavior (as indicated by the dye injection) as the back pressure was increased. An unsteady separated flow region was observed to move forward to reach the injection location (tap #10 in Figure D7) at a pressure ratio of about 2.04, and to leave fully reattached flow at the injection location at a pressure ratio of about 2.11.

III. NUMERICAL SIMULATION

A. GRID GENERATION

A C-grid was used for the numerical simulation. The original grid was generated by Collins [Ref. 6] with the GRAPE grid generation code. GRAPE (GRids about Airfoils using Poisson's Equation) was written by Sorenson [Refs. 11 and 12] and revised by Chima [Ref. 13] to accomodate periodic cascades for turbomachinery. The original grid contained 169 x 31 points. The grid was increased in size to 250 x 49 points, more grid points were placed at the leading and trailing edges of the blade, and a finer grid mesh was formed near the blade surface to capture the boundary layer for a viscous solution. The grid is shown in Figures 19 through 21. The GRAPE input file for this grid is listed in Appendix G.

B. COMPUTATIONAL SCHEME

1. The Solution Method

The numerical scheme used in this study was RVCQ3D (Rotor Viscous Code Quasi-3-D). The code was developed by Rodrick V. Chima at the NASA Lewis Research Center in Cleveland, Ohio. As stated by Chima [Ref. 14], RVCQ3D was designed for the analysis of both inviscid and viscous blade-to-blade flows in turbomachinery. An ideal gas is assumed in the solution. The code uses an explicit multistage Runge-

Kutta scheme to solve the Euler and Navier-Stokes Equations. It also incorporates a spatially varying time step and implicit residual smoothing. When calculating viscous derivatives, those in the streamwise direction are dropped as for the thin shear layer approximation. The Baldwin-Lomax turbulence model is used for turbulent flows. The solution is found by calculating an initial one-dimensional guess and then time marching to a steady-state solution. All spatial derivatives are central differenced, making the scheme second order accurate in space and fifth order accurate in time since the five stage Runge-Kutta option was used. A complete mathematical description of the code is presented in a paper by Chima [Ref. 15], and a comparison of his scheme with other multigrid methods is given in a report by Chima, Turkel, and Schaffer [Ref. 16].

2. Solution Inputs

While the code can account for the effects of rotation, it was implemented in the present study on a purely two-dimensional basis. Throughout this investigation, the five stage Runge-Kutta scheme was selected. An adiabatic wall temperature boundary condition was imposed. The dynamic viscosity was derived from tables provided by Schlichting [Ref. 17] for the design stagnation pressure of 14.7 PSI and static temperature of 463.3°R (corresponding to a total temperature of 518.7°R, or 15°C) for the transonic fan

compressor. The Courant number had to be kept low due to the unsteady nature of the flow, which required a very short time step to maintain stability. Reference 14 contains a complete glossary of the input variables for RVCQ3D.

A transonic compressor cascade test case was supplied by Chima [Ref. 14]. A viscous solution for the present simulation was obtained by substituting the proper grid and flow parameters, and then iteratively modifying the algorithm controls and blade row rotational speed until the solution output variables matched the fan design flow. The RVCQ3D input code is listed in Appendix H.

C. COMPUTATIONAL SOLUTION

The viscous solution required 4000 iterations to fully develop the flow. The solution for the Mach number distribution is pictured in Figure 22. The normal shock merges with the leading edge bow shock on the pressure surface and with the turbulent boundary layer on the suction surface. The lambda foot is not visible in the solution, however a sudden increase in boundary layer thickness is apparent. Laminar to turbulent transition of the suction surface boundary layer is predicted by the solution to occur at X/C = 0.1. The predicted flow incidence angle is 57.87°, giving a relative incidence angle of 2.53°. (The fan design flow incidence angle is 1.15°.) Figure 23 shows the velocity profile within the lambda foot. The flow velocity decreases

markedly upon entering the region of interaction, however no boundary layer separation is predicted.

A convergence history of the solution is presented in Figure 24. The solution residuals converged by only two orders of magnitude, flattened, and then slowly increased. A steady-state solution could not be obtained during the present study, therefore this solution is a "snap shot" of an unsteady process. A plot of the coefficient of pressure, Cp, is given in Figure 25.

IV. DISCUSSION OF RESULTS

A. EXPERIMENTAL RESULTS

1. Cascade Inlet Flow

Normalized test section inlet static pressures from Runs 26, 27, and 28 are shown in Figures 26, 27, and 28, respectively. The figures are drawn to scale. Pressure taps were located only at the far upstream inlet station (the left end of each of the seven lines) and where deviations were expected to occur in front of the side boundary layer scoop. Note the decrease in the four pressures along Row 3 (entering the lower passage) in each of the figures, which indicates an expansion fan emanating from the lower blade leading edge. In Figure 26 the back pressure valve is fully open, and in Figure 27 the normal shock is positioned in the lower passage. The similarity between these two figures indicates that unstarting the lower passage does not disturb the inlet conditions. A marked change in inlet conditions does occur when the upper passage is unstarted as in Figure 28. Here the shock in the lower passage has been pushed forward of the middle blade leading edge, and the two passages see entirely different inlet flows. Note the expansion fan that is indicated by the pressure decrease along the last five holes of Row 5 in front of the upper passage.

There are two possible causes for the lack of uniformity in the static pressure distribution in front of the cascade: either the upper boundary layer scoop is unstarted or the blade passages are, in some way, different. A close examination of the shadowgraphs in Figures 16 through 18 shows that oblique shocks are present in the upper boundary layer scoop, which is visible above the test section window. While not conclusive, the presence of these shocks indicates that at least part of the flow entering the upper scoop is supersonic. A more likely explanation for the upstream pressure field is a difference in how each passage dumps downstream: the air flow from the lower passage must dump across a recirculation region that is behind and below the lower blade that the air flow from the upper passage does not encounter. The differences in starting behavior between the two passages does not preclude the use of each passage separately to collect information on shock-boundary layer interactions, as has been done in this study.

2. Lower Blade Pressure Data

Figure 29 shows the normalized static pressures on the centerline of the lower blade surface. The shock is located at approximately half the chord length. The shape of the distribution is typical of the pressure variation through a shock-turbulent boundary layer interaction region. Figure 30 shows the normalized static pressures over the entire lower

blade pressure tap array and indicates that the transonic cascade is highly two-dimensional. Deviations from the mean pressure in the interaction region are less than two percent.

Two of the five runs that involved positioning the normal shock in the lower passage did not produce data that were as two-dimensional as those presented in Figure 30. In Runs 22 and 24, pressures from the far left row of taps, Row "A", deviated by as much as 0.04 x Pt, and pressures from the second from the right row, Row "D", deviated by as much as 0.02 x Pt. The cause of this is unknown. The other three rows of taps produced repeatably similar data in each run.

Figure 31 shows the variation of blade centerline static pressures with increasing back pressures. The large pressure spike in the lower curve is due to the oblique shock when the back pressure valve is in the fully open position.

3. Side Wall Pressure Data

Figure 32 shows normalized static pressures taken from the lowest row of taps along the wall of the lower cascade passage. Pressures from the lower blade centerline are plotted for comparison. The figure shows that the shock-boundary layer interaction occurs somewhat similarly over the side wall of the passage. Clearly, the wall interaction is not too different from that on the blade surface. This would indicate that three-dimensional effects are modest, since they would be greatest at the corners of the passage where two-

dimensional shock structures meet edge on. Graphs of all nine rows of wall data are presented in Appendix E.

4. Flow Symmetry

The data obtained from the right and left sides of the cascade were compared to examine the symmetry of the flow. This was done with the COMPARE program listed in Appendix F with data comparisons for Runs 26, 27, and 28. At the design conditions of Run 27, and including all data, the standard deviation was 0.9778 PSI. A singular point appeared in comparing the vertical column of taps on the two sides of the lower passage in all cascade runs. This was probably due to a leak in the tube leading from one port. Neglecting this one pair of corresponding taps, the standard deviation was 0.5890 PSI. Thus, flow symmetry and two-dimensionality were well demonstrated.

B. NUMERICAL RESULTS

Numerous attempts were made to achieve a steady-state solution to the flow by varying the Courant number, the fourth order artificial viscosity term, and the implicit residual smoothing coefficients. While the slope of the increasing residuals could be reduced, it could not be eliminated. As can be seen by refering to the grid in Figures 19 and 20 and the solution in Figure 22, the shock below the leading edge of the blade is skewed to the angle of the grid. This introduces errors which might be overcome by constructing a new grid with

a structure more in line with the shock, as is the case on the suction surface.

A comparison of the numerical and experimental static pressure distributions along the blade centerline is shown in Figure 33. Though the numerical solution is not considered to be final, the computed pressure distribution is certainly qualitatively similar to that found in the experiment.

V. CONCLUSIONS AND RECOMMENDATIONS

In the present study, a two-dimensional experimental simulation of the flow through a fan passage was established, controlled, and measured. Baseline pressure data for the interaction of the passage shock with the suction surface boundary layer were obtained in the experiment. Also, a viscous prediction of transonic flow behavior was produced computationally.

From the experiment, the following conclusions were drawn:

- The new design of the back pressure valve was fully successful. A normal shock could be positioned wherever desired within the cascade by adjusting the pressure ratio across the model. Adjustment to within 0.5% of the design pressure ratio was achieved easily and repeatably.
- The data acquisition system was also successful. Using an on-line readout of cascade pressure ratio to adjust the sensitive back pressure valve, experimental conditions were easily repeated from test to test. This feature will be valuable when the effects of vortex generators are studied.
- The flow in the cascade was found to be highly two-dimensional in the lower passage.
- A baseline static pressure database was created for the intended experiment.
- The necessary programs were created to facilitate the presentation and interpretation of results. This included the display of normalized blade static pressures as distributions along a single line and as distributions along multiple lines on a given surface.

From the numerical simulation, the following were concluded:

- The solution to the flow was highly grid dependent. Progressively increasing the grid size eventually reversed the early apparent progress toward a converged steady-state solution.
- The steady-state solution was not attained possibly due to the oblique angle with which some of the grid lines intersected the normal shock.
- In spite of climbing residuals, a "snap shot" of the solution was obtained which was observed to be qualitatively similar to the results of the experiment.

The following are recommended to advance the experiment:

- Manufacture additional windows for the test secton. Particles in the air flow continuously scratch the Plexiglas, which cannot be repolished to its original optical quality. Consequently, the quality of the optical system is degraded further with each operation of the tunnel.
- Design and implement a total pressure probe to survey the flow leaving the test section.
- Investigate further the reasons for the higher static pressures in front of the upper passage of the cascade. This may involve installing more pressure taps in the test section side plate, reshaping the side wall slots near the top, or experimenting with an extension to the inner side plates to fully contain the flow laterally until it completely exits the narrow aluminum test section (Figure 8). The extension could be used to mount adjustable "tail-boards" to effect control of the flows from the upper and lower passages separately.

TABLE I. STATIC PRESSURE TAP DISTRIBUTION

COMPONENT	NUMBER OF TAPS
Right Sideplate	50
Left Sideplate	21
Right Window Blank	124
Left Window Blank	30
Lower Blade	73
Plenum	1
Cascade Exit Plane	6
TOTAL	305

TABLE II. TEST PROGRAM SUMMARY

RUN NUMBER	CONFIGURATION			EXPERIMENT PROGRESSION
	INLET WALLS	LOWER BLADE	CASCADE WALLS	
1	*	*	Windows	Test of New Back Pressure Valve
2	*	*	"	Check of Boundary Layer Scoops
3 - 4	*	*	"	Video
5 - 7	*	*	"	Shadowgraphs
8 - 10	*	*	"	Video and Shadowgraphs
11 - 13	*	*	"	Spark Shadowgraphs
14	*	*	"	Shadowgraphs
15 - 17	Pressure Taps	*	"	Shadowgraphs/Upstream Pressure Data
18 - 20	"	Pressure Taps	"	Video/Upstream, Blade Pressure Data
21 - 23	"	"	Pressure Taps	First Full Static Pressure Survey
24 - 28	"	"	"	Static Pressure Distributions
29	"	"	Windows	Video/Surface Flow Visualization

* Indicates No Instrumentation

" Indicates Same As Above

TABLE III. DATA FROM RUN 26--OPEN BACK PRESSURE VALVE

SCAN Program Output
Pressure data from File RUN26OPEN
(File data has been multiplied by 1000.)

Atmospheric Pressure = 14.889316519 PSIA

Gauge pressures:

PORT #	SCANIVALVE NUMBER 1	2	3	4	5	6	7
1	.0282	-.2874	.008	.002	.0042	.038	-.0066
2	24.9996	24.7392	25.0022	24.9944	24.998	25.0448	25.0134
3	37.3458	4.3718	1.4752	2.6174	1.7404	-.4084	1.858
4	1.7484	4.9242	1.143	.5804	1.3978	4.7004	1.7986
5	7.6126	4.8688	.9186	1.4886	1.3432	4.5284	1.602
6	2.5928	4.0782	1.1172	1.3598	1.2668	1.2908	1.2038
7	3.181	4.0274	1.5344	1.684	1.1296	1.3356	.4996
8	2.696	4.6446	1.4882	1.3296	1.1638	1.5264	1.7692
9	2.5364	4.5466	2.3138	.6556	1.1892	1.3904	2.7894
10	4.7264	5.3976	3.9962	2.4174	1.1114	1.3956	3.759
11	4.956	5.1776	3.6192	2.741	.934	1.4492	4.479
12	7.1448	4.349	3.1924	.3652	1.3504	1.0936	2.2376
13	4.723	3.6912	2.7888	1.2028	1.478	.2928	3.1916
14	3.367	5.2696	2.5962	1.125	1.473	-.5164	3.6754
15	3.8036	4.2644	1.3414	.6936	1.5264	-1.0008	1.7388
16	1.8772	4.5398	1.3918	.9302	1.5082	-1.06	1.8468
17	3.3478	5.4434	1.3962	1.337	1.4178	-.5888	3.6368
18	4.8886	4.9808	1.342	.6682	1.1684	1.556	1.963
19	4.1364	4.2806	1.4258	.126	.8366	2.1324	3.0718
20	3.8156	3.2642	1.562	2.2642	.4696	1.994	1.5752
21	2.5454	2.1034	1.2922	1.8724	-.0756	1.7484	1.95
22	3.1612	4.9618	2.4258	.7636	-.6484	1.3812	3.06
23	2.7406	4.0852	1.4178	.9576	4.8192	1.1376	1.7806
24	2.7896	4.8596	2.9502	.6308	-1.1586	.7324	1.917
25	3.334	5.0292	2.3826	.482	2.0756	.0132	2.2358
26	3.9496	4.743	2.5852	.3456	.2066	-.5844	.9134
27	4.1336	4.0906	3.286	.8012	1.888	-.6604	2.0606
28	3.9254	3.0524	1.4372	.571	1.183	-.5604	2.4802
29	2.5284	.8742	1.233	-.4062	1.505	4.424	1.3828
30	1.0134	1.571	1.401	.314	1.3168	3.7884	-.0114
31	.9606	3.5028	1.4252	.7944	1.1978	2.8208	-.0124
32	1.8674	4.0442	1.3292	-.218	1.5854	.9744	-.0126
33	1.8594	4.7094	1.2502	-.8752	1.5594	-.1032	-.015
34	3.2958	4.294	.9418	.757	1.1642	1.3584	-.0152
35	4.4684	4.2288	1.1004	1.1938	.5416	1.5208	-.0148
36	3.7468	3.8008	1.1796	1.0864	.355	1.678	-.0144
37	3.0604	2.656	1.385	1.2926	.1854	1.344	-.0142
38	2.5774	.9428	2.2416	2.8516	.0294	1.2968	-.0144
39	1.9334	.8298	3.1374	3.7716	3.4178	.4388	-.014
40	1.5918	1.6262	1.282	3.6534	1.1946	1.4232	-.014
41	-.9048	1.8346	2.483	3.9112	1.0714	1.5564	-.0118
42	1.782	3.4114	4.6976	3.9044	1.3454	1.2936	-.0104
43	1.9156	4.475	4.1258	3.5572	1.4204	.4584	-.0104
44	.8908	3.79	1.9672	2.8244	1.4102	1.8056	7.6256
45	.7914	3.8156	1.84	4.6968	1.5174	1.0416	7.523
46	1.4466	3.3092	1.135	4.1318	1.3148	.0416	7.355
47	1.8718	2.4534	2.875	3.6554	.6822	.0444	.214
48	1.6246	1.1862	3.565	3.3878	.0848	.0456	8.0618

TABLE III. (CONT.) DATA FROM RUN 26--OPEN BACK PRESSURE VALVE

PORT #	SCANIVALVE NUMBER 8	9	10	P2/P1
1	1.9636	7.9108	0	1.35288847442
2	1.85	7.8104	0	1.3560718858
3	1.7608	7.714	0	1.35754704739
4	1.7068	7.6136	0	1.35591458961
5	1.6348	7.6252	0	1.36252467677
6	1.7512	7.6756	0	1.35602260262
7	1.8076	7.7724	0	1.35723961327
8	1.9132	7.7984	0	1.35025705782
9	1.9736	7.8772	0	1.35009365037
10	1.918	7.878	0	1.3546074707
11	1.98	7.8356	0	1.3471154266
12	1.9956	7.8988	0	1.34961381025
13	1.9976	7.9364	0	1.35168054472
14	1.9792	7.9028	0	1.3511630672
15	1.9504	7.8916	0	1.35280878946
16	1.9708	7.8644	0	1.34955867555
17	1.9848	7.92	0	1.35173397039
18	1.9652	7.8908	0	1.35157341911
19	1.97	7.8992	0	1.35168685476
20	1.972	7.8572	0	1.34903561613
21	2.0088	7.8928	0	1.34820448737
22	1.9636	7.8408	0	1.34873489069
23	1.9324	7.8216	0	1.35009506868
24	1.9484	7.8664	0	1.35147283738
25	1.98	7.9064	0	1.35131239569
26	1.9528	7.8616	0	1.35083476553
27	1.9804	7.874	0	1.34935975322
28	1.9464	7.8736	0	1.35206104791
29	1.9492	7.8824	0	1.35235883121
30	1.9648	7.9112	0	1.35281588289
31	1.956	7.8512	0	1.34996077357
32	1.9664	7.926	0	1.35356550956
33	1.9972	7.9364	0	1.3517125627
34	1.9696	7.8844	0	1.35084105158
35	1.9588	7.8656	0	1.35059111761
36	2.002	7.9136	0	1.349978641
37	2.0036	7.8832	0	1.34805120794
38	1.9976	7.9152	0	1.35042513495
39	1.9716	7.9008	0	1.35165348179
40	1.9712	7.8984	0	1.35154320411
41	2.0128	7.9132	0	1.34909237511
42	1.9988	7.8888	0	1.34876594991
43	2.01	7.8984	0	1.34844012735
44	2.0316	7.9228	0	1.34816080993
45	2.0408	7.9172	0	1.34709743394
46	1.9944	7.9184	0	1.35087061509
47	2.036	7.9064	0	1.34684137182
48	2.0296	7.91	0	1.34756362758

TABLE IV. DATA FROM RUN 27--LOWER PASSAGE SHOCK POSITIONED

SCAN Program Output
Pressure data from File RUN27LOWER
(File data has been multiplied by 1000.)

Atmospheric Pressure = 14.9086532937 PSIA

Gauge pressures:

PORT #	SCANIVALVE NUMBER 1	2	3	4	5	6	7
1	.0172	.0284	.0092	-.0006	.0008	.0144	-.0144
2	25.0024	25.0472	25.0134	25.0024	25.01	25.0328	25.0024
3	38.7742	16.058	2.0404	3.4302	2.0594	13.6236	2.288
4	2.276	16.518	2.8908	.6926	1.7446	14.8832	2.3944
5	19.8442	16.4198	5.0722	1.372	1.7266	14.7416	2.253
6	2.8946	16.5458	9.1428	1.1496	1.7308	1.7048	1.7064
7	3.5344	16.62	11.003	1.7284	1.5516	1.6656	.9118
8	2.9336	15.3596	12.1192	1.3284	1.5466	1.7992	2.1556
9	2.7288	16.1748	12.9534	.982	1.5366	1.7808	3.0604
10	4.9486	16.2724	13.9972	2.6498	1.524	5.0268	3.9232
11	5.0958	16.3926	14.724	2.9856	1.3752	7.8308	4.8226
12	7.4696	16.5958	15.3684	.4314	1.7824	10.6456	2.5482
13	5.0524	16.6488	15.5082	1.0848	2.5266	11.5656	3.1374
14	3.6624	13.6948	16.2468	1.1752	4.132	12.8088	3.7314
15	3.9028	15.2992	1.6896	.8132	6.0904	13.3296	2.0466
16	2.1526	15.7778	1.8128	.7188	7.8474	14.308	1.8984
17	3.3138	16.2824	2.8888	1.1386	8.927	14.2052	3.65
18	5.1402	16.442	5.6318	.7702	10.3904	1.7856	2.3462
19	4.3704	16.4646	8.4632	.3398	10.9734	2.3484	3.3586
20	3.898	16.731	9.416	2.2734	11.4878	2.2232	1.7122
21	2.8418	10.9564	10.8862	3.5532	12.5474	2.0088	2.2538
22	3.0084	12.94	13.5986	.7444	13.3718	3.1528	3.334
23	2.9872	14.1396	8.4482	.8714	14.7462	8.3748	1.9906
24	3.0718	15.3492	14.5502	.611	13.9516	10.2412	2.2582
25	3.6042	15.9988	15.2666	.6744	16.1282	11.7444	2.5742
26	4.0254	16.3038	15.7166	.4362	17.6134	12.8164	1.1038
27	4.0936	16.5782	15.5234	.6658	18.952	13.4336	2.3868
28	4.2632	16.6752	1.684	.5668	2.06	14.1208	2.7624
29	3.0328	9.1008	1.8448	-.2194	2.0952	14.8396	.1.643
30	1.2468	11.5044	3.5146	1.0698	1.572	14.3332	-.0112
31	1.0586	12.694	6.5118	2.8464	1.6476	14.068	-.011
32	1.8588	13.759	12.1332	-.5386	4.177	13.9172	-.0112
33	2.2108	14.6456	9.174	-.4742	7.5572	13.4696	-.0116
34	3.6296	15.139	10.6574	2.8844	10.077	1.598	-.0112
35	4.6754	15.6342	11.966	4.0204	10.9254	1.564	-.0124
36	4.0338	16.1522	12.94	8.7152	11.9046	1.7456	-.01
37	3.2512	16.4562	14.0672	10.5958	13.0664	1.7	-.0082
38	2.7968	4.6412	14.6778	12.074	13.929	1.4116	-.0072
39	2.1682	9.094	15.3148	13.8382	14.671	.9184	-.0082
40	1.8094	10.7964	1.4374	14.7876	1.4712	1.5176	-.0084
41	-.7552	12.3698	2.1476	15.5396	1.6202	1.5112	-.007
42	2.0092	13.3538	5.0608	15.7308	1.8494	1.944	-.0064
43	2.102	14.1974	3.8392	15.9658	1.7786	.786	-.006
44	1.0096	15.032	1.588	16.2584	3.2084	1.638	19.8422
45	1.0082	15.247	1.9404	15.7692	7.827	.3104	19.9904
46	1.6666	15.7876	1.238	15.5906	10.3426	.032	19.7472
47	2.025	16.17	2.9492	15.243	11.5248	.0308	.3014
48	1.773	2.105	3.1634	14.9558	12.5384	.0312	20.2466

TABLE IV. (CONT.) DATA FROM RUN 27--LOWER PASSAGE SHOCK POSITIONED

PORT #	SCANIVALVE NUMBER 8	9	10	P2/P1
1	2.1524	19.6844	0	2.02760361264
2	2.2116	19.8404	0	2.02970439149
3	2.3248	19.9244	0	2.02124627607
4	2.376	19.9264	0	2.01537472009
5	2.3276	19.9036	0	2.01971116927
6	2.302	19.9156	0	2.02341263283
7	2.3104	19.8724	0	2.01991669928
8	2.296	19.8376	0	2.01958462635
9	2.3196	19.8936	0	2.02006858736
10	2.3484	19.9048	0	2.01734633956
11	2.3516	19.8564	0	2.01416819916
12	2.3216	19.8444	0	2.01697866545
13	2.37	19.8856	0	2.01371326239
14	2.3196	19.8796	0	2.01925596871
15	2.328	19.8584	0	2.01704198032
16	2.3324	19.8332	0	2.01506559384
17	2.312	19.794	0	2.01517635259
18	2.3316	19.8764	0	2.01766486264
19	2.3036	19.8052	0	2.01681050711
20	2.3352	19.8116	0	2.01348577388
21	2.3032	19.8344	0	2.01855388266
22	2.2956	19.8036	0	2.01765532634
23	2.344	19.8352	0	2.01382666783
24	2.3176	19.7948	0	2.01456768933
25	2.33	19.8384	0	2.01564778302
26	2.3104	19.8428	0	2.0181976733
27	2.3016	19.7888	0	2.01609195992
28	2.284	19.782	0	2.01776030151
29	2.3332	19.8068	0	2.01344093946
30	2.2952	19.76	0	2.01516792208
31	2.2924	19.7348	0	2.01403092602
32	2.2936	19.7352	0	2.01391368341
33	2.3188	19.8064	0	2.01510070594
34	2.3028	19.7584	0	2.01418513022
35	2.2456	19.6996	0	2.01747360851
36	2.2812	19.7716	0	2.01748395994
37	2.3372	19.788	0	2.01188382522
38	2.254	19.7276	0	2.01811763607
39	2.2784	19.74	0	2.01597404172
40	2.29	19.6752	0	2.01084658799
41	2.3004	19.688	0	2.01037516145
42	2.266	19.6664	0	2.01314417837
43	2.284	19.6272	0	2.00875645566
44	2.2812	19.6692	0	2.01152695738
45	2.2688	19.628	0	2.01058053852
46	2.2556	19.6044	0	2.01075180511
47	2.2576	19.5932	0	2.00986509423
48	2.2332	19.5708	0	2.01141922655

TABLE V. DATA FROM RUN 28--UPPER PASSAGE SHOCK POSITIONED

SCAN Program Output
Pressure data from File RUN28UPPER
(File data has been multiplied by 1000.)

Atmospheric Pressure - 14.9086532937 PSIA

Gauge pressures:

PORT #	SCANIVALVE NUMBER 1	2	3	4	5	6	7
1	.005	.1394	.015	-.0024	.0042	.0368	-.0052
2	25.0146	25.1584	25.032	25.0118	25.0248	25.0648	25.0178
3	39.5462	19.9376	11.573	14.8424	2.328	18.0492	2.5336
4	2.4182	20.0976	12.247	4.5128	8.4744	18.9464	2.6122
5	22.4134	20.1782	12.95	5.7832	13.0462	19.0048	2.4408
6	7.1104	20.4728	14.0412	9.2156	13.2532	13.89	1.8934
7	9.6048	20.6956	15.2864	10.9394	13.5572	14.6484	1.1042
8	9.9054	19.569	16.1546	12.4814	13.6808	15.0348	2.3386
9	8.4668	19.7534	17.1652	13.108	13.8756	15.5008	3.2432
10	6.6706	19.819	18.0234	13.9144	14.1698	16.0412	6.1302
11	5.9384	20.0756	18.513	14.7208	13.936	16.2836	6.0138
12	7.0148	20.3354	19.2068	3.0404	14.557	16.7316	2.7512
13	5.7236	20.4378	19.311	4.5216	14.712	17.1056	7.7426
14	7.9138	18.51	20.0016	7.5496	14.8526	17.4792	5.0546
15	9.8372	18.8228	10.5926	8.4016	15.3212	18.032	2.2272
16	9.9504	19.235	11.2126	9.6846	15.515	18.5236	10.158
17	7.681	19.625	11.6836	10.9438	15.6918	18.5352	4.437
18	6.0578	19.8428	12.6196	12.2794	15.9364	13.9272	2.4996
19	5.4016	20.1354	13.8436	13.4424	16.4214	14.7876	4.4382
20	4.7076	20.4228	14.7022	14.5042	16.654	15.4456	13.3882
21	8.6938	17.2002	16.0184	15.2068	17.1136	16.1628	2.4258
22	11.8666	17.82	17.5864	3.934	17.8606	16.5056	3.5122
23	10.3236	18.288	13.7502	5.1552	18.7152	16.8364	2.1086
24	8.9266	19.0612	18.6186	7.4352	18.29	17.1112	2.478
25	7.3666	19.4116	19.098	7.472	19.8754	17.3304	2.7886
26	6.1348	19.7464	19.4942	8.4196	20.913	17.7356	1.2338
27	4.538	20.1906	19.1182	9.8276	21.9034	18.1464	2.5372
28	4.4344	20.434	11.0562	11.2662	11.0548	18.454	2.9402
29	4.1404	15.4742	11.1896	13.5292	11.0924	18.9544	1.8296
30	11.262	16.3022	11.918	14.5138	11.306	18.6152	-.0054
31	12.6092	17.138	12.9424	15.1024	11.9658	18.5456	-.0058
32	11.8272	17.9062	16.9038	13.2512	12.8646	18.4776	-.0054
33	2.3666	18.4132	14.9088	14.2412	13.871	18.0616	-.0054
34	3.8594	19.0784	15.973	15.09	14.9764	4.866	-.0054
35	4.863	19.3834	16.827	17.948	16.183	6.7156	-.006
36	4.1568	19.9884	17.7604	18.6314	17.1048	8.544	-.0068
37	3.3792	20.2532	18.5468	18.661	17.9842	9.528	-.0078
38	2.8324	13.675	19.082	18.706	18.6474	10.9324	-.0078
39	2.2816	14.668	19.4952	18.554	19.1582	11.8584	-.0086
40	1.9446	15.5258	10.1706	18.8298	11.9336	12.8976	-.0098
41	-.6792	16.5034	12.6258	18.9292	12.1112	13.672	-.0084
42	2.1648	17.3294	13.903	19.1956	12.2726	12.2464	-.0078
43	2.2744	18.0672	14.1332	19.003	12.5386	12.0244	-.0076
44	1.1174	18.7418	6.8264	19.5812	13.4018	9.186	22.717
45	1.135	19.0532	10.6652	19.6864	14.2854	8.8168	22.5556
46	1.8532	19.591	12.407	19.429	15.215	.0336	22.483
47	2.1696	19.9512	13.2516	19.277	16.1186	.0344	.3826
48	1.8576	11.2586	13.4698	18.6954	16.9334	.0324	22.6006

TABLE V. (CONT.) DATA FROM RUN 27--UPPER PASSAGE SHOCK POSITIONED

PORT #	SCANIVALVE NUMBER 8	9	10	P2/P1
1	2.4988	22.4708	0	2.1473246352
2	2.4692	22.5036	0	2.15286967046
3	2.4576	22.4452	0	2.15094486197
4	2.4968	22.4692	0	2.14747945158
5	2.4892	22.46	0	2.14788874598
6	2.4636	22.446	0	2.15024802265
7	2.4548	22.4364	0	2.15078490793
8	2.4688	22.4204	0	2.14813141274
9	2.4572	22.4048	0	2.14866800166
10	2.4804	22.4472	0	2.1482396231
11	2.4808	22.4092	0	2.14600497574
12	2.486	22.45	0	2.14770899212
13	2.5324	22.4256	0	2.14059625098
14	2.5124	22.4132	0	2.14234195054
15	2.468	22.4108	0	2.14767784469
16	2.48	22.3892	0	2.14495353169
17	2.4552	22.3628	0	2.14649667118
18	2.4584	22.3796	0	2.14706851318
19	2.4928	22.4156	0	2.14489288129
20	2.488	22.4288	0	2.14624345633
21	2.4864	22.4632	0	2.14841844188
22	2.4748	22.384	0	2.14529602741
23	2.4988	22.42	0	2.14440634502
24	2.5008	22.4164	0	2.14395321117
25	2.512	22.4808	0	2.14627159288
26	2.4812	22.408	0	2.14588660775
27	2.5012	22.4428	0	2.14542033546
28	2.446	22.3648	0	2.14774980882
29	2.456	22.4144	0	2.1493693345
30	2.4828	22.4084	0	2.14571218768
31	2.4548	22.3668	0	2.14677648871
32	2.4872	22.416	0	2.14560635018
33	2.4784	22.3412	0	2.14239024086
34	2.5268	22.3784	0	2.13857664986
35	2.4772	22.3332	0	2.14207796791
36	2.4424	22.306	0	2.14480658112
37	2.4564	22.23	0	2.13870079553
38	2.4344	22.2476	0	2.14242859458
39	2.4436	22.1896	0	2.13795019389
40	2.4172	22.1964	0	2.14160033937
41	2.4244	22.1528	0	2.13819531191
42	2.422	22.1424	0	2.13789132272
43	2.4472	22.196	0	2.13787548591
44	2.4344	22.1788	0	2.13846158837
45	2.3592	22.0668	0	2.14128836195
46	2.336	22.058	0	2.14365882944
47	2.3872	22.0456	0	2.1365961347
48	2.3816	22.0564	0	2.13791276888

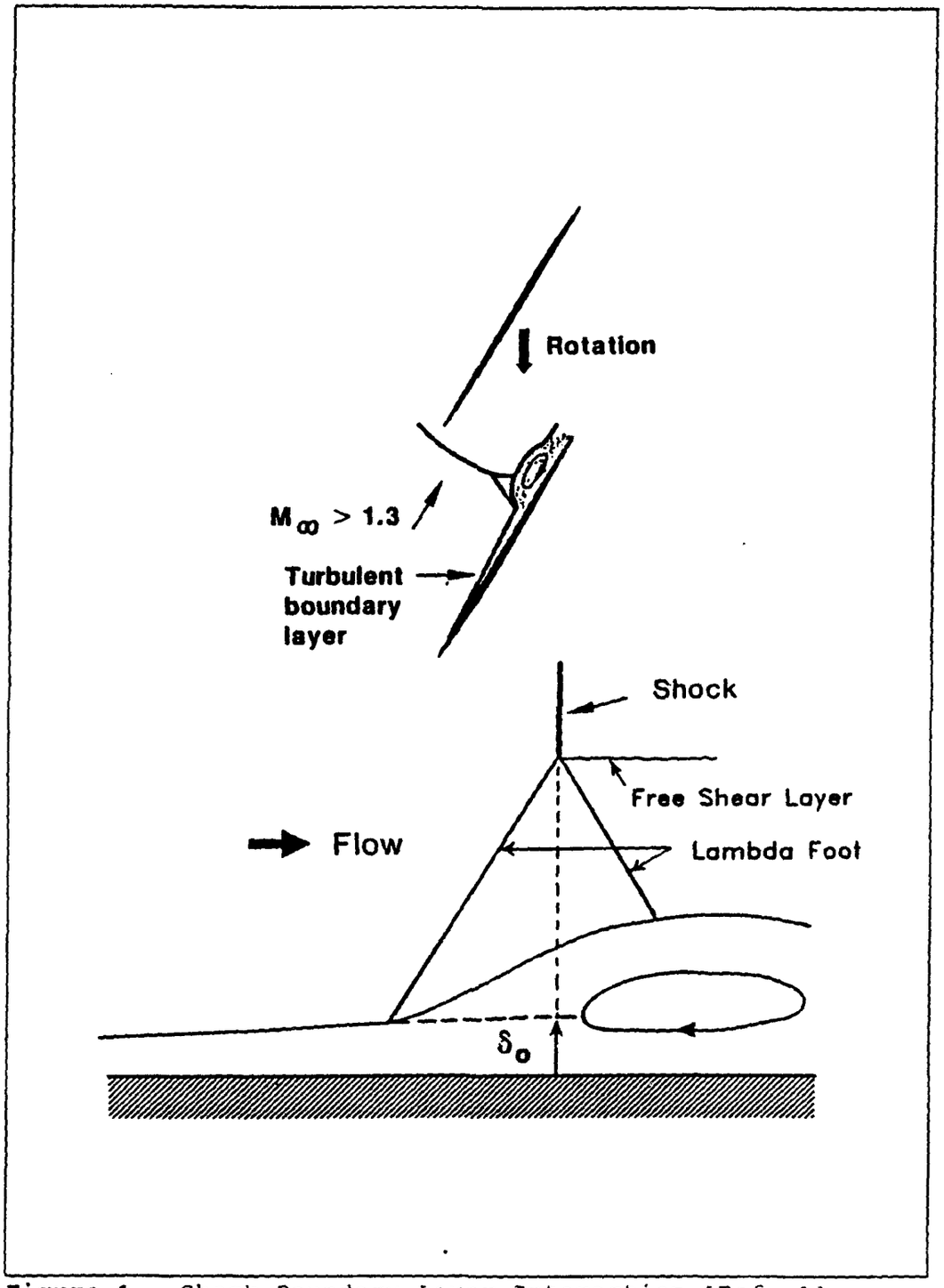

Figure 1. Shock-Boundary Layer Interaction [Ref. 1]

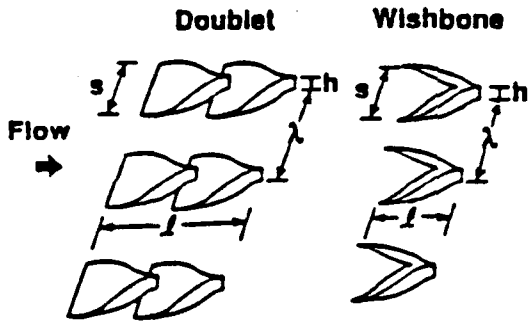

Doublet

h	ℓ	s	λ
0.11"	1.25"	0.42"	0.50"
0.125"	1.60"	0.80"	1.00"
0.15"	1.65"	0.56"	0.75"
0.50"	3.35"	1.62"	2.00"

Wishbone

h	ℓ	s	λ
0.11"	0.35"	0.25"	0.50"
0.25"	0.84"	0.70"	1.00"
0.50"	1.88"	1.60"	2.00"

Figure 2. Low-Profile Vortex Generator Operation [Ref. 4]

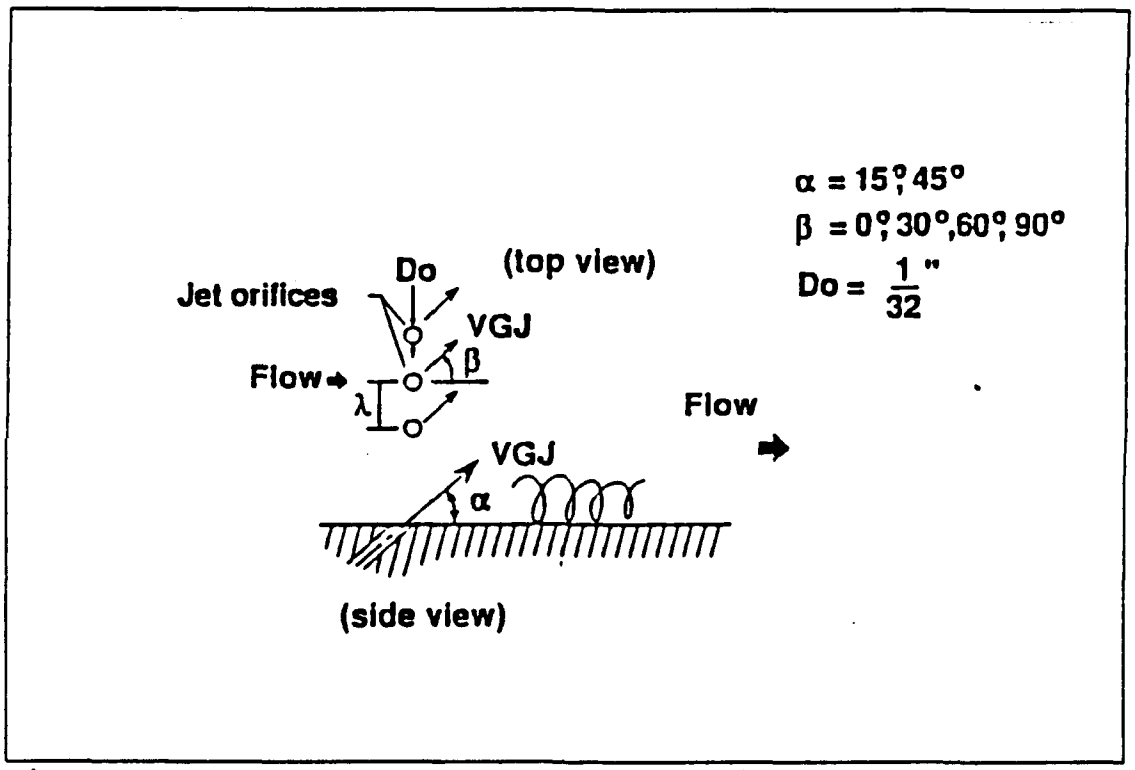

Figure 3. Vortex Generator Jet Operation [Ref. 4]

Blade Geometry

L.E. Radius	= 0.015 in
T.E. Radius	= 0.015 in
Wedge Angle	= 3.5°
Wedge Length	= 2.85 in
Suction Surface Arc Radius	= 13.53 in

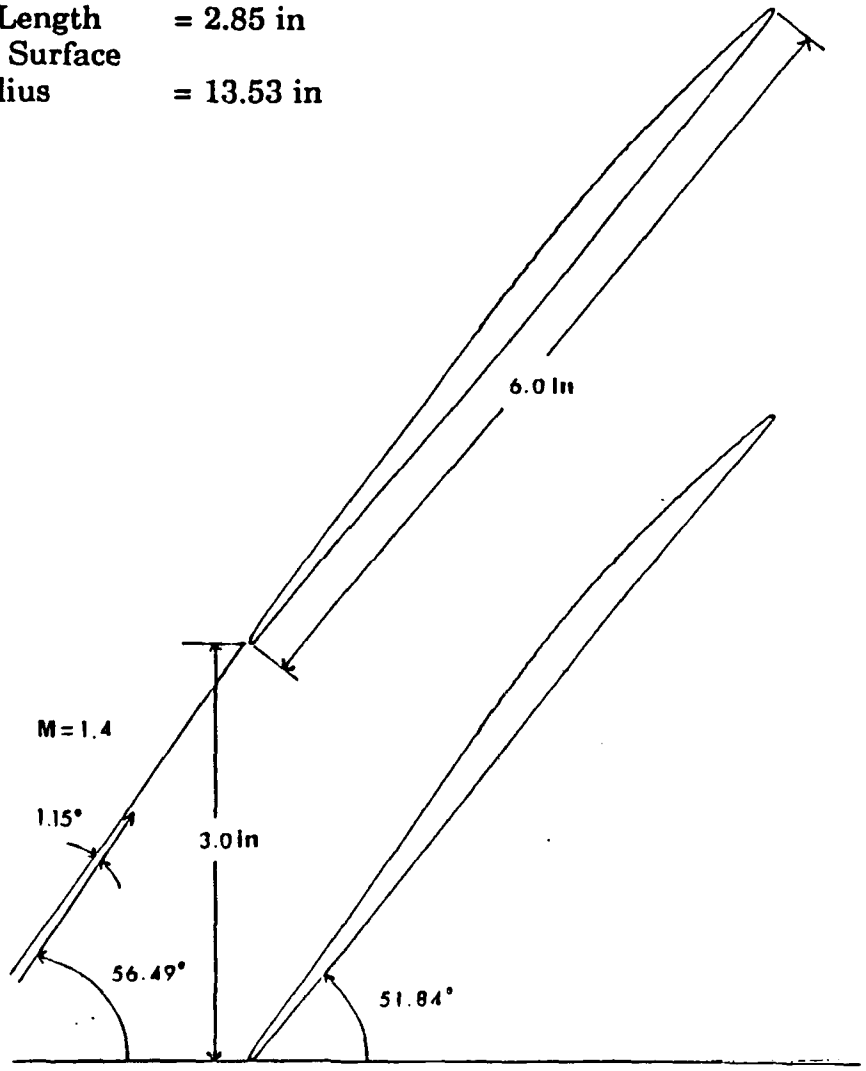

Figure 4. Transonic Cascade Blade Geometry

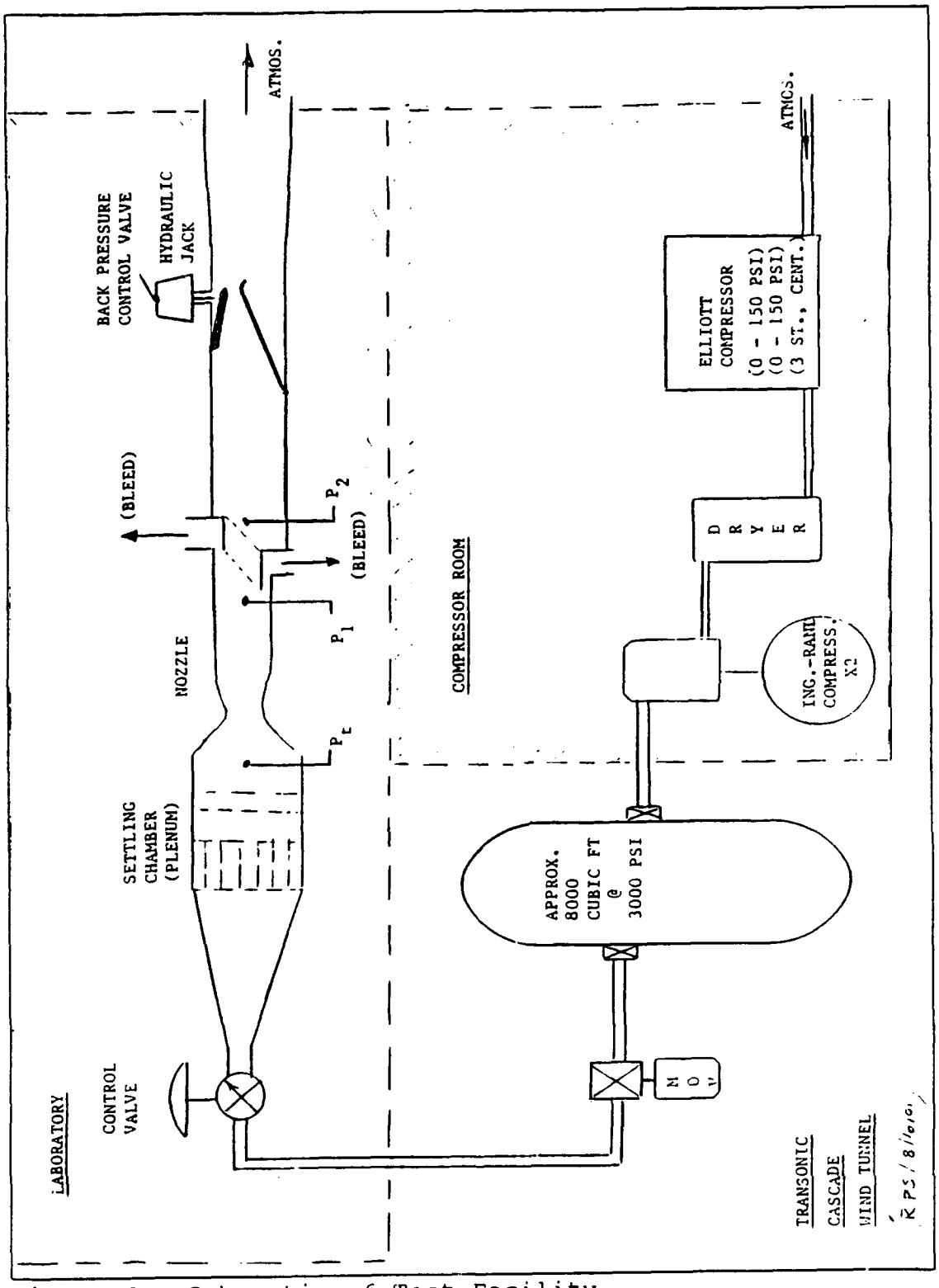

Figure 5. Schematic of Test Facility

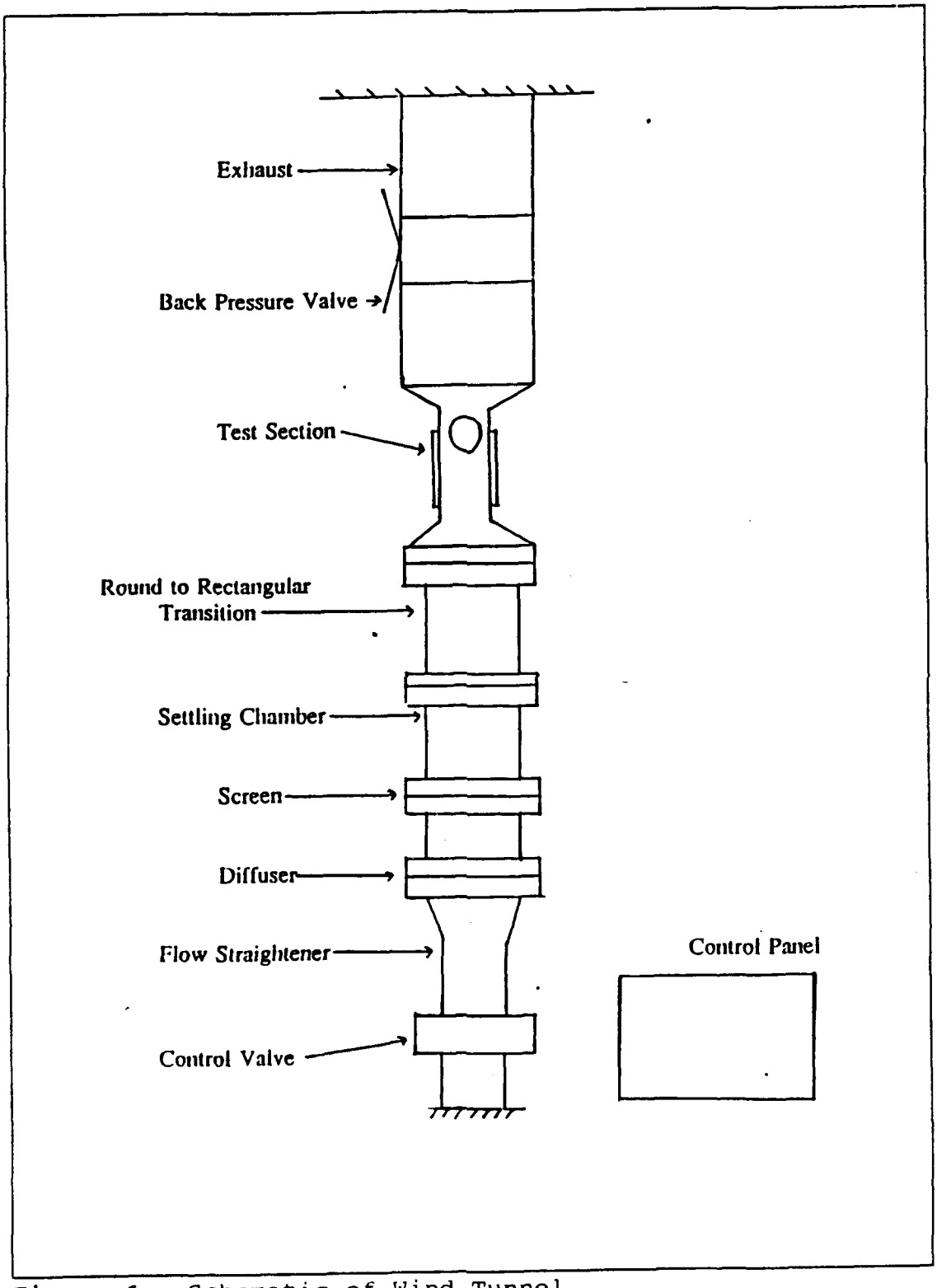

Figure 6. Schematic of Wind Tunnel

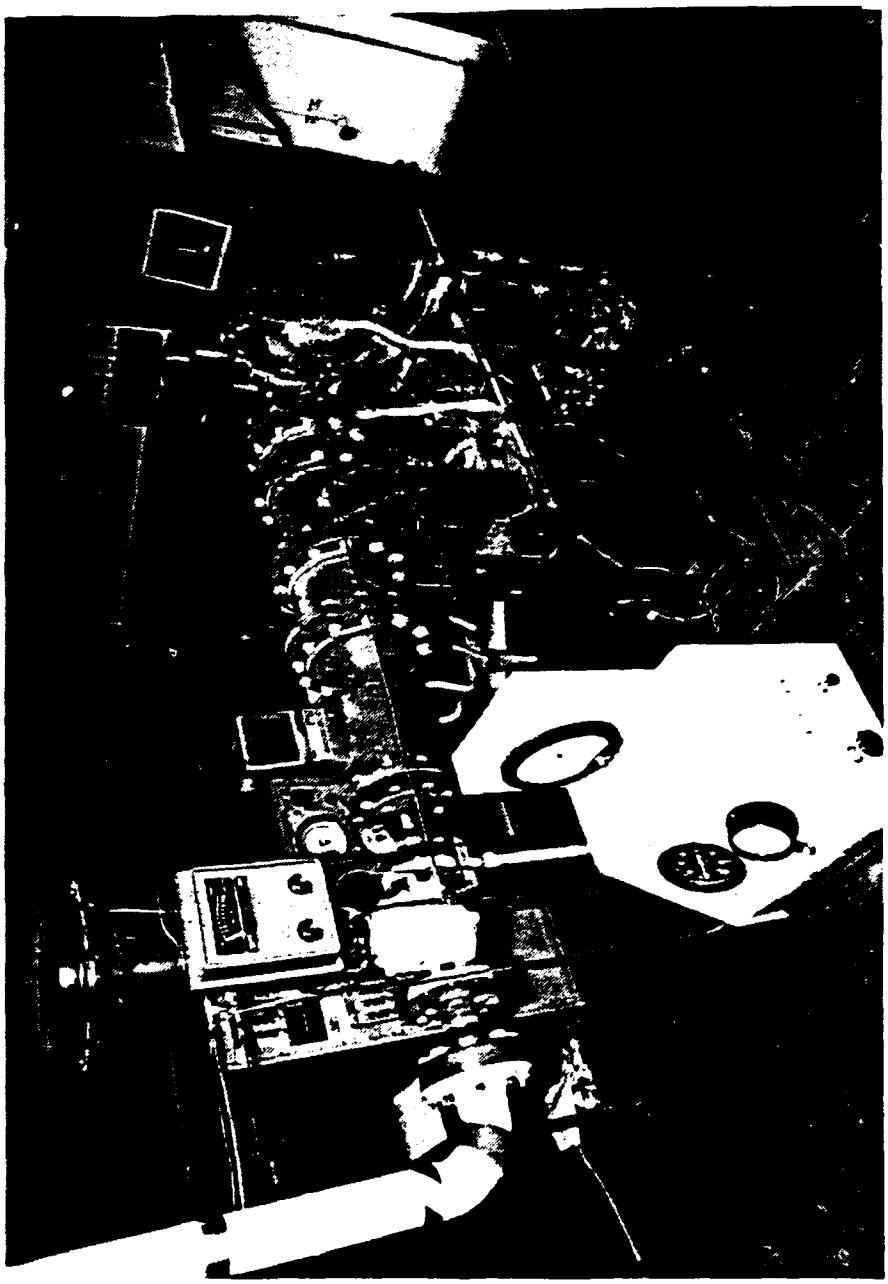

Figure 7. Transonic Cascade Wind Tunnel

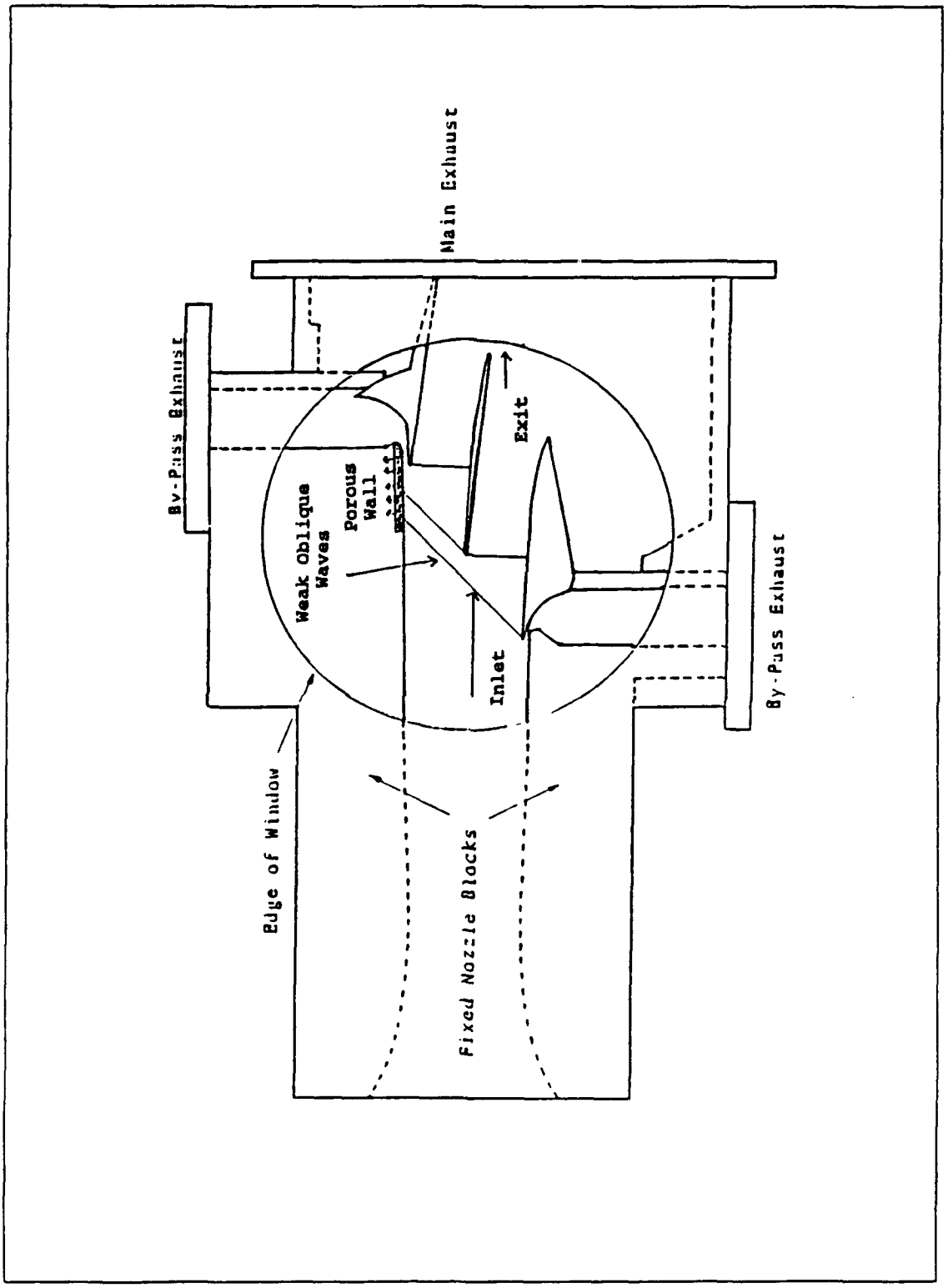

Figure 8. Schematic of Test Section

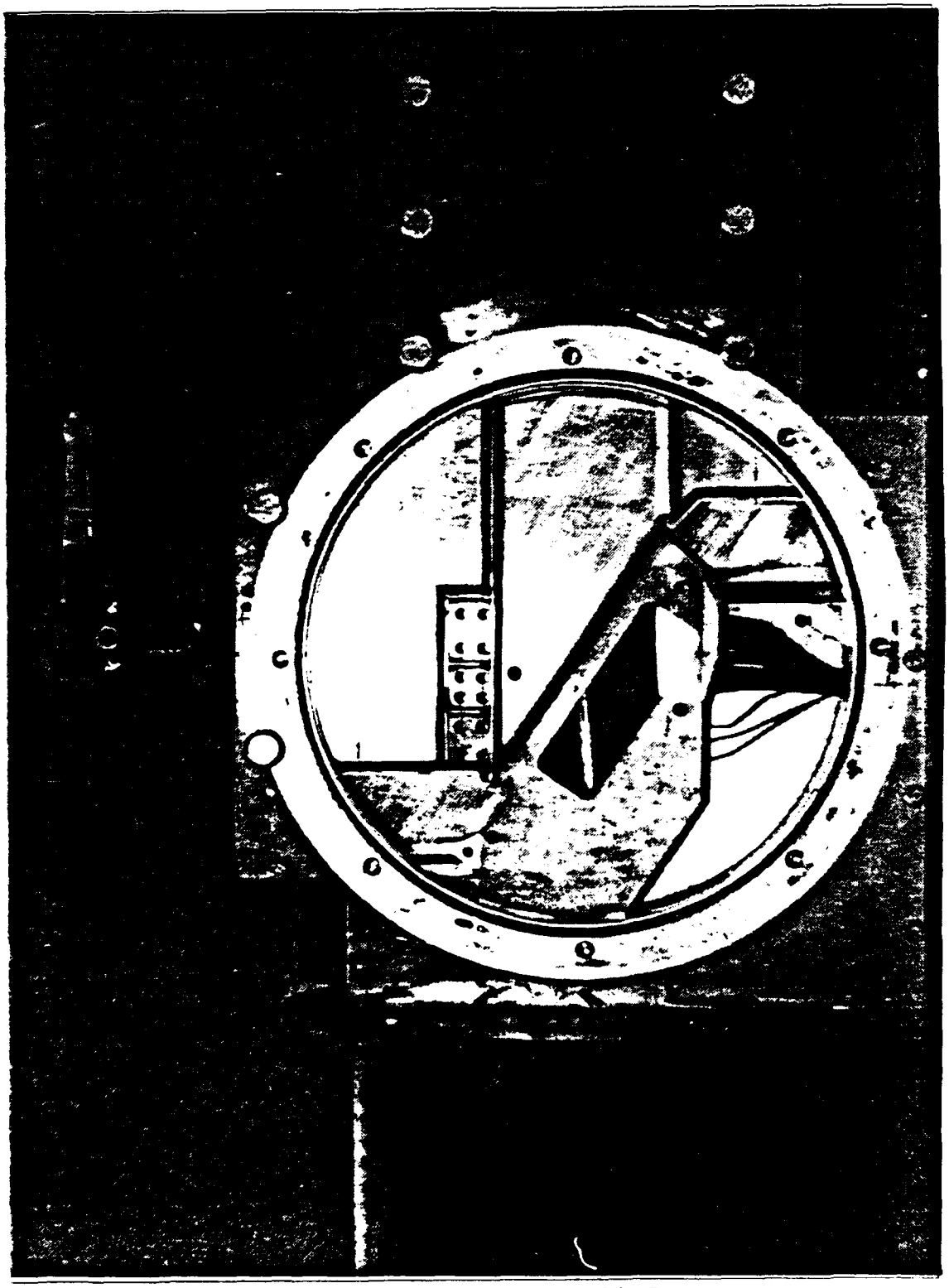

Figure 9. Test Section (with Side-Wall Removed)

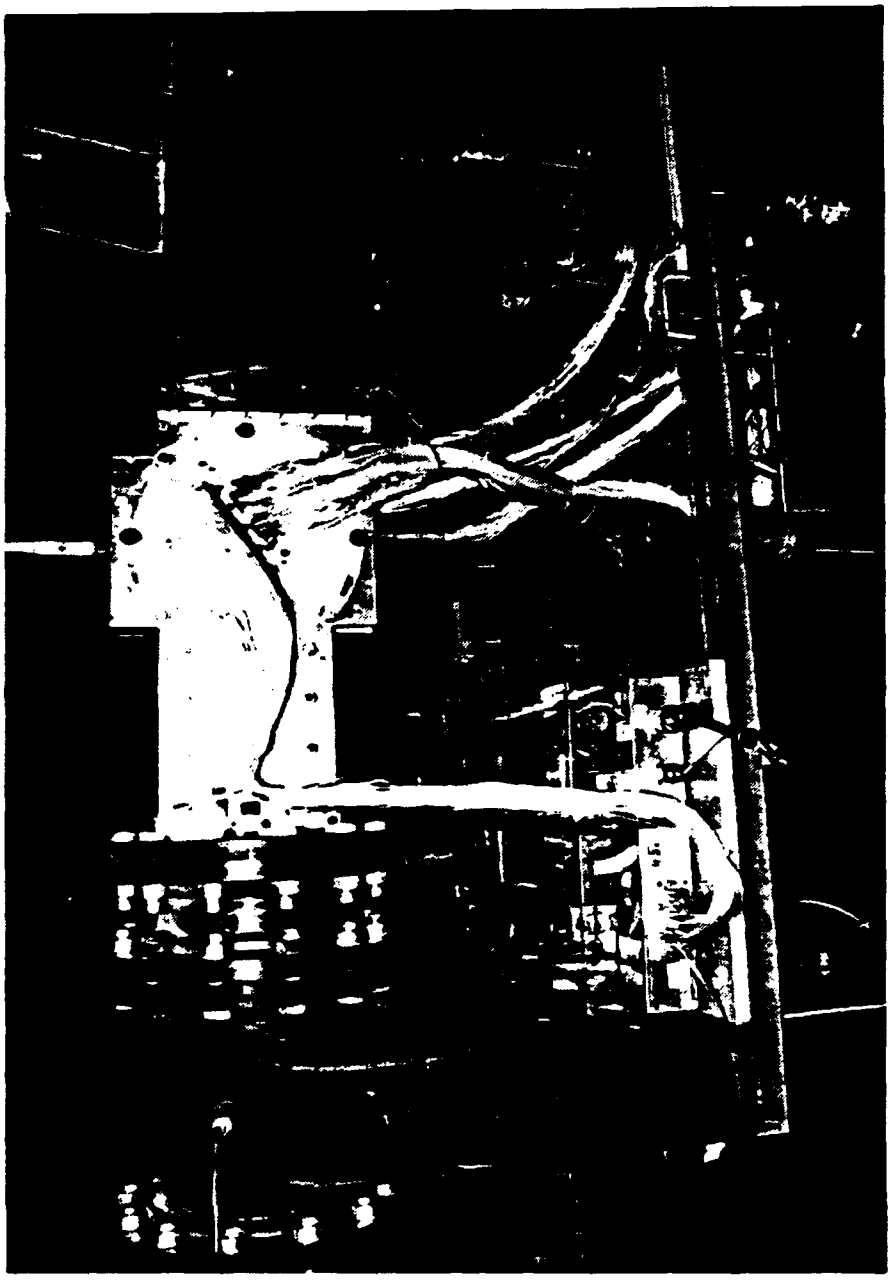

Figure 10. Test Section And Instrumentation

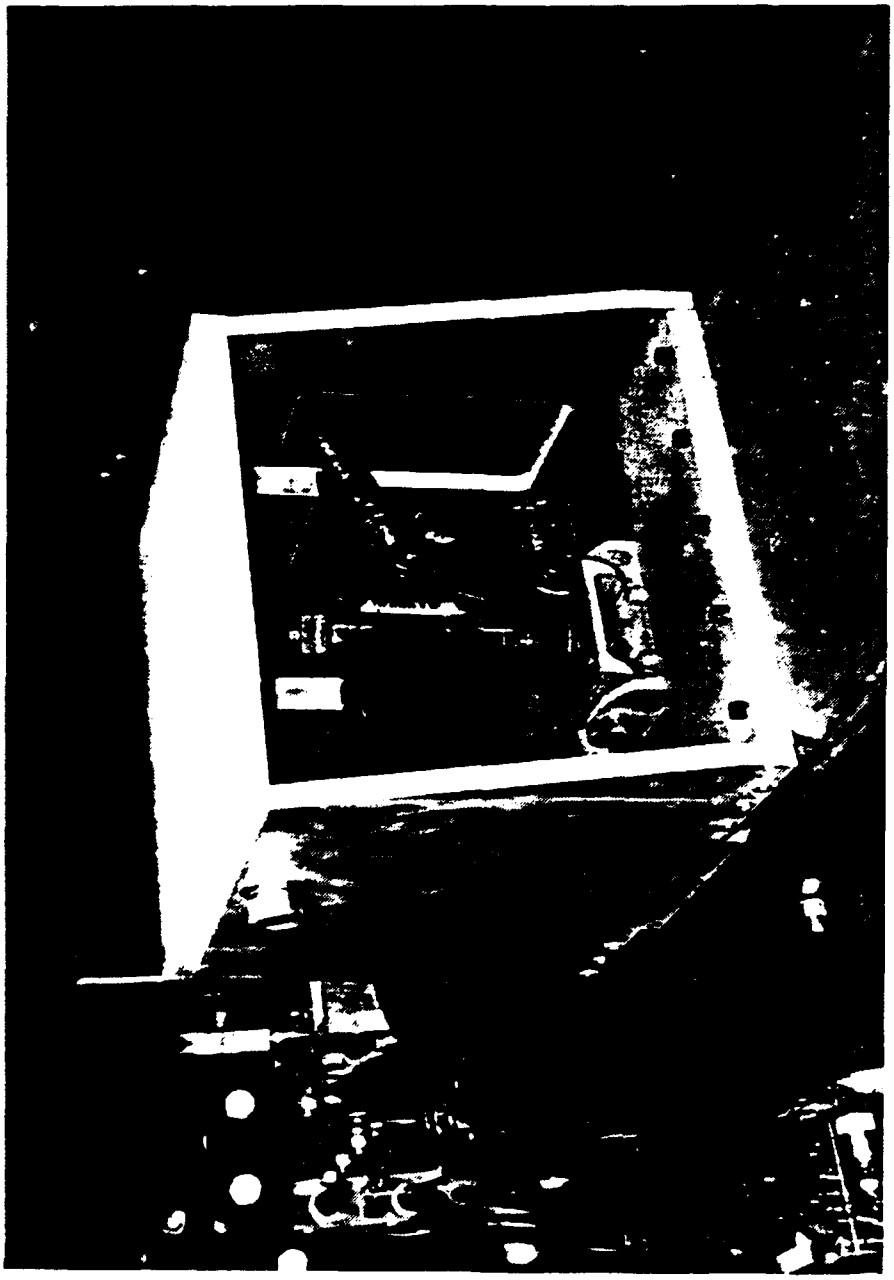

Figure 11. Back Pressure Valve

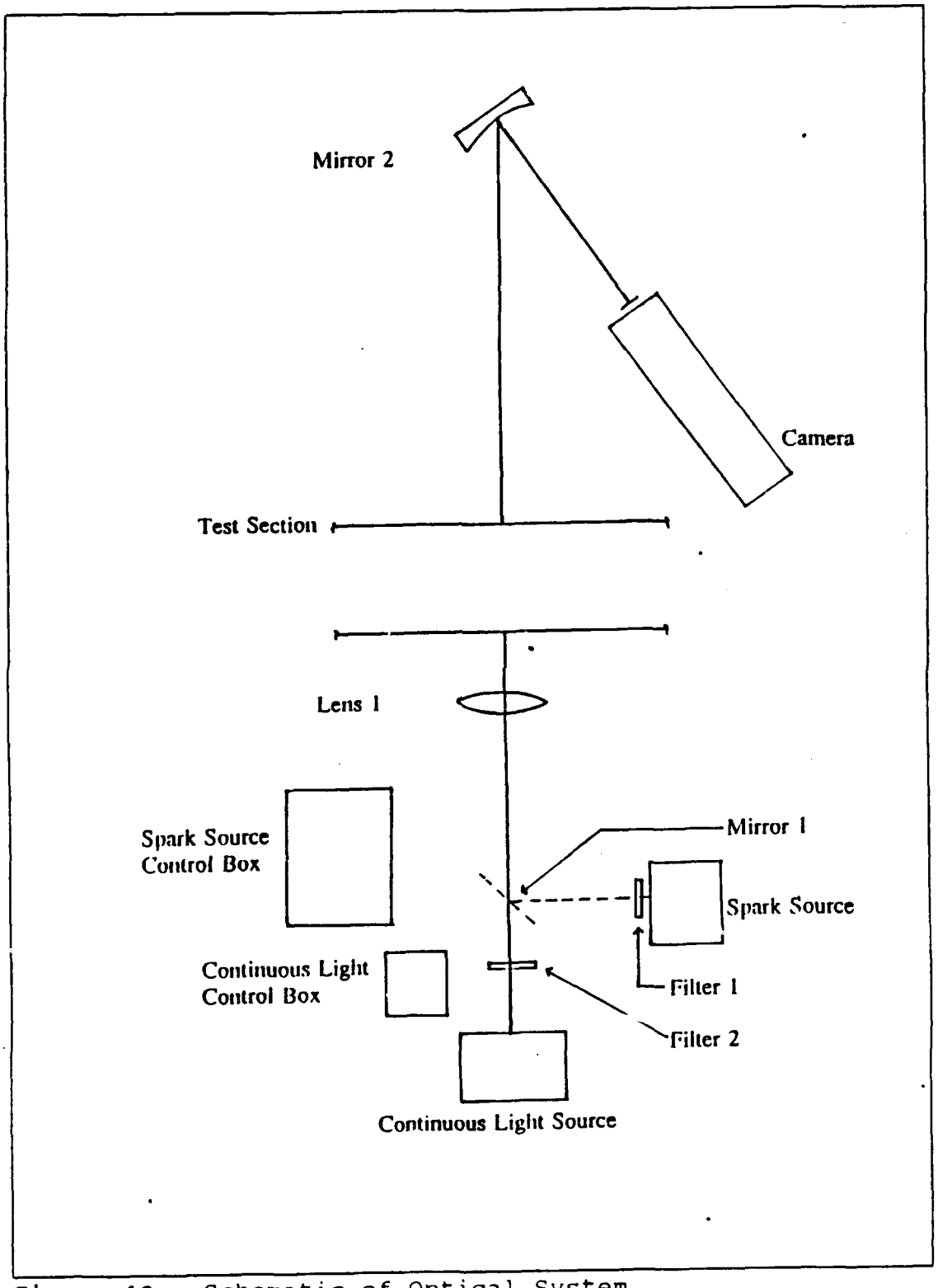

Figure 12. Schematic of Optical System

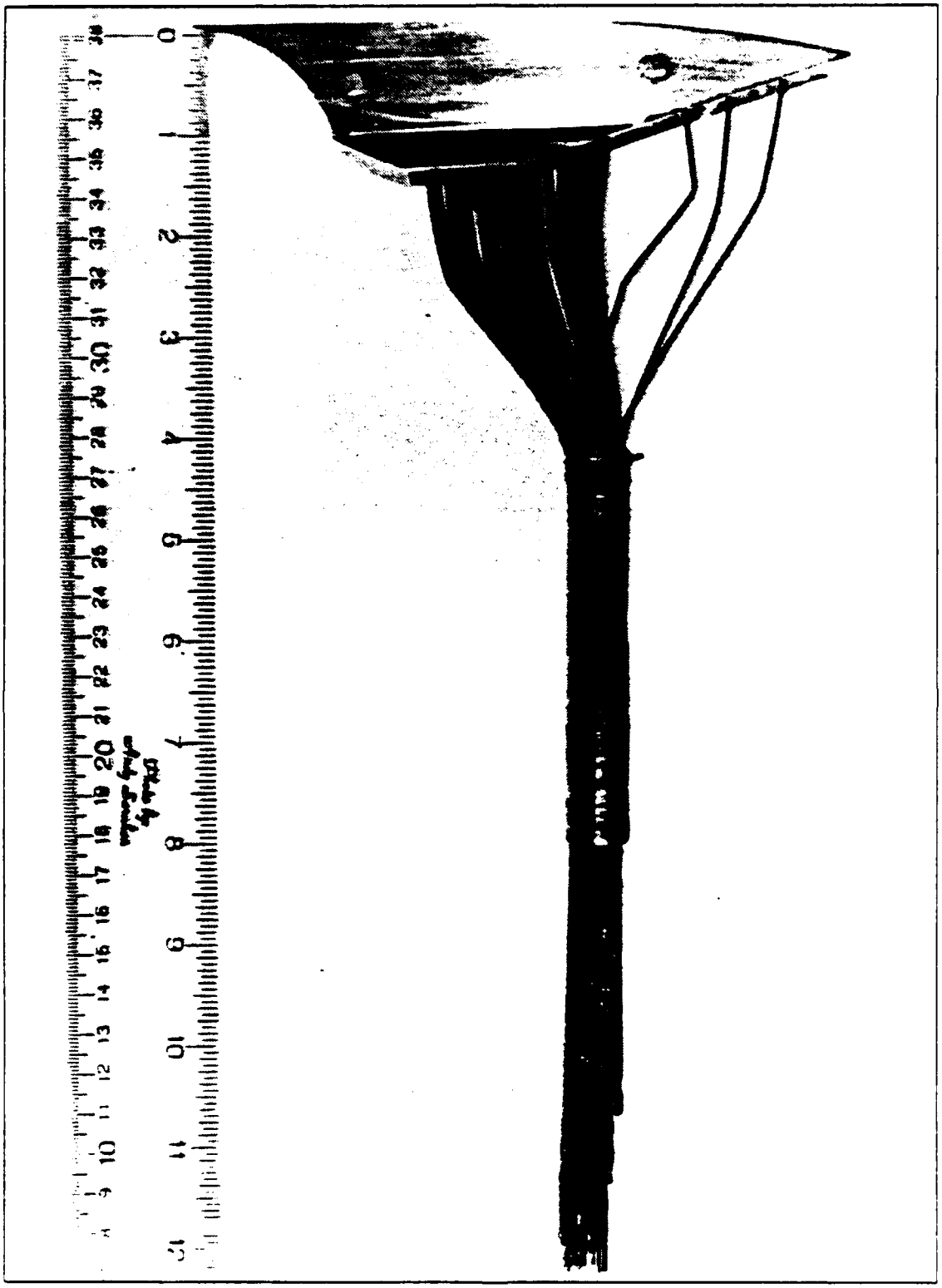

Figure 13. Instrumented Test Section Lower Blade

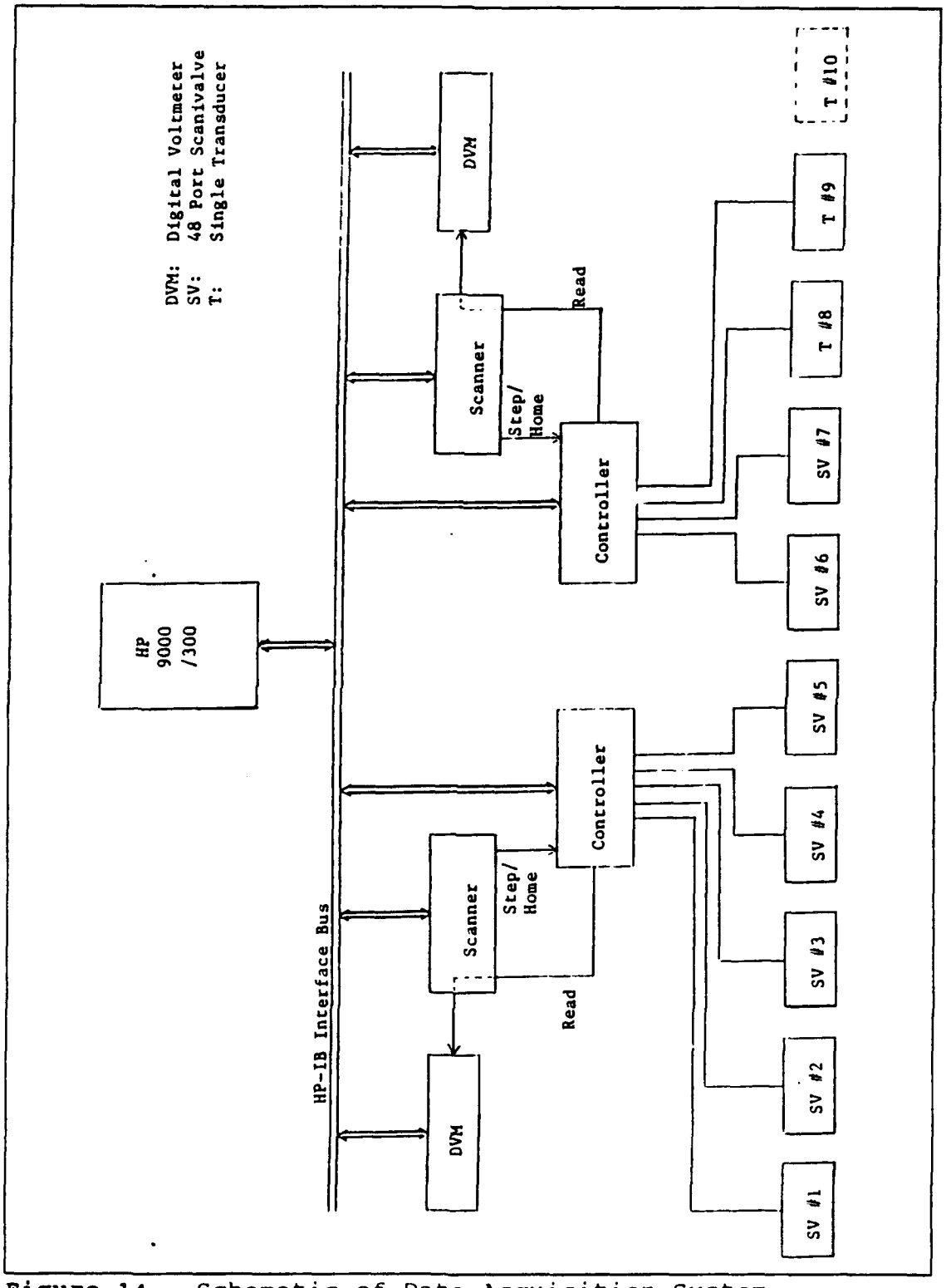

Figure 14. Schematic of Data Acquisition System

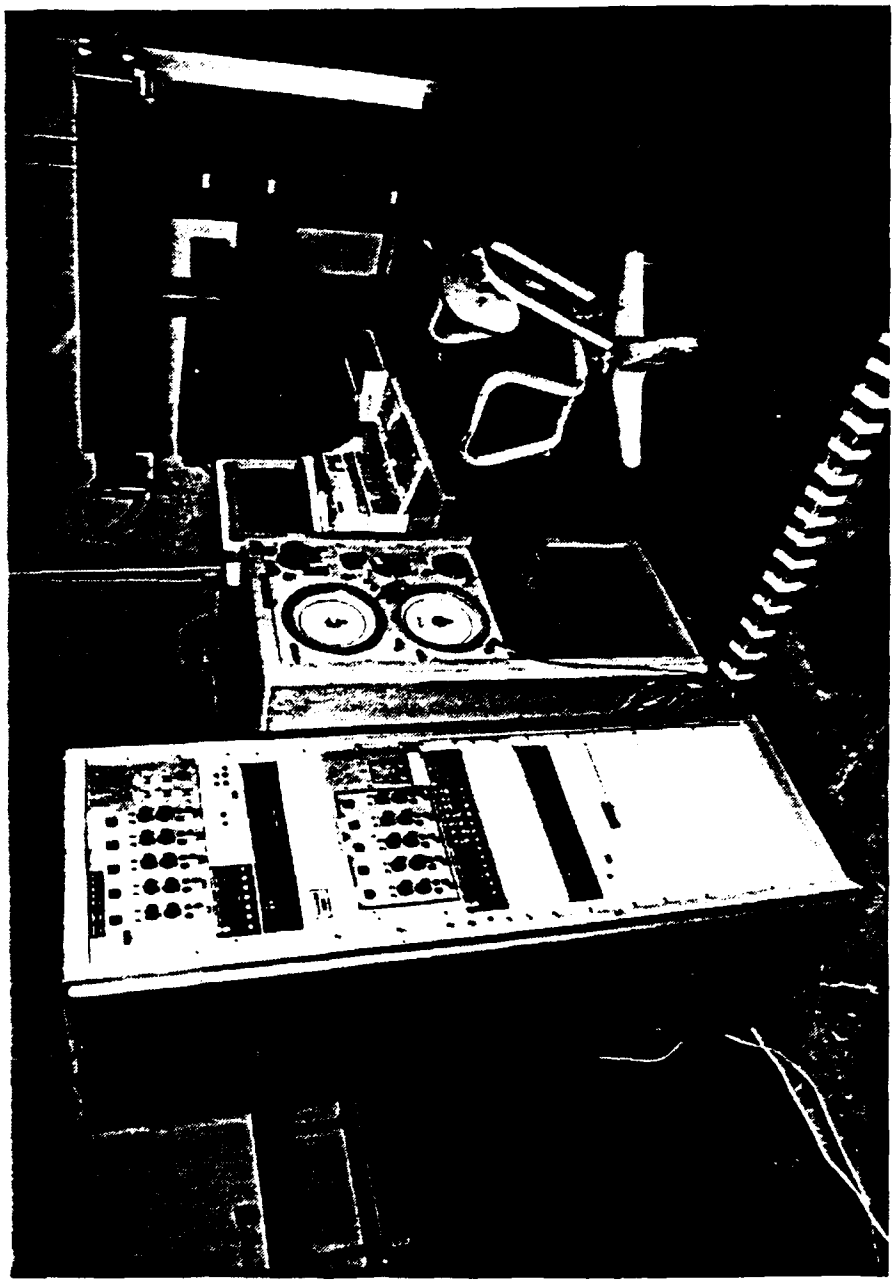

Figure 15. Data Acquisition System

ENLARGE

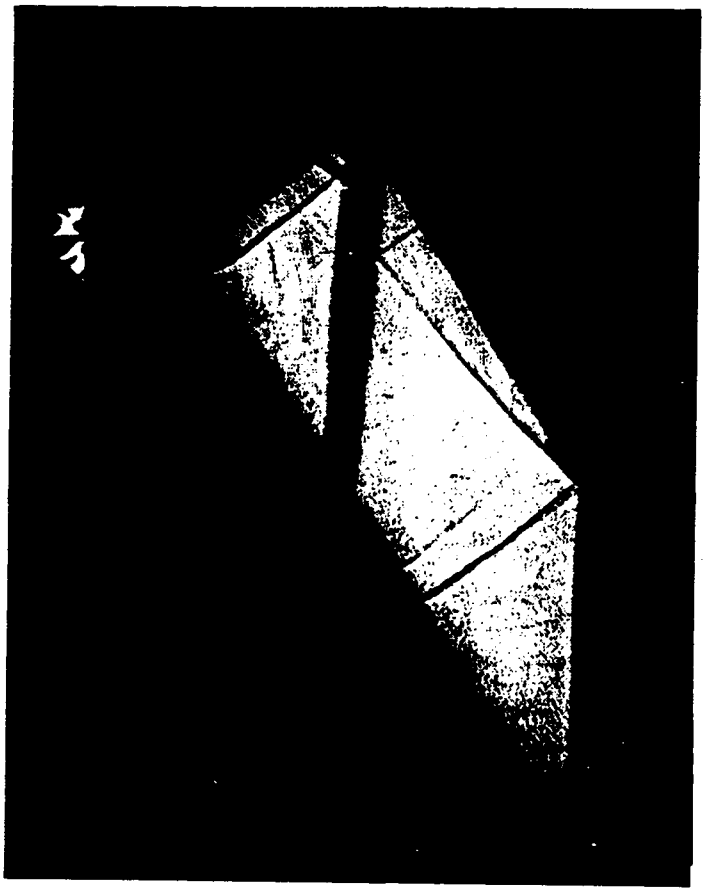

Figure 16. Shock Structure with Open Back Pressure Valve

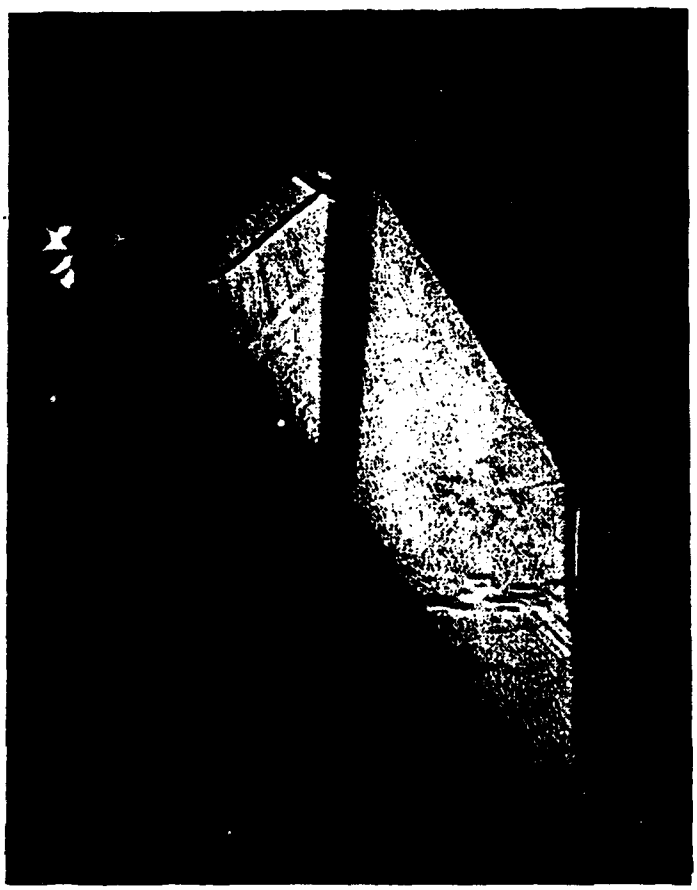

Figure 17. Shock Structure with Lower Shock in Position

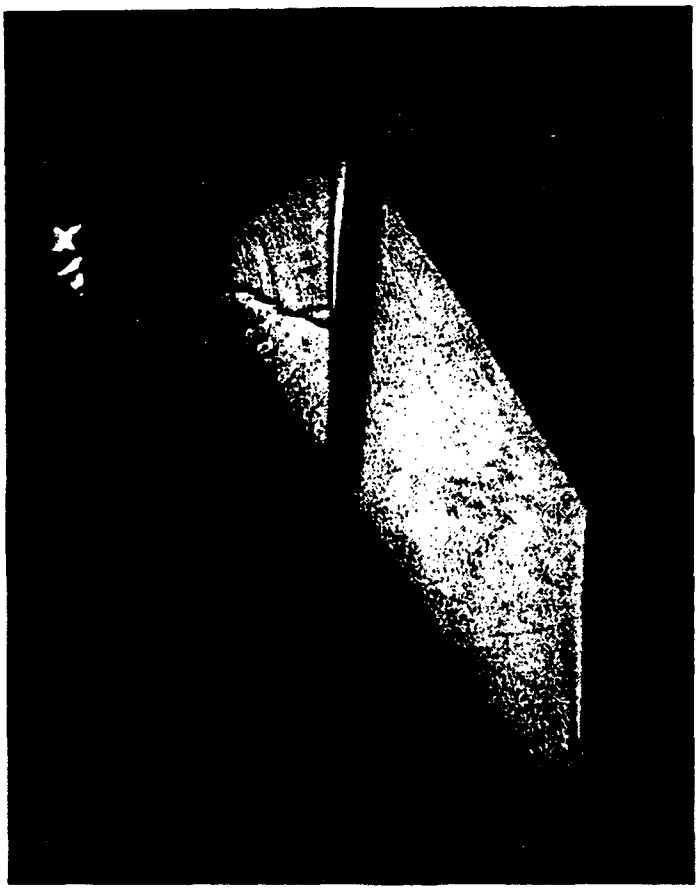

Figure 18. Shock Structure with Upper Shock in Position

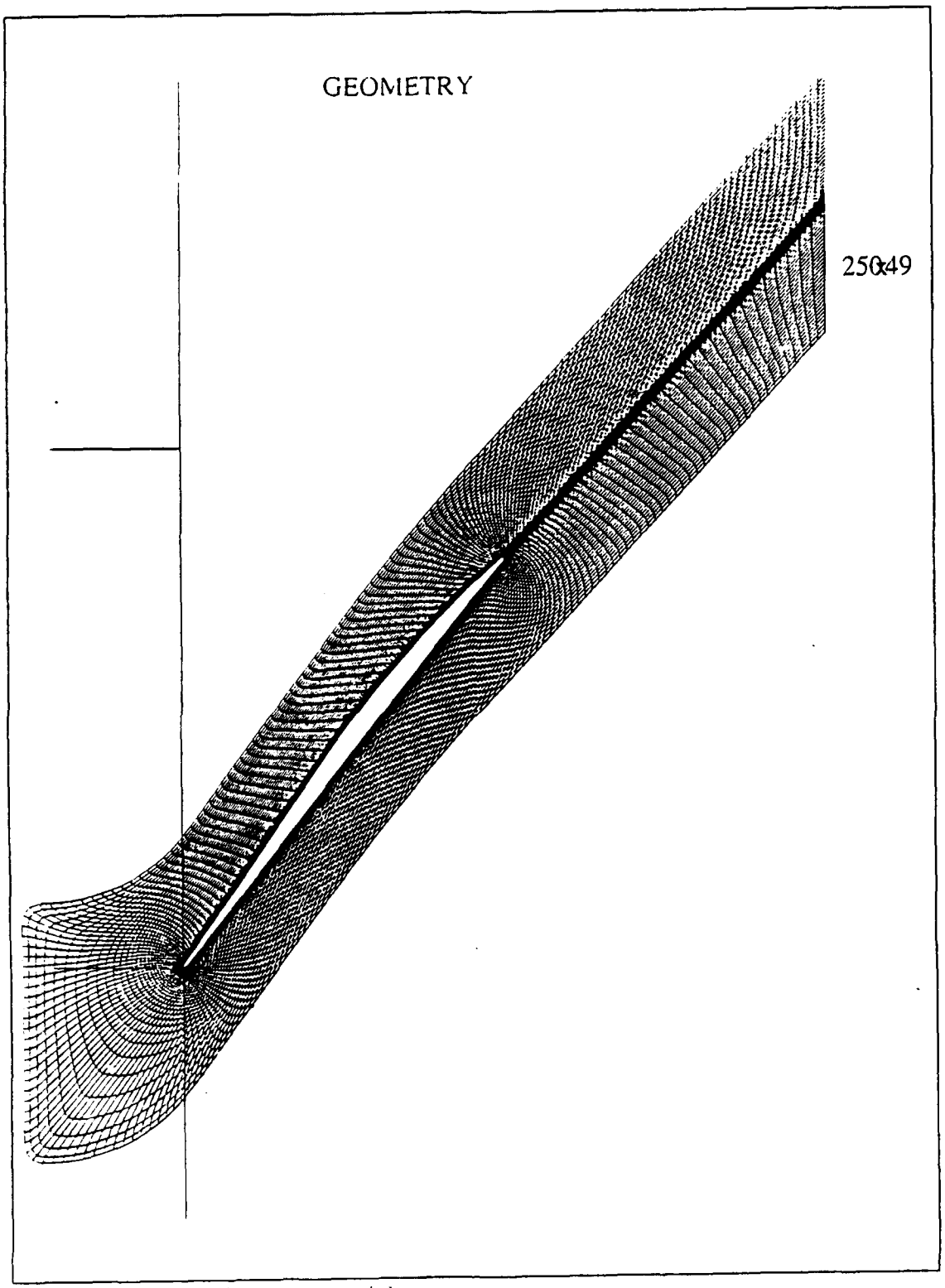

Figure 19. Viscous Grid

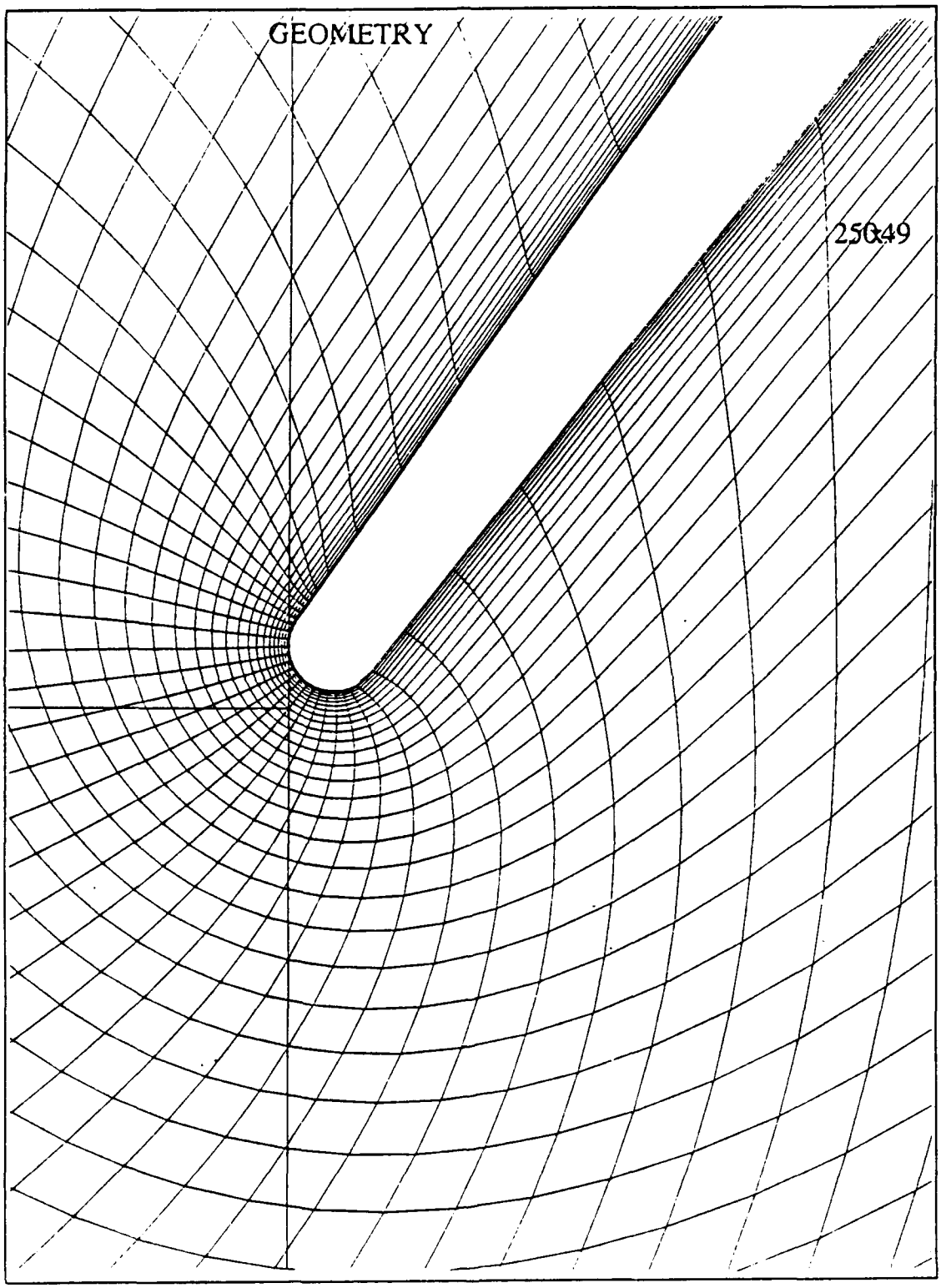

Figure 20. Viscous Grid Leading Edge

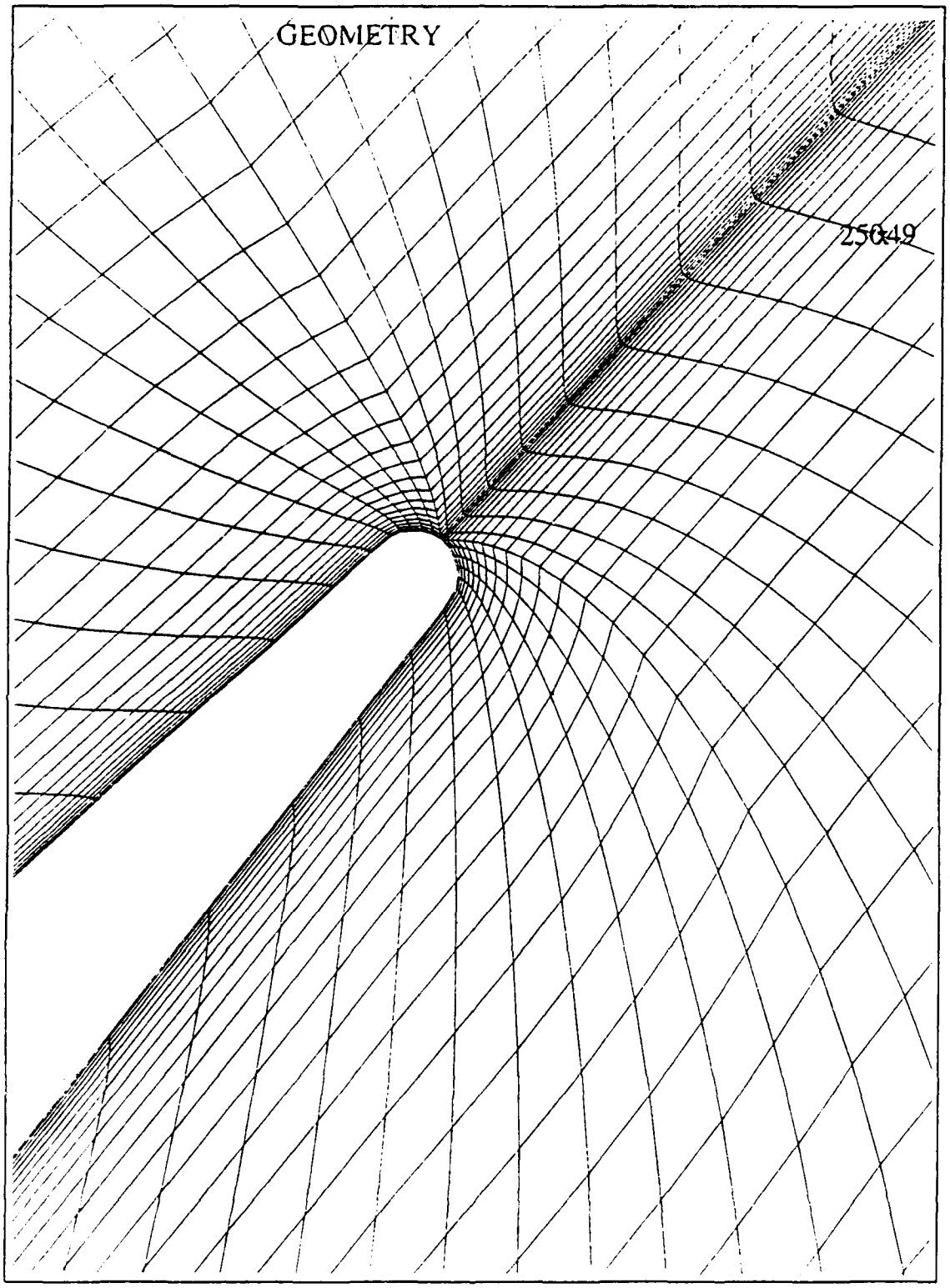

Figure 21. Viscous Grid Trailing Edge

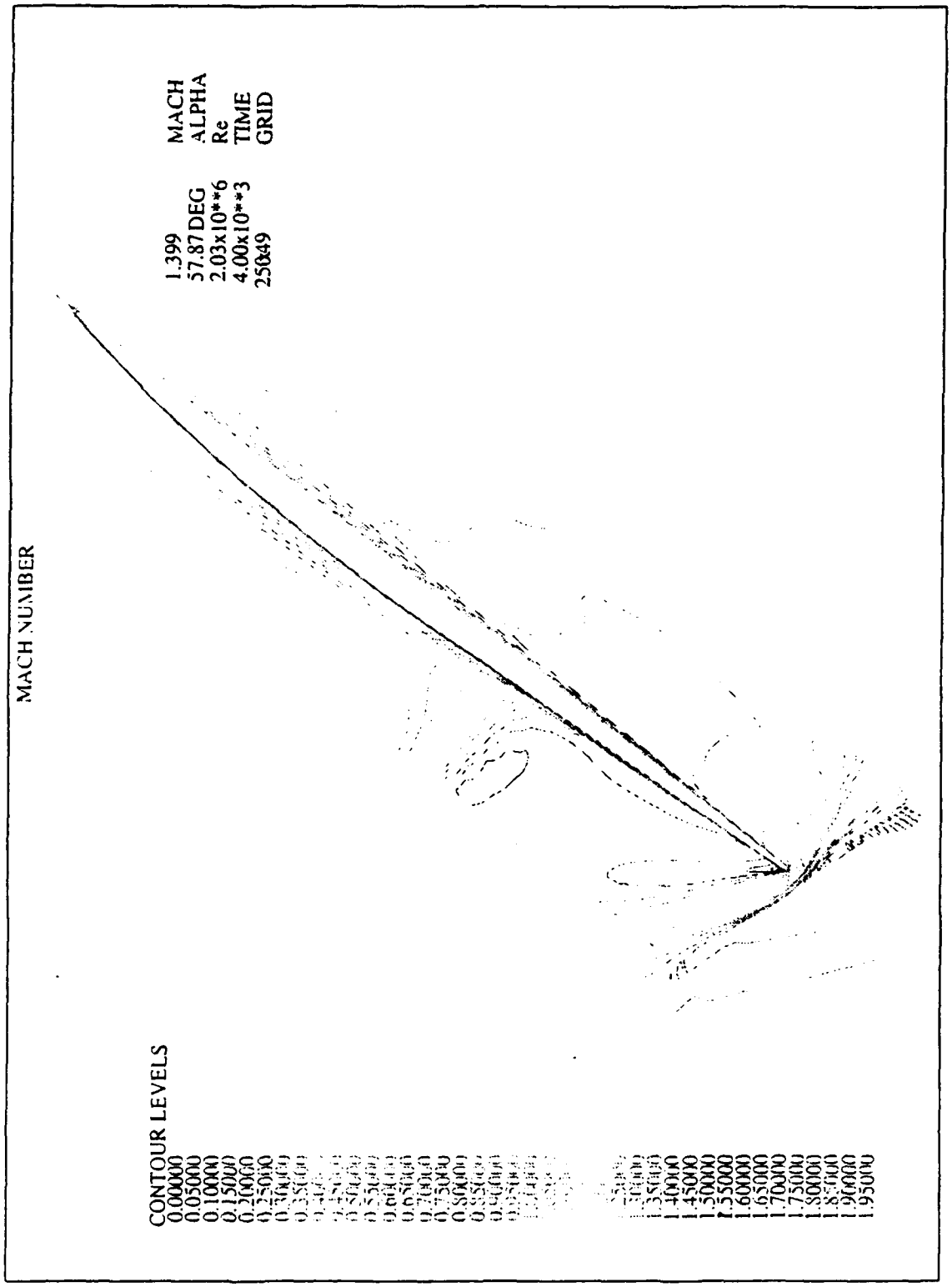

Figure 22. Viscous Solution Mach Number Profile

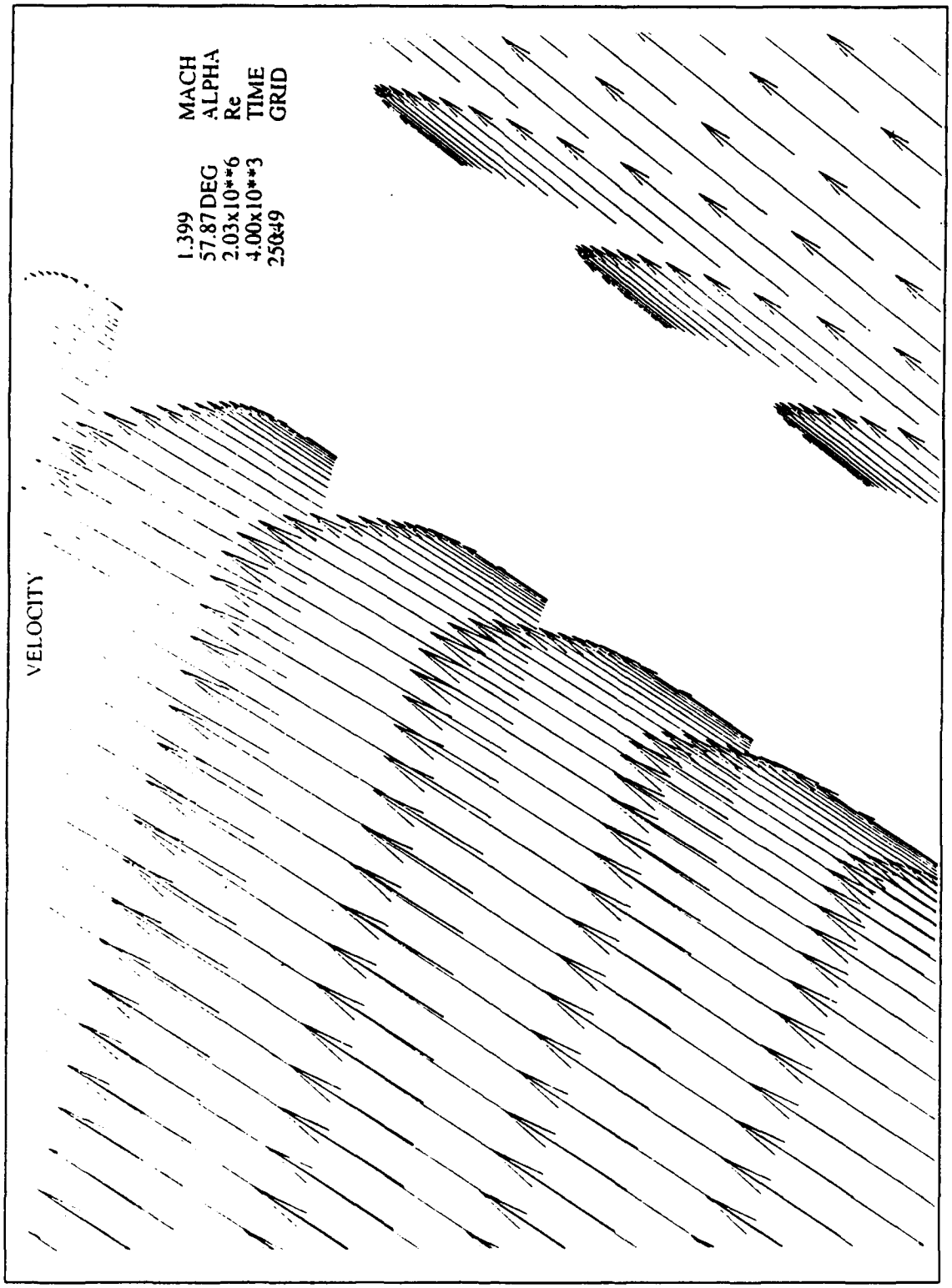

Figure 23. Viscous Solution Velocity Profile

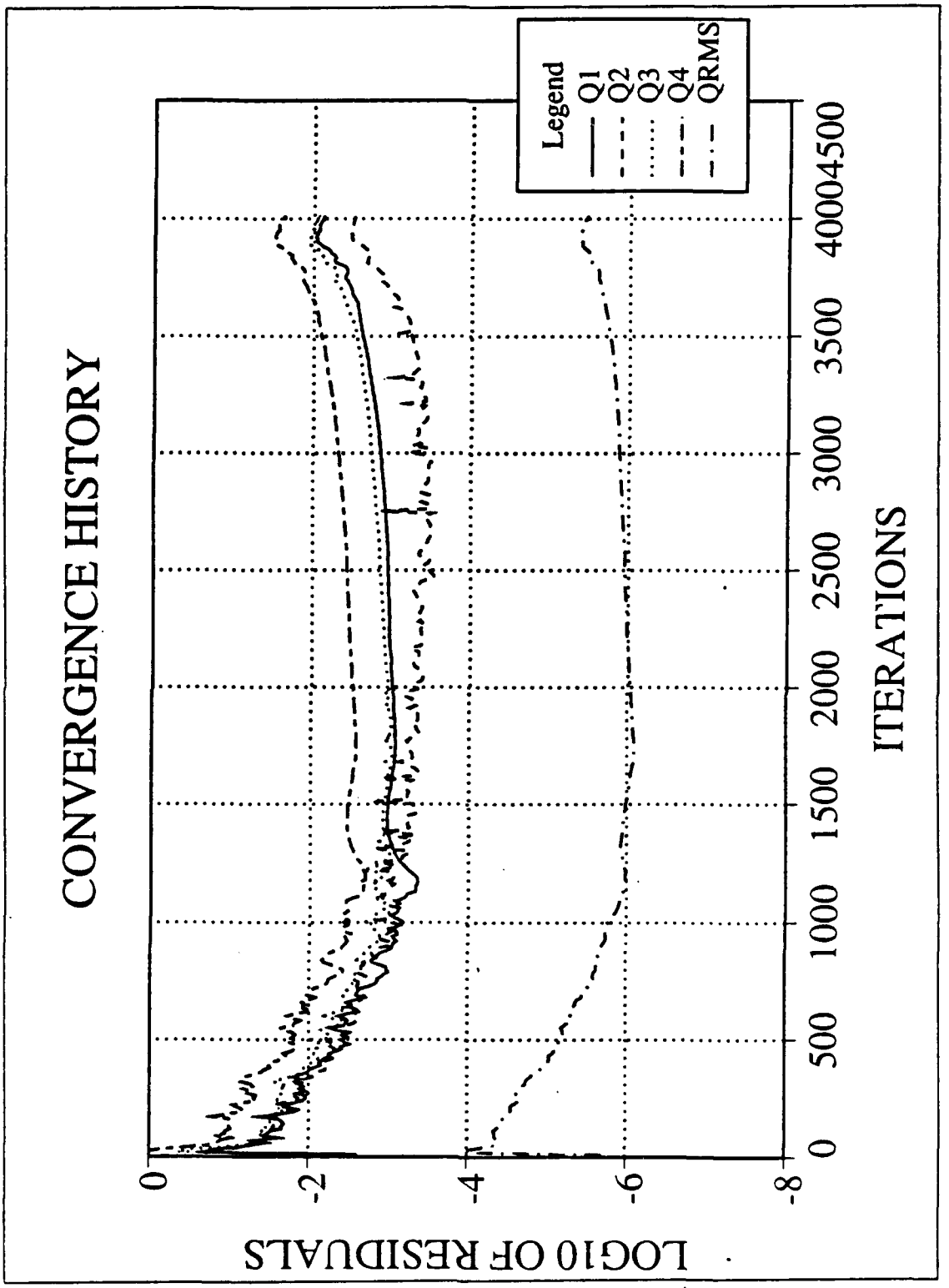

Figure 24. Viscous Solution Convergence History

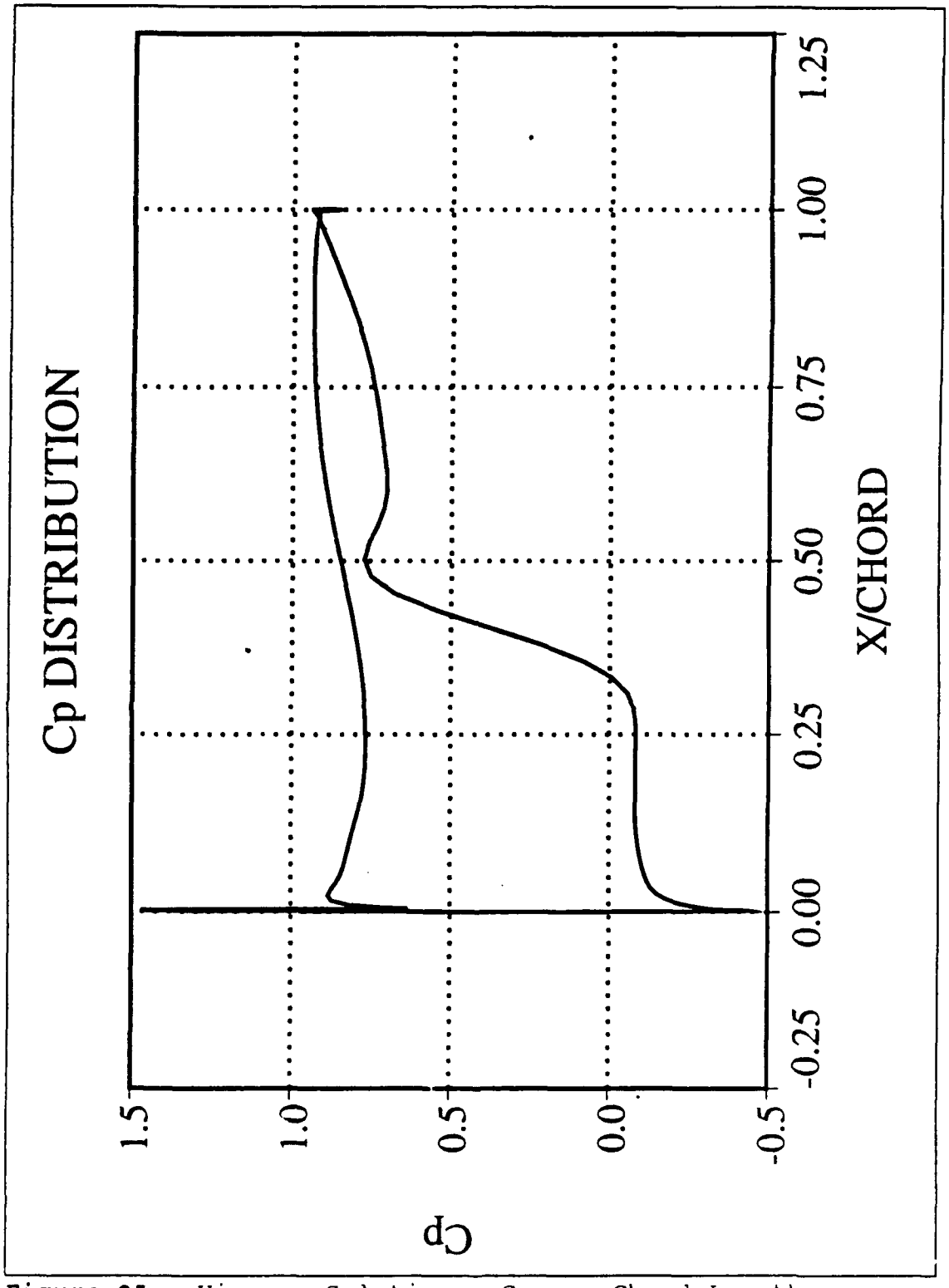

Figure 25. Viscous Solution: Cp vs. Chord Length

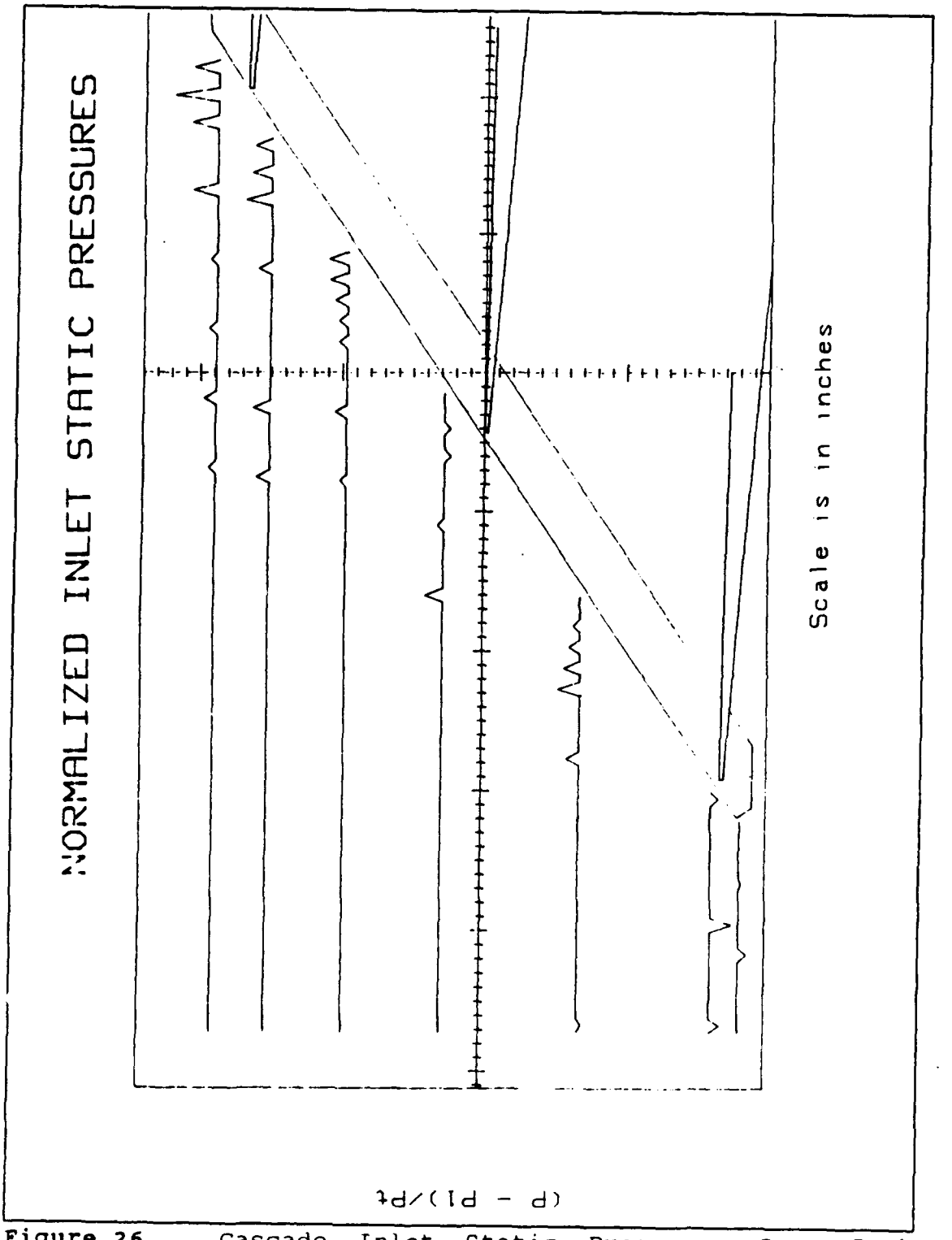

Figure 26. Cascade Inlet Static Pressures--Open Back Pressure Valve

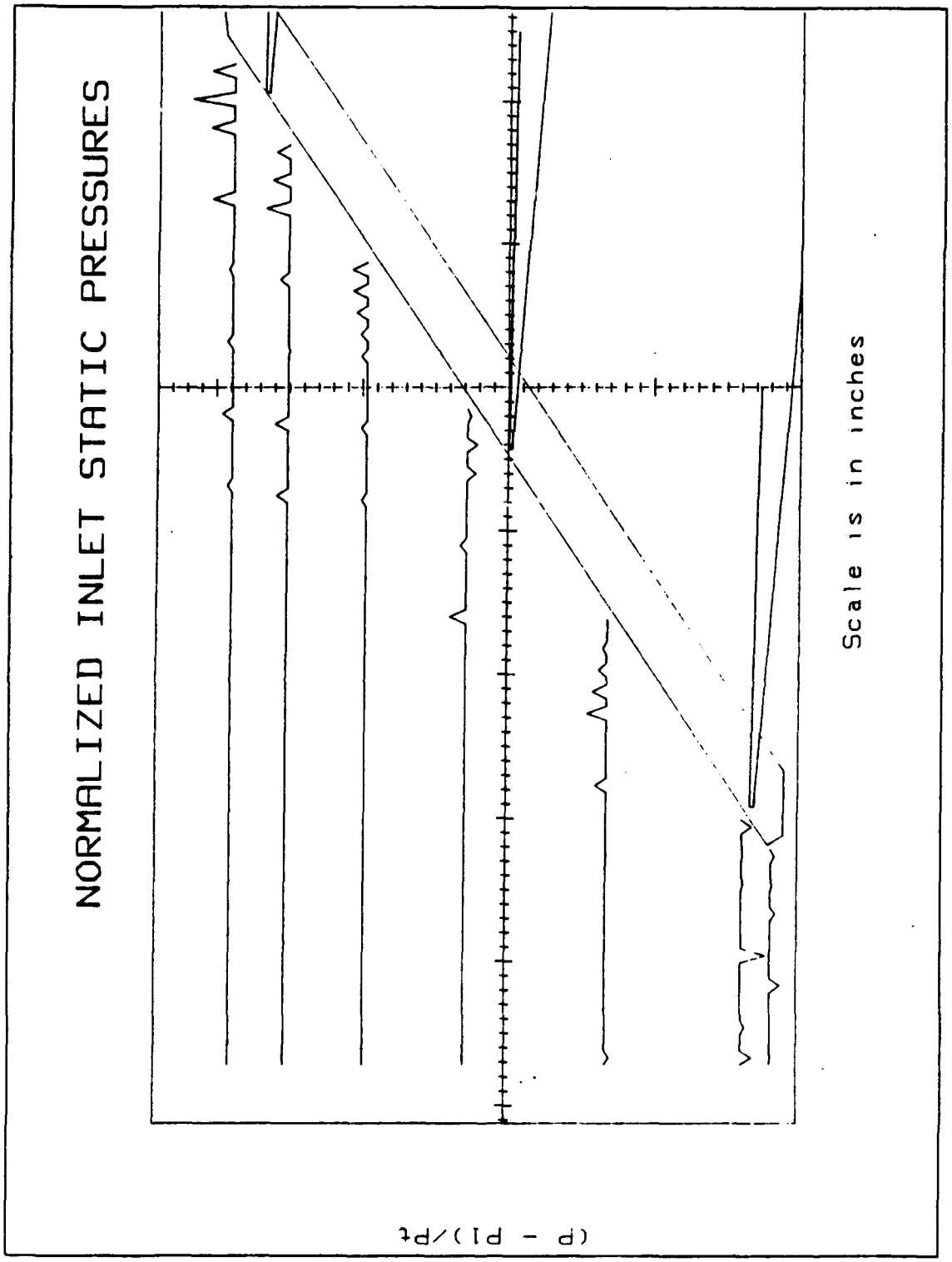

Figure 27. Cascade Inlet Static Pressures--Lower Shock in Position

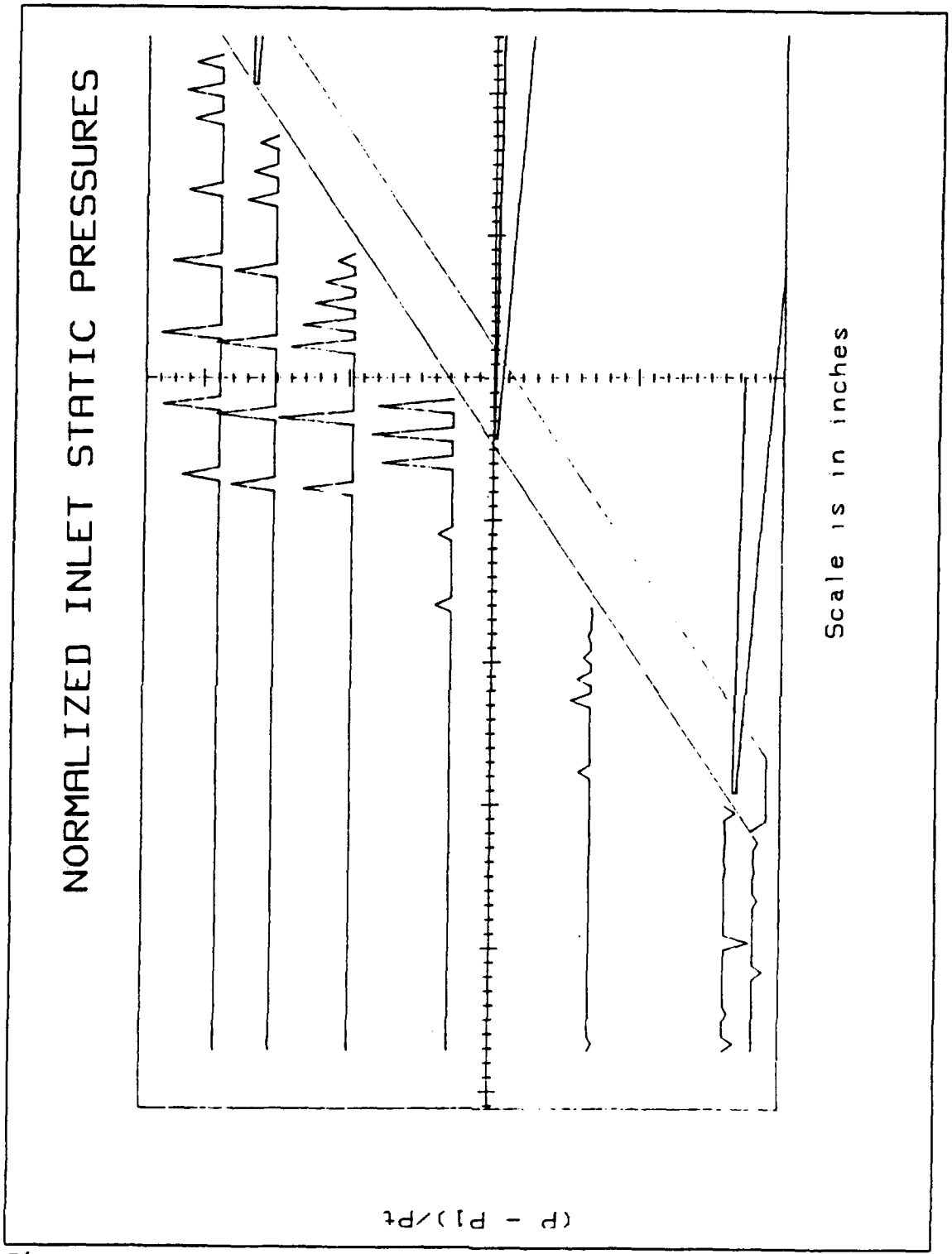

Figure 28. Cascade Inlet Static Pressures--Upper Shock in Position

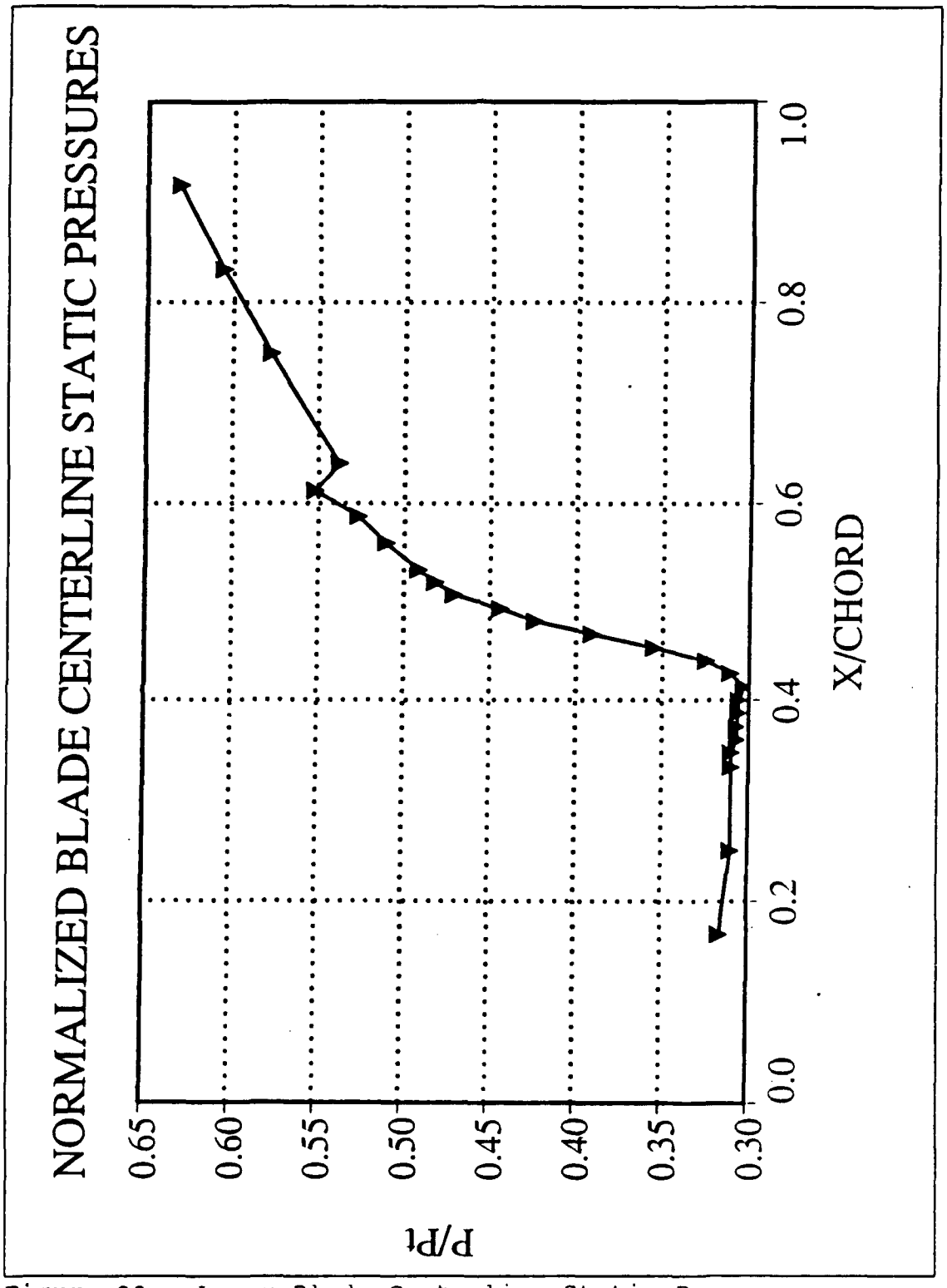

Figure 29. Lower Blade Centerline Static Pressures

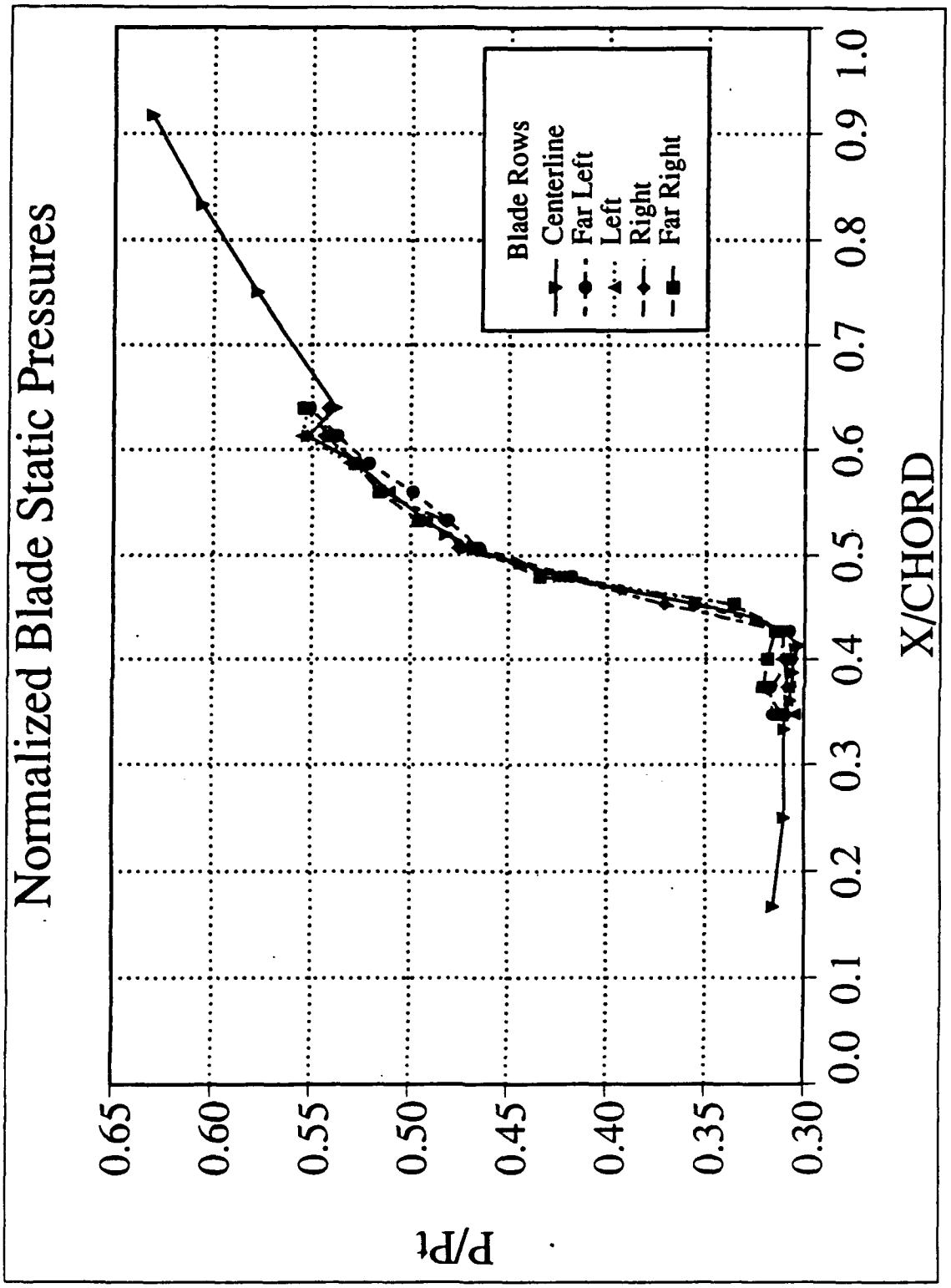

Figure 30. Lower Blade Static Pressures (All Rows)

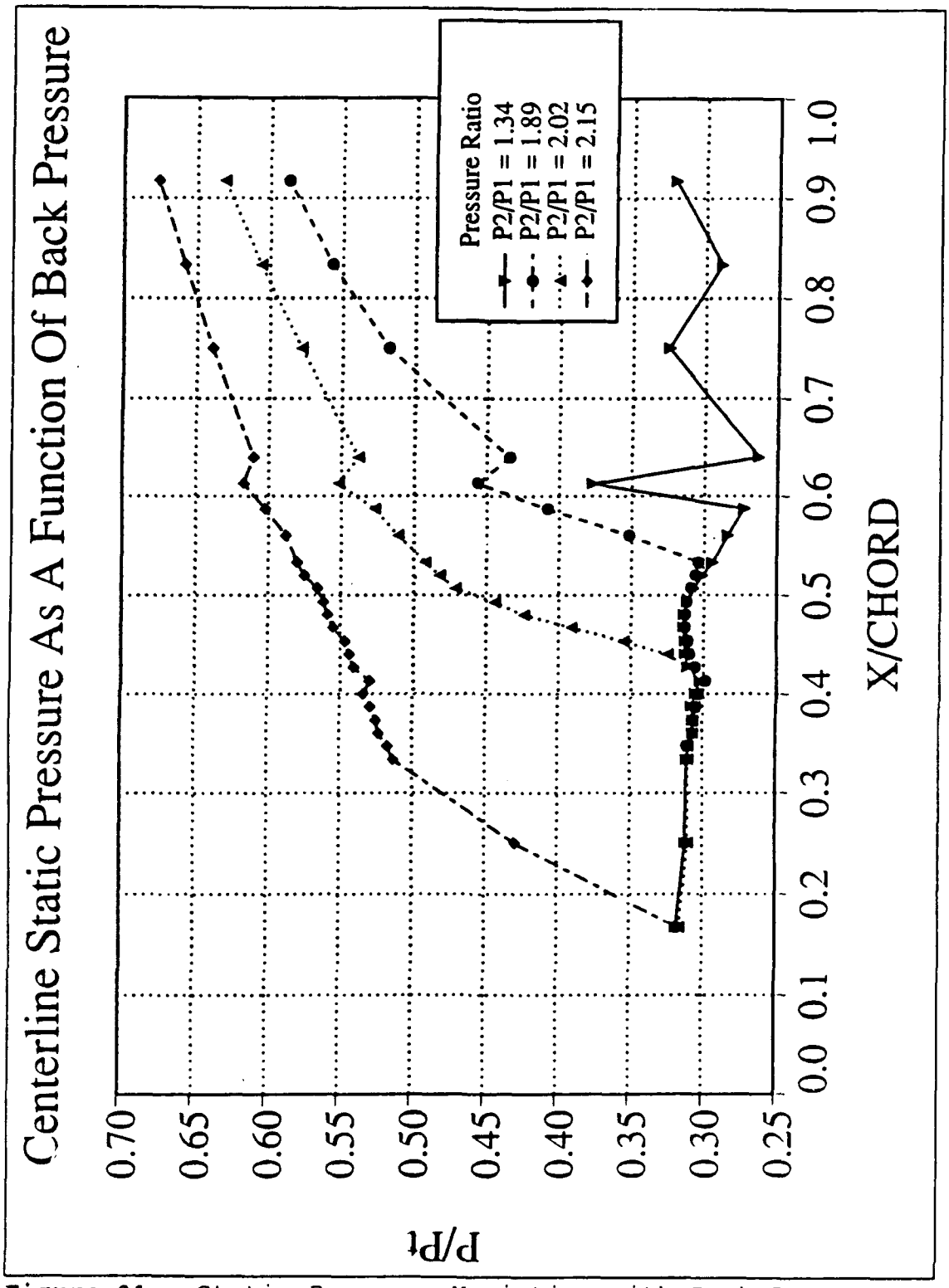

Figure 31. Static Pressure Variation with Back Pressure

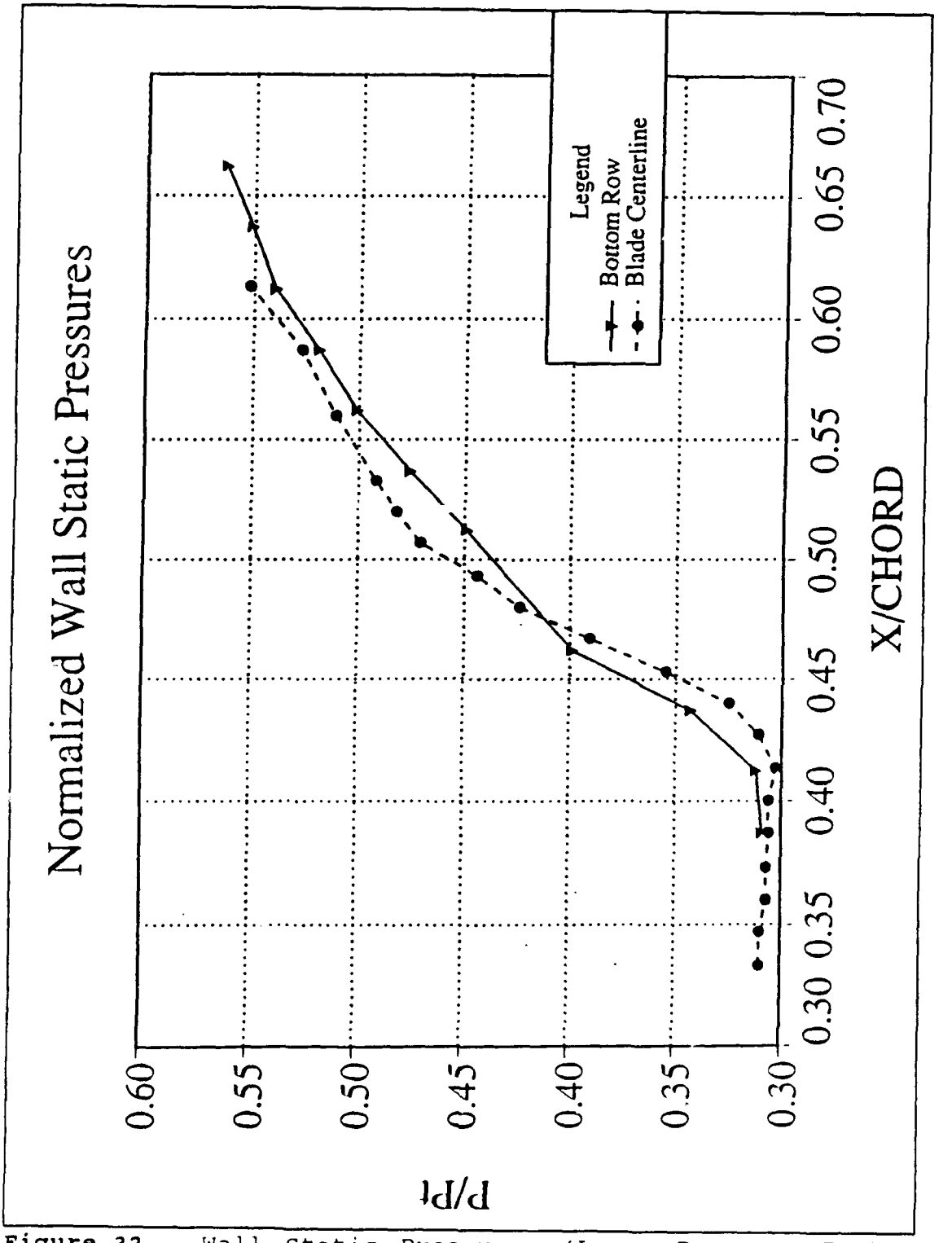

Figure 32. Wall Static Pressures (Lower Passage, Bottom Row)

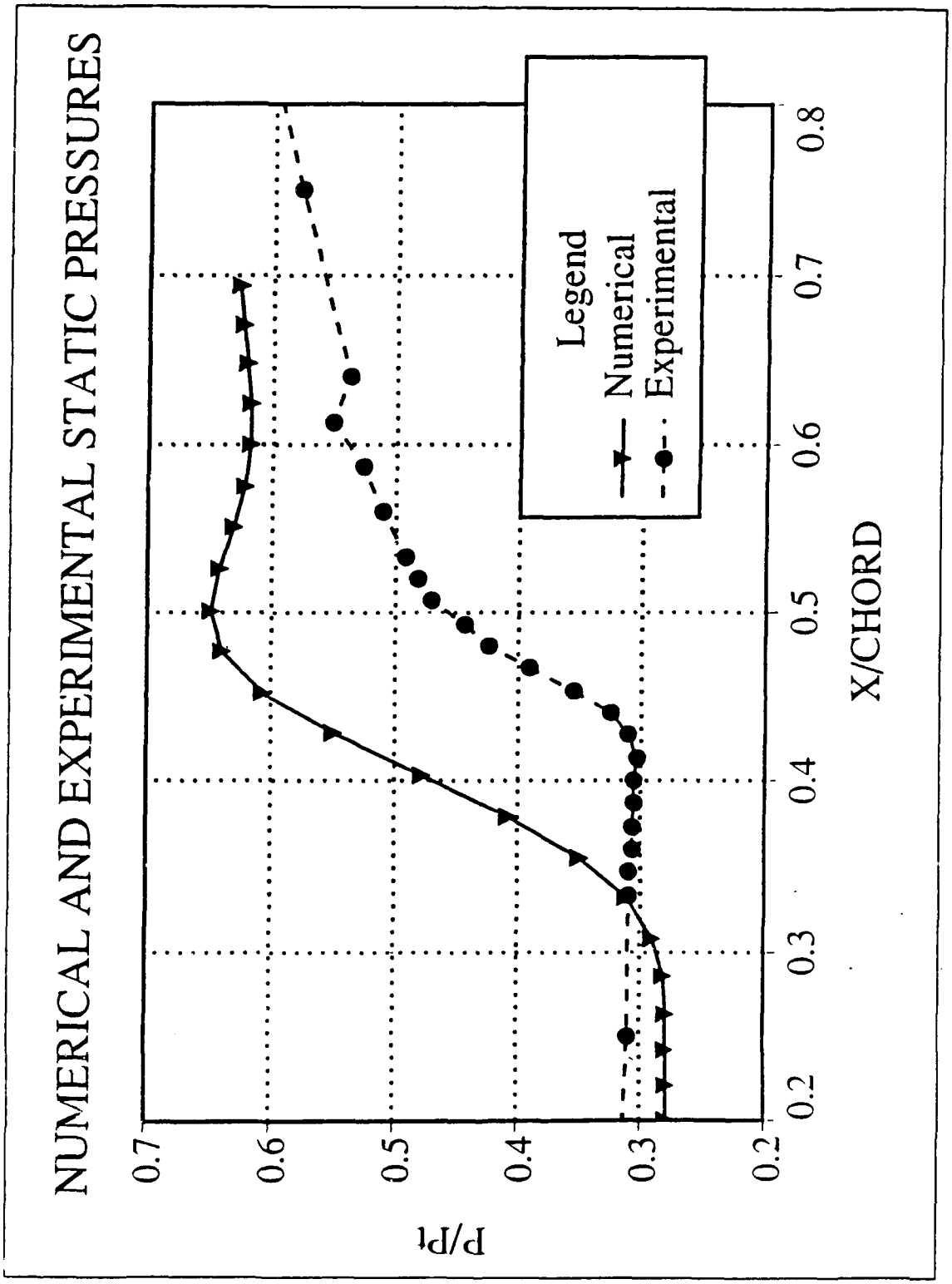

Figure 33. Comparison of Blade Centerline Results

APPENDIX A

MACHINE DRAWINGS OF THE BACK PRESSURE VALVE

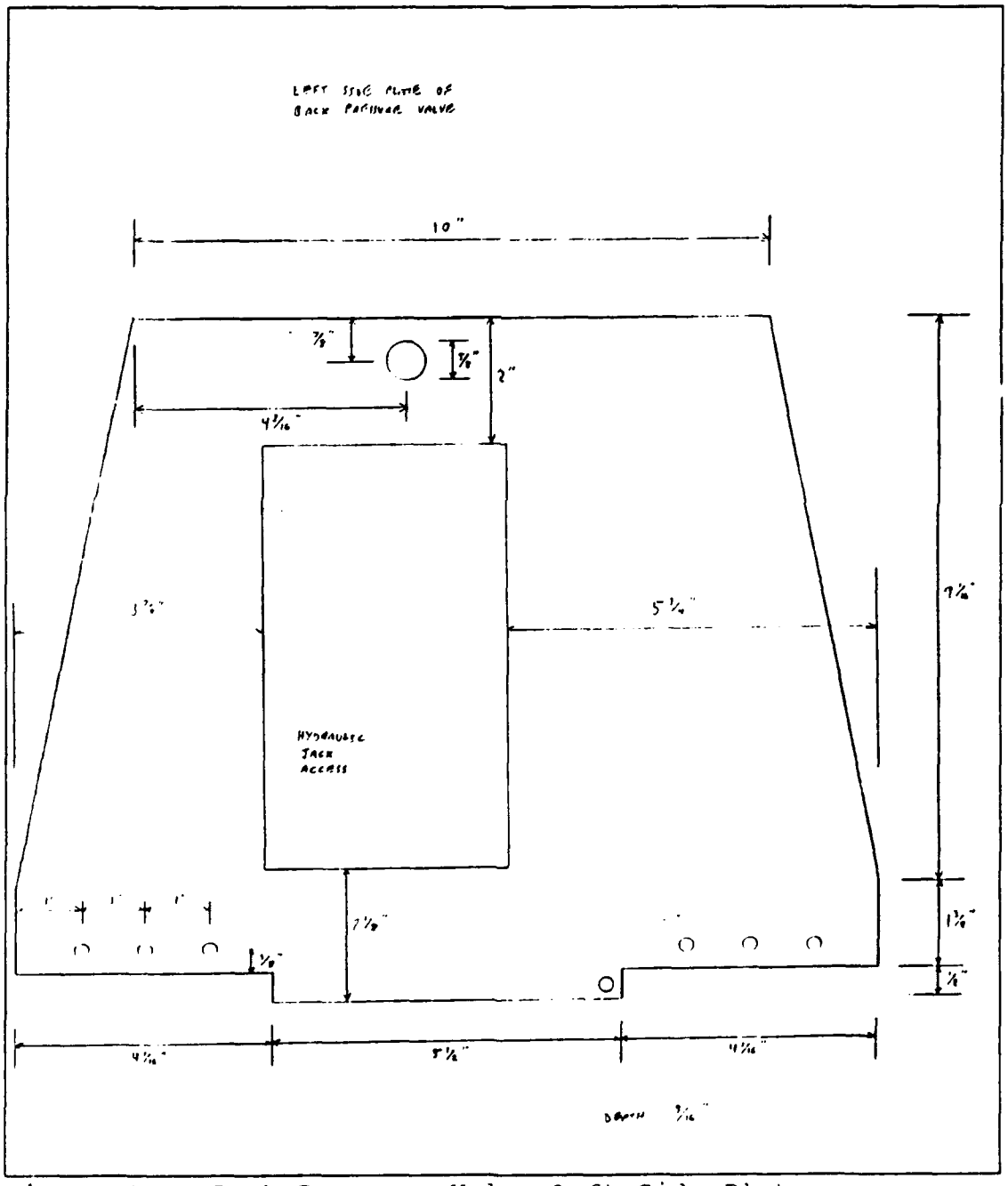

Figure A1. Back Pressure Valve Left Side Plate

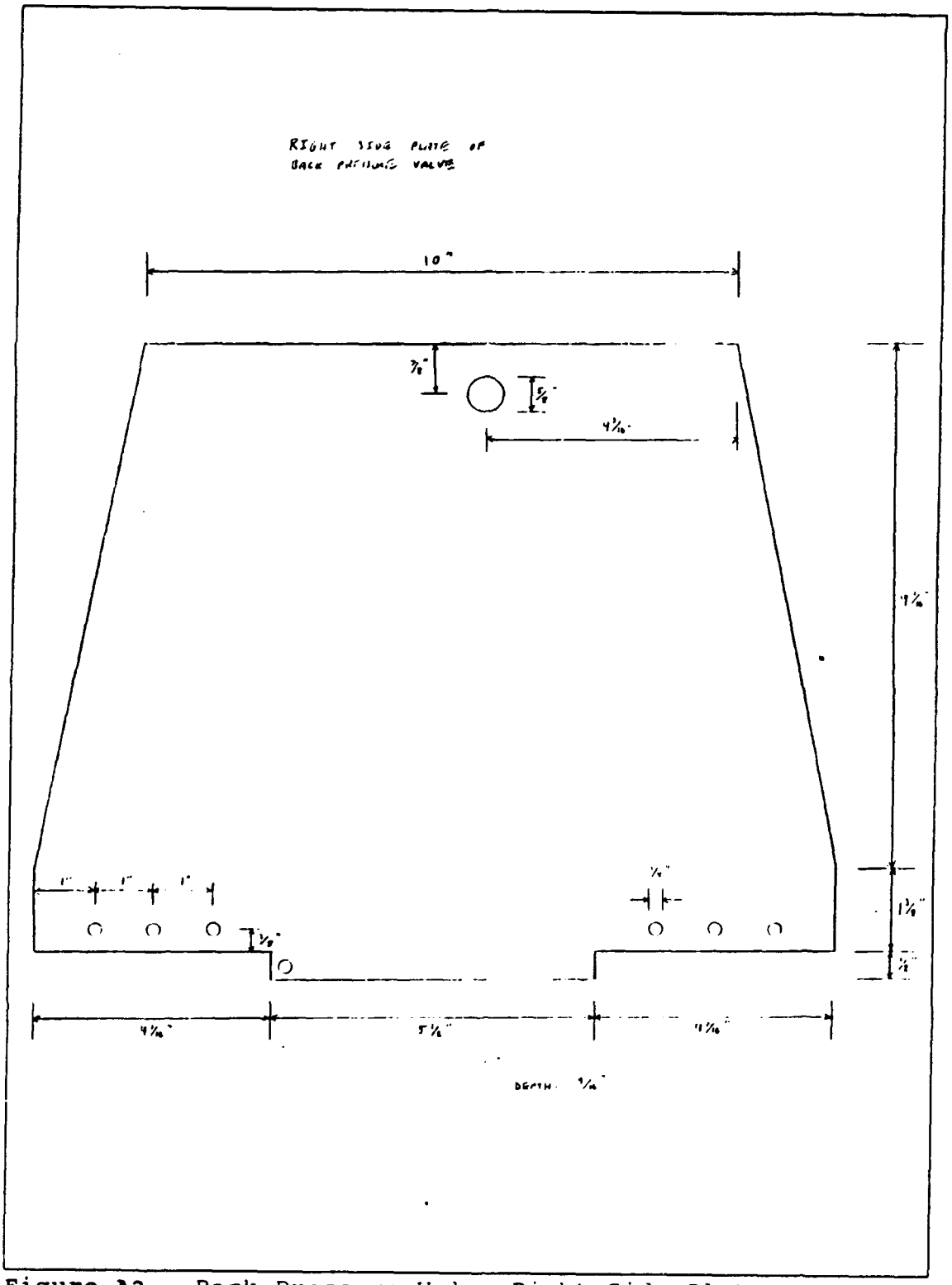

Figure A2. Back Pressure Valve Right Side Plate

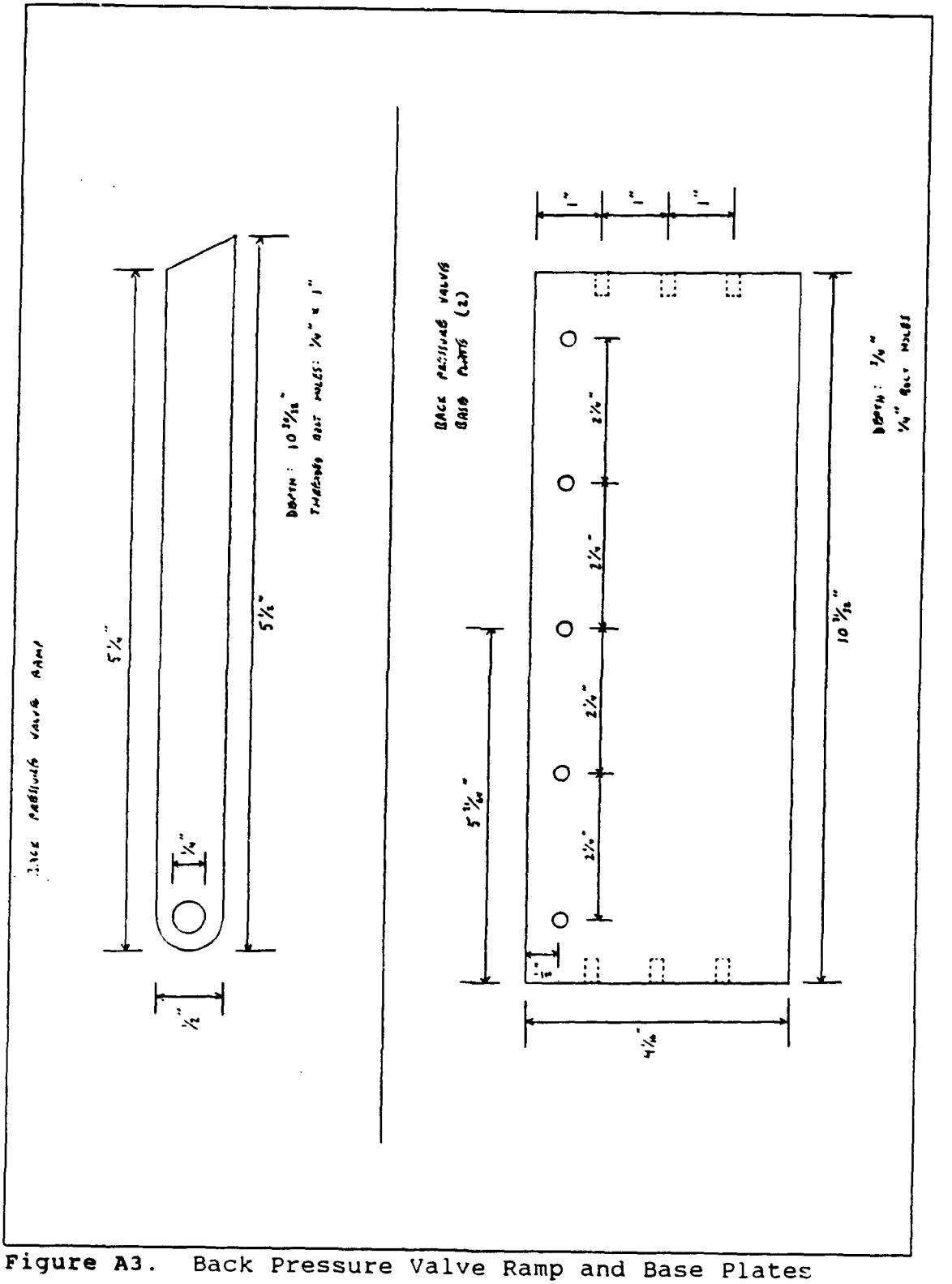

Figure A3. Back Pressure Valve Ramp and Base Plates

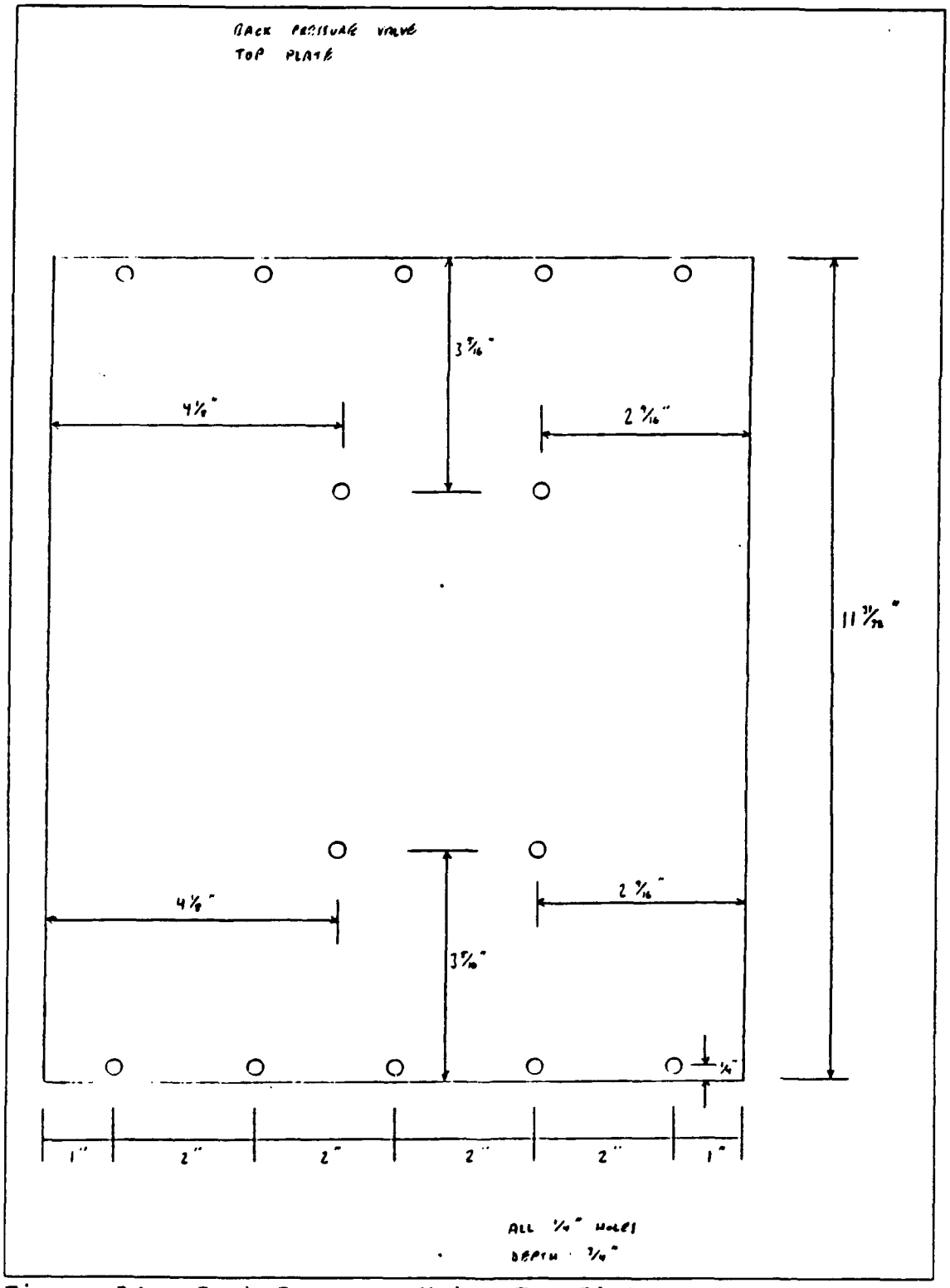

Figure A4. Back Pressure Valve Top Plate

APPENDIX B

MACHINE DRAWINGS OF TEST SECTION INSTRUMENTATION

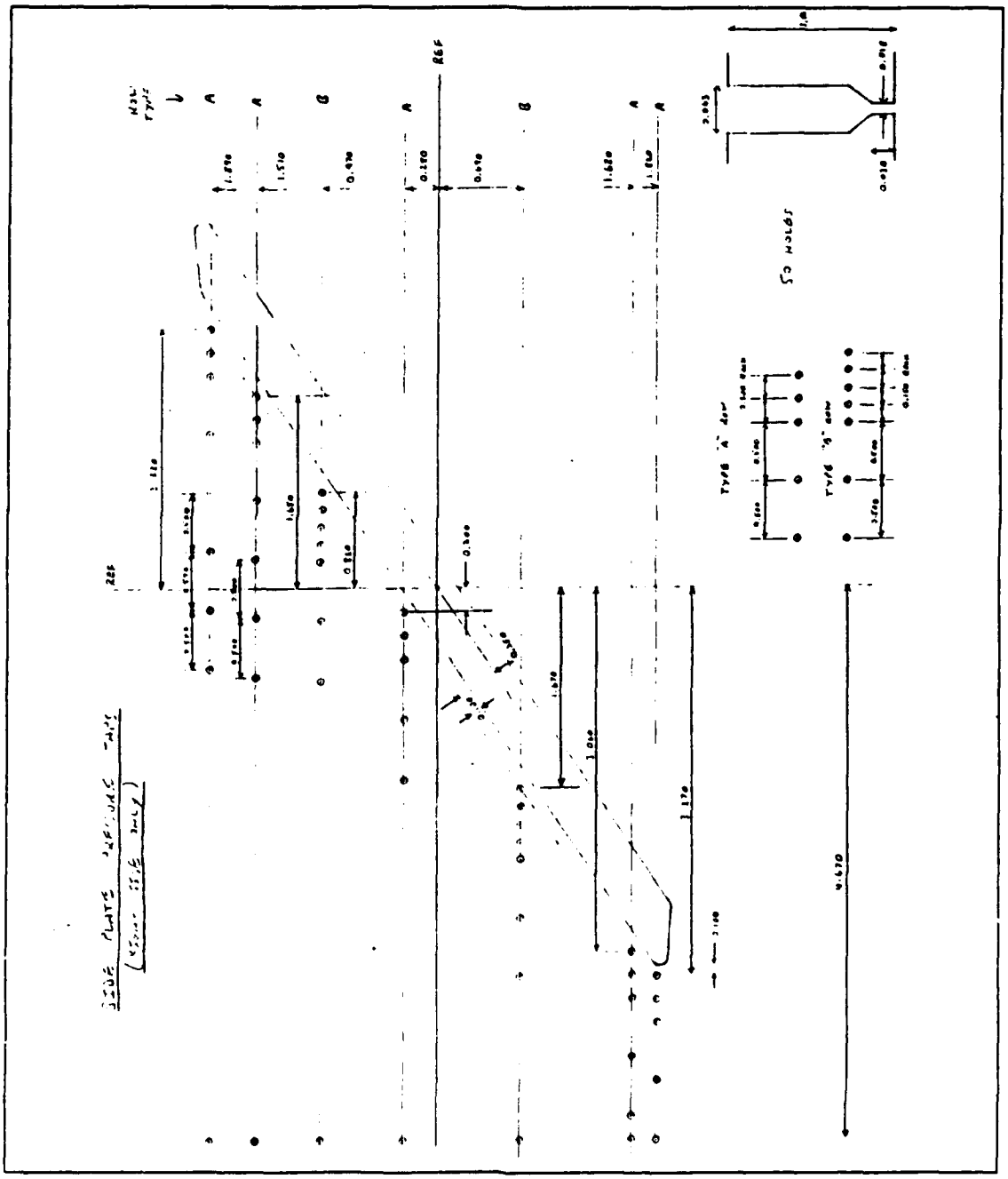

Figure B1. Right Side Plate Instrumentation

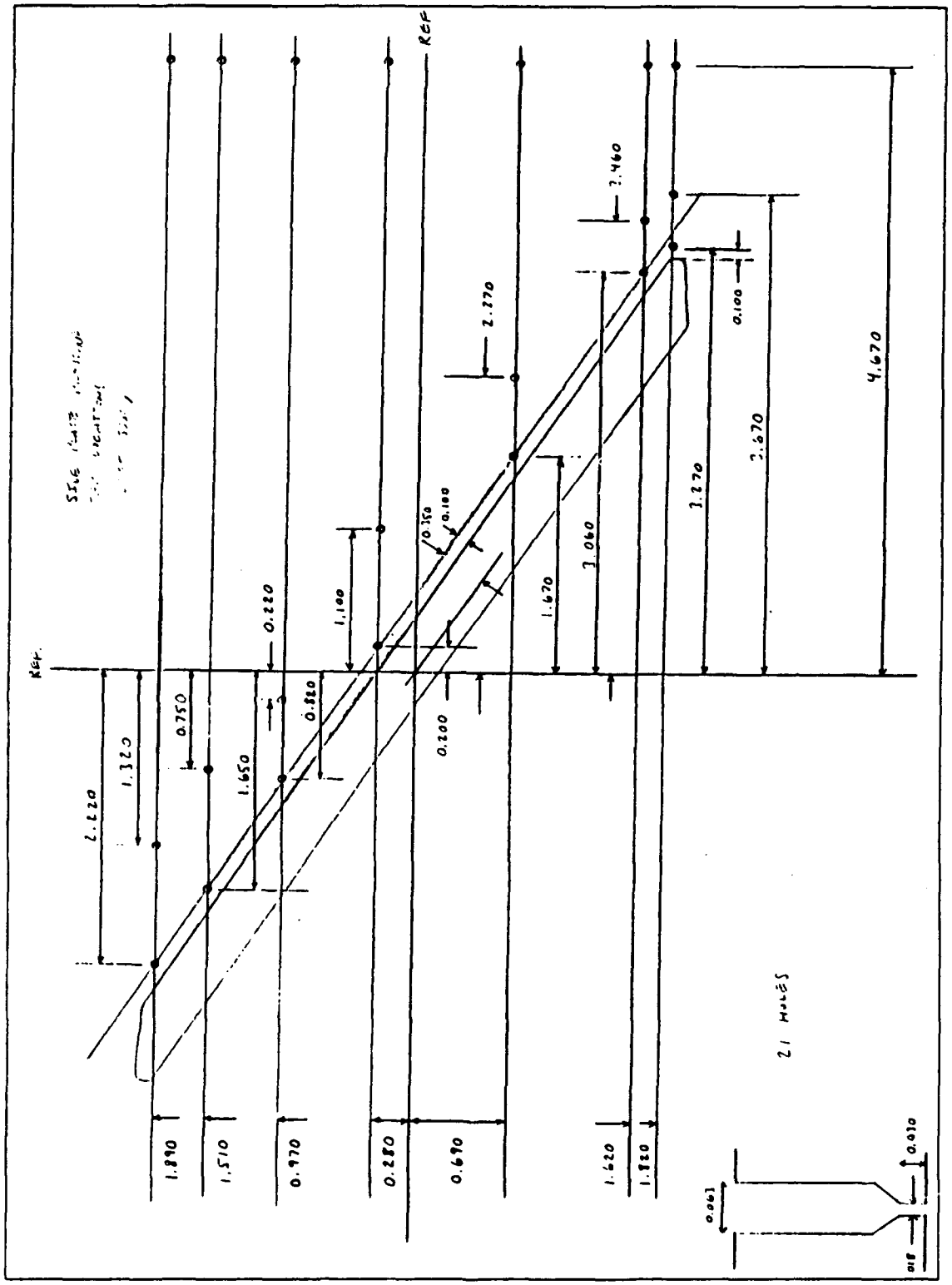

Figure B2. Left Side Plate Instrumentation

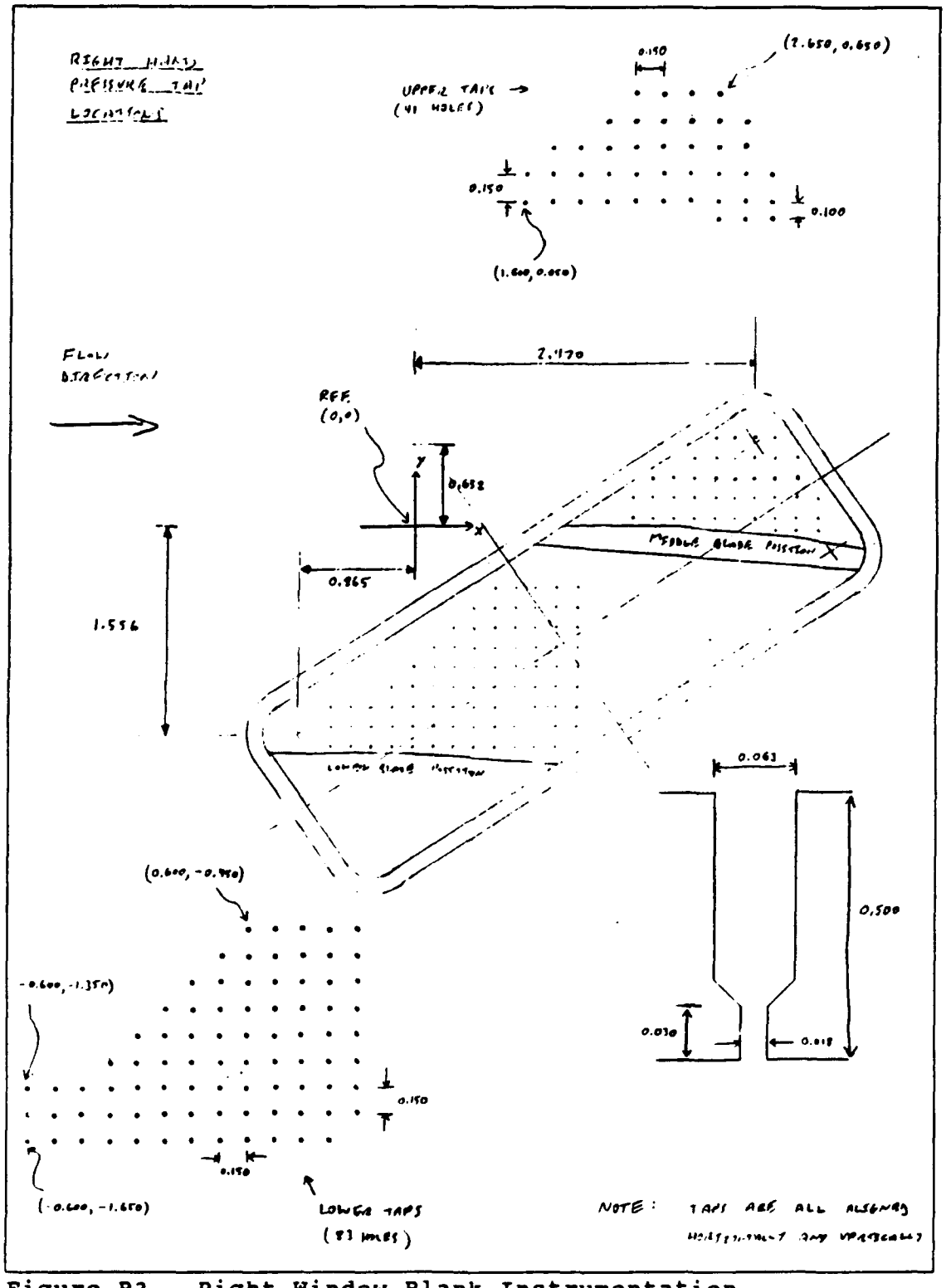

Figure B3. Right Window Blank Instrumentation

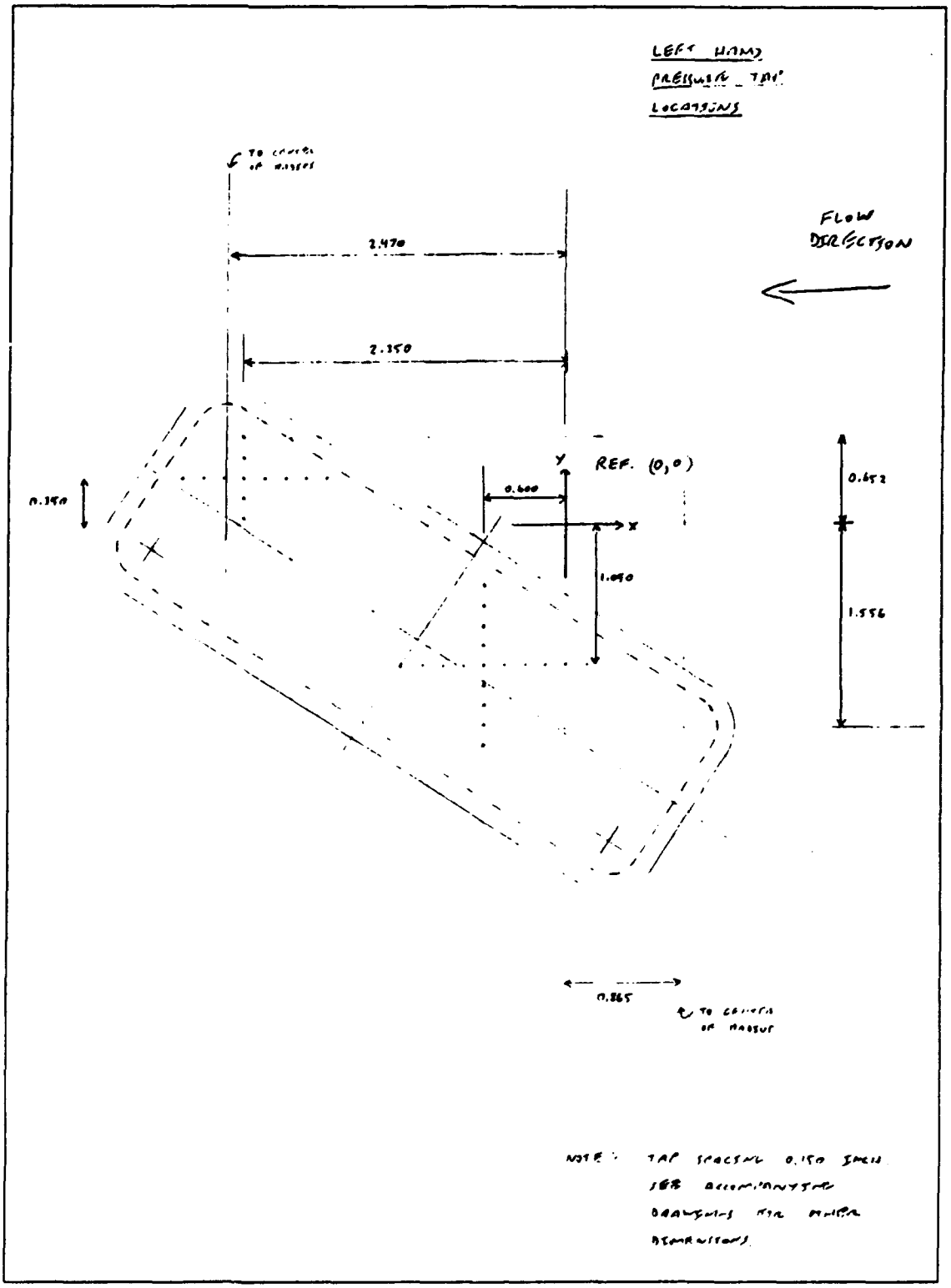

Figure B4. Left Window Blank Instrumentation

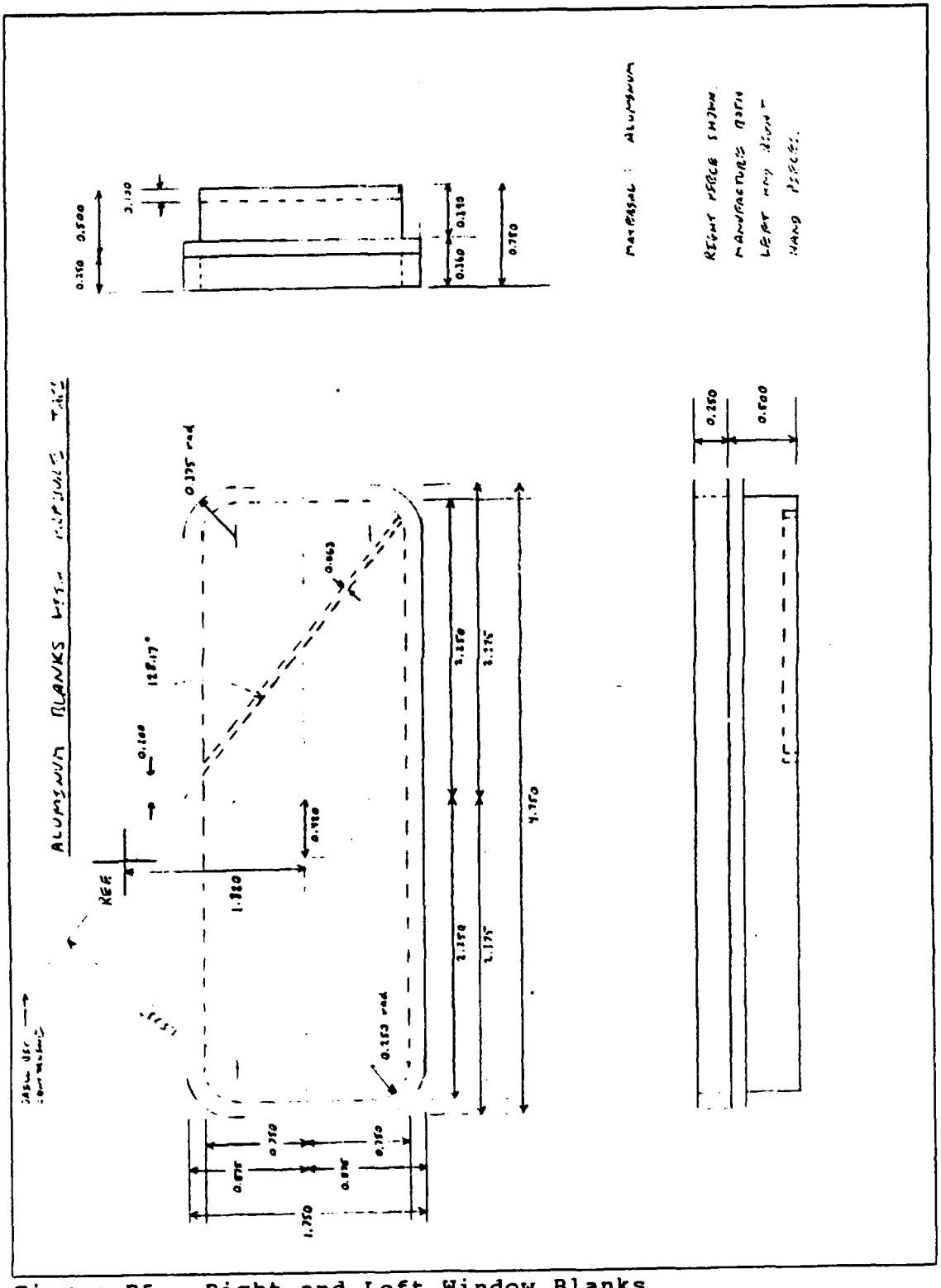

Figure B5. Right and Left Window Blanks

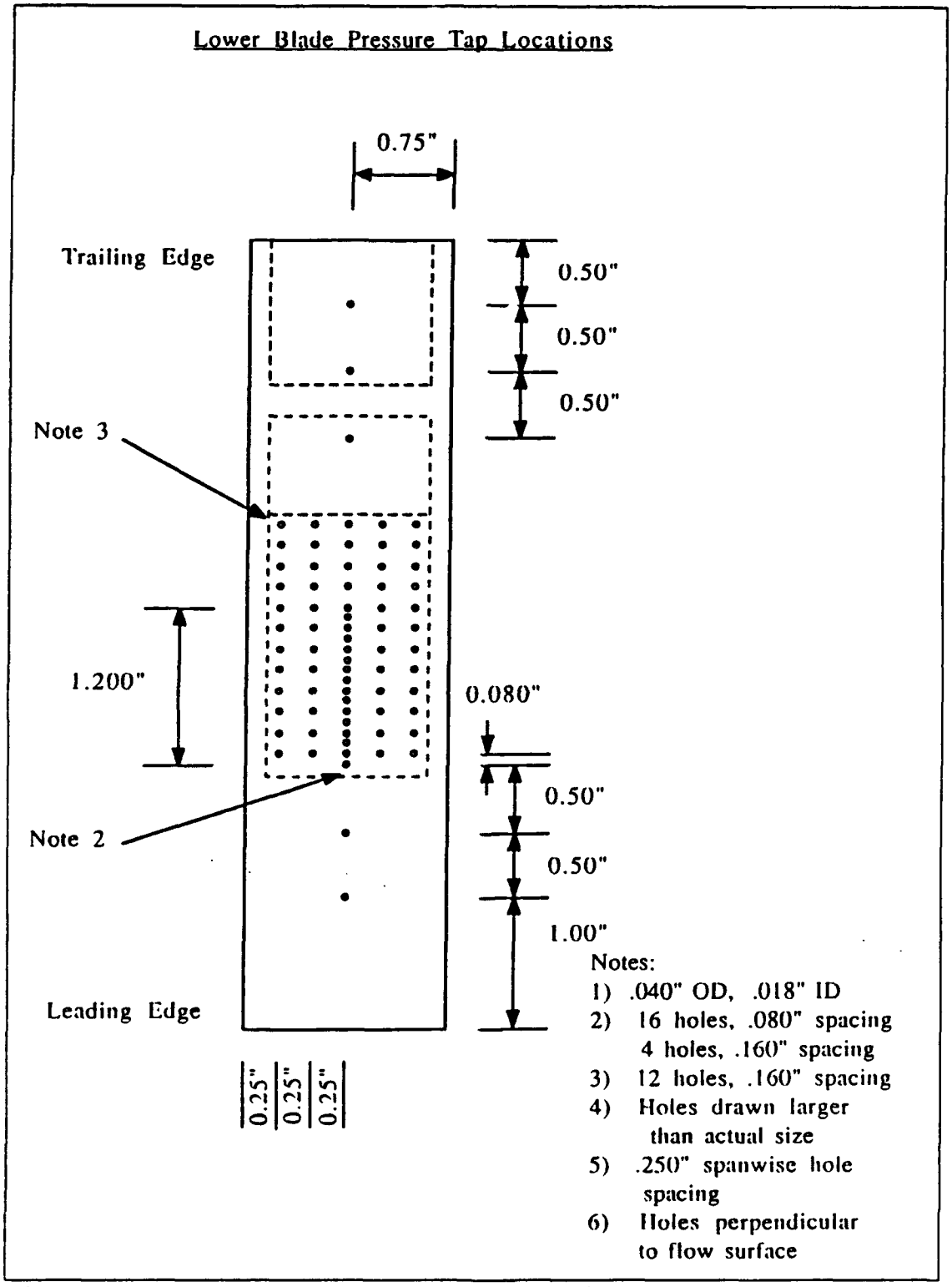

Figure B6. Lower Blade Instrumentation (Top View)

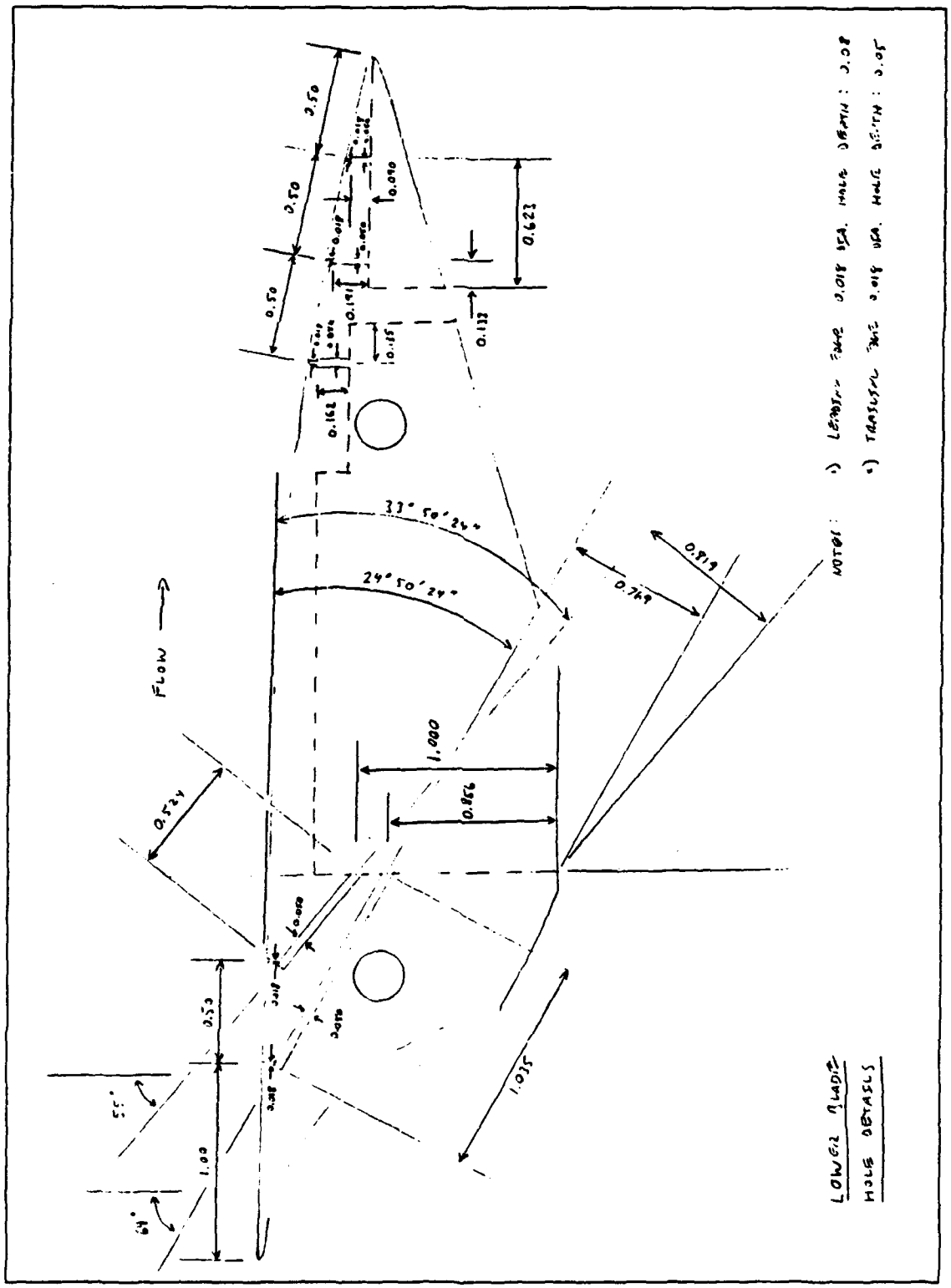

Figure B7. Lower Blade Instrumentation (Side View)

APPENDIX C

DATA ACQUISITION PROGRAMS

```
10    !Title:     CALIBRATE
20    !Author:    LT Bill Golden
30    !Date:      1991
40    !Updated:   21 February 1992
50    !Purpose:   Used to set-up Scanivalve controller by adjusting bridge
60    !           for zero and max values, or to sample data from a
70    !           particular Scanivalve and port.
80    !
90    !           Configured for two scanners.
100   !
110   !Device addresses:
120   Dvm1=720            !HP3455A      Scanivalves 1-5 on this set
130   Scanner1=701        !HP3495A
140   Controller1=706     !HG-78K
150   !
160   Dvm2=722                          !Scanivalves 6-10 on this set
170   Scanner2=709
180   Controller2=707
190   !
200   !Initial devices:
210   Dvm=Dvm1
220   Scanner=Scanner1
230   Controller=Controller1
240   ASSIGN @Listeners TO Dvm1,Dvm2,Scanner1,Scanner2,Controller1,Controller2
250   !
```

Figure C1. CALIBRATE Program

```
260   !
270   !Begin Main Program
280   CLEAR @Listeners      !Initialize all instruments on bus
290   OUTPUT Dvm1;"F1R7M3A0H0T1"
300   OUTPUT Dvm2;"F1R7M3A0H0T1"
310   CLEAR SCREEN
320   PRINT "        Scanivalve CALIBRATION Program"
330   PRINT
340   PRINT
350   PRINT "Directions:"
360   PRINT
370   PRINT "1) Type in Scanivalve ID (1-10) of transducer to be examined."
380   PRINT
390   PRINT "2) Step and Reset the Scanivalves using manual buttons on"
400   PRINT "   the HG-78K Controllers."
410   PRINT
420   PRINT "3) An out of range value will exit the program."
430   !
440 A:INPUT "Input desired Scanivalve to be calibrated(1-10):",Id
450   IF Id<1 OR Id>10 THEN Quit                !Exit trap
460   GOSUB Switch
470   OUTPUT Scanner USING "DDD";V+9            !Scanivalve output on Dvm
480   GOTO A
490   !***********END OF MAIN PROGRAM****************************
500   !
510   !*****SUBROUTINE:  DETERMINE WHICH SET OF DEVICES TO USE*****
520 Switch:!
530   IF Id<6 THEN
540     Scanner=Scanner1            !For Scanivalves 1 through 5
550     Controller=Controller1
560     Dvm=Dvm1
570     V=Id
580   ELSE
590     Scanner=Scanner2            !For Scanivalves 6 through 10
600     Controller=Controller2
610     Dvm=Dvm2
620     V=Id-5                      !S/V must be 1-5 for controller
630   END IF
640   RETURN
650   !
660   !***********END OF SUBROUTINES****************************
670 Quit:CLEAR Scanner
680   CLEAR Dvm
690   CLEAR SCREEN
700   LOAD "ACQ_MENU",10        !Return to menu selection screen.
710   END
```

Figure C1. (Cont.) CALIBRATE Program

```
10    !Title:     SCAN
20    !Author:    LT Bill Golden
30    !Date:      November 1991
40    !Updated:   28 February 1992
50    !Purpose:   Reads voltages from designated scanivalves, prints psi gauge
60    !           data to CRT, and stores raw data in a 10 x 48 element array
70    !           within an ASCII file.  A hard copy of data is an option.
80    !           Currently 7 Scanivalves and 9 transducers are in operation.
90    !           Configured for two scanners.
100   !
110   !
120   !Variable declaration:
130   INTEGER Printer,Scanner,Scanner1,Scanner2,Controller,Controller1
140   INTEGER Controller2,Dvm,Dvm1,Dvm2,First_sv,Last_sv,First_port,Last_port
150   INTEGER Port_reqd,Port_read,Id,N,V
160   REAL P,Pt,P1,P2,Atm_mmhg,Atm_inhg,Atm_psia,Pratio,Total
170   !
180   !Devices addresses:
190   Printer=702       !HP ThinkJet Printer
200   !
210   !Device Set #1 (For Scanivalves 1 through 5):
220   Scanner1=701      !HP3495A Scanner
230   Controller1=706   !HG-78K Scanivalve Controller
240   Dvm1=720          !HP3455A Digital Voltmeter
250   !
260   !Device Set #2 (For Scanivalves 6 through 10):
270   Scanner2=709
280   Controller2=707
290   Dvm2=722
300   !
310   !Initial device address set up:
320   Scanner=Scanner1
330   Controller=Controller1
340   Dvm=Dvm1
350   ASSIGN @Instruments TO Dvm1,Dvm2,Scanner1,Scanner2,Controller1,Controller2
360   ASSIGN @Dvms TO Dvm1,Dvm2
370   ASSIGN @Scanners TO Scanner1,Scanner2
380   ASSIGN @Controllers TO Controller1,Controller2
390   !
400   !Arrays
410   DIM Press(1:10,1:48)    !Scanivalve Raw Pressure Data
420   DIM Pg(1:10,1:48)       !Gauge Pressures (Press*1000.)
430   !
440   !Default values for variables:
450   First_sv=1                !Read first 9 Scanivalves
460   Last_sv=9                 !Pt transducer (10) not yet installed
470   First_port=1              !Read all 48 ports
480   Last_port=48
490   Atm_psia=14.7             !Generic atmospheric pressure
500   MAT Press= (0.)           !Zero out arrays
510   MAT Pg= (0.)
520   P1=0.                     !Individual measurements
530   P2=0.
540   Pt=0.
550   Pratio=0.                 !P2 divided by P1
560   Filename$="SCAN_OUTPUT"   !Raw data output file
570   !
580   !
```

Figure C2. SCAN Program

```
600   !Create Hot Keys and Initial Screen Display
610   CLEAR SCREEN
620   ON KEY 1 LABEL "Ambient Pressure" GOTO Ambient
630   ON KEY 2 LABEL "S/V ID  & Home  " GOTO Svid
640   ON KEY 3 LABEL "Ports   To Read " GOTO Ports
650   ON KEY 4 LABEL "Create  Filename" GOTO Name
660   ON KEY 5 LABEL "P2/P1   Ratio   " GOTO P2p1
670   ON KEY 6 LABEL "Take    Data    " GOTO Measure
680   ON KEY 7 LABEL "Hard    Copy    " GOTO Hardcopy
690   ON KEY 8 LABEL "Exit    Program " GOTO Done
700   !
710   PRINTER IS CRT
720   PRINT "   Transonic Cascade Data Acquisition Program"
730   PRINT
740   PRINT "                Select A Function"
750   PRINT
760   PRINT "(Initial selections should be made from left to right.)"
770   PRINT
780   PRINT
790   PRINT "               ***** WARNING *****"
800   PRINT "    The current directory must NOT include the "
810   PRINT "    Filename to which you plan on writing your"
820   PRINT "    data.  It is created in this program."
830   !
840   !
850   !*****Hot Key Routines*****
860 Hold:!Holding pen for when no action is selected
870   GOTO Hold
880   !
890   !
900 Ambient:!Manual input of atmospheric pressure from mm Hg gauge
910   CLEAR SCREEN
920   INPUT "Input Atmospheric Pressure in mm Hg:",Atm_mmhg
930   Atm_inhg=Atm_mmhg*.03937007874
940   Atm_psia=Atm_mmhg*.0193367747
950   CLEAR SCREEN
960   PRINT "Atmospheric Pressure is ",Atm_psia,"PSIA"
970   GOTO Hold
980   !
990   !
1000 Svid:!Designate Scanivalves to be read and home them
1010  CLEAR SCREEN
1020  PRINT "Select and Home Scanivalves."
1030  PRINT
1040  PRINT "Scanivalves must be read from first to last"
1050  PRINT "in ascending order."
1060  !
1070  INPUT "Input Scanivalves to be read (First,Last):",First_sv,Last_sv
1080  N=Last_sv-First_sv+1      !N is total # of Scanivalves to read
1090  CLEAR SCREEN
1100  PRINT "First Scanivalve is number ",First_sv
1110  PRINT
1120  PRINT "Last Scanivalve is number ",Last_sv
1130  !
1140  GOSUB Home            !Home all selected Scanivalves
1150  PRINT
1160  PRINT "Scanivalves are homed on Port #1."
1170  GOTO Hold
1180  !
1190  !
```

Figure C2. (Cont.) SCAN Program

```
1200 Ports:!Designate First and Last S/V Ports to read, and position Scanivalves
1210  CLEAR SCREEN
1220  INPUT "Input first port and last port (First,Last):",First_port,Last_port
1230  CLEAR SCREEN
1240  PRINT "First port is number ",First_port
1250  PRINT
1260  PRINT "Last port is number ",Last_port
1270  !
1280  Port_reqd=First_port            !Set all Scanivalves to First_port
1290  FOR Id=First_sv TO Last_sv
1300    GOSUB Switch                  !Decide which device set to address
1310    IF Id<8 THEN GOSUB Posit      !Rotate Scanivalves 1-7 (8-10 stationary)
1320  NEXT Id
1330  PRINT
1340  PRINT "Scanivalves are set to first port."
1350  GOTO Hold
1360  !
1370  !
1380 P2pl:!Continuous cascade pressure ratio (P2/P1) readout
1390  Id=8                     !Corresponds to P1
1400  V=1                      !Inputs for Switch routine--Sets up Scanner,Dvm
1410  Port_reqd=First_port
1420 P_loop:GOSUB Switch
1430  GOSUB Read               !Read transducers
1440  SELECT Id
1450    CASE 8                 !P1 is on Scanivalve #8
1460      P1=P*1000.
1470    CASE 9                 !P2 is on Scanivalve #9
1480      P2=P*1000.
1490    CASE 10                !Pt is on Scanivalve #10
1500      Pt=P*1000.
1510  END SELECT
1520  Id=Id+1
1530  IF Id<10 THEN P_loop     !Read S/V 8,9 only  (Pt not installed)
1540                           !Add S/V 10 when transducer available
1550  !
1560  Pratio=(P2+Atm_psia)/(P1+Atm_psia)
1570  PRINT "  Pt  "," P1  "," P2  ","Pratio"
1580  PRINT Pt,P1,P2,Pratio
1590  PRINT
1600  WAIT .5                   !Time available to read line on CRT
1610  GOTO P2pl
1620  !
1630  !
1640 Name:!Create a filename other than the default string (SCAN_OUTPUT)
1650  !    for use in the "Store" data storage subroutine.
1660  CLEAR SCREEN
1670  INPUT "Enter a Filename for Data Storage:",Filename$
1680  CLEAR SCREEN
1690  PRINT "Output Filename is ",Filename$
1700  GOTO Hold
1710  !
1720  !
1730 Measure:!Take Pressure Measurements on Selected Ports and Scanivalves
1740  CLEAR SCREEN
1750  PRINT "Taking Pressure Measurements.  Please wait."
1760  PRINT
1770  !
1780  FOR Port_reqd=First_port TO Last_port   !Outer loop for each port
1790  !
```

Figure C2. (Cont.) SCAN Program

```
1800    FOR Id=First_sv TO Last_sv   !Read same port from each Scanivalve
1810      GOSUB Switch               !Decide which device set to address
1820      GOSUB Read                 !Read pressure transducer, return "P"
1830      Press(Id,Port_reqd)=P
1840    NEXT Id
1850    GOSUB Step                   !Step all Scanivalves once
1860    WAIT .5                      !Transient settling time
1870  NEXT Port_reqd
1880  !
1890  MAT Pg= Press*(1000.)          !Actual gauge pressures.
1900  CLEAR SCREEN
1910  GOSUB Write                    !Writes data to the screen.
1920  PRINT
1930  PRINT "Data Acquisition Complete"
1940  PRINT
1950  GOSUB Store                    !Stores data in an ASCII file
1960  GOTO Hold
1970  !
1980  !
1990 Hardcopy:!Sends a copy of the data to the printer
2000  CLEAR SCREEN
2010  PRINTER IS Printer
2020  GOSUB Write
2030  PRINTER IS CRT
2040  GOTO Hold
2050  !*****END OF MAIN PROGRAM and HOT KEY ROUTINES*****
2060  !
2070  !
2080  !*****SUBROUTINE: HOME ALL SELECTED SCANIVALVES*****
2090 Home:!
2100  CLEAR @Scanners
2110  FOR I=First_sv TO Last_sv        !Home command is (S/V#)+4
2120    IF I<6 THEN                    !First Controller
2130        OUTPUT Scanner1 USING "DDD";I+4
2140        CLEAR Scanner1
2150    ELSE                           !Second Controller
2160        OUTPUT Scanner2 USING "DDD";(I-5)+4
2170        CLEAR Scanner2
2180    END IF
2190  NEXT I
2200  WAIT 5.0       !Allow time for Scanivalves to home
2210  RETURN
2220  !
2230  !
2240  !*****SUBROUTINE:  STEP ALL SELECTED SCANIVALVES*****
2250 Step:!
2260  CLEAR @Scanners
2270  FOR I=First_sv TO Last_sv        !Step command is (S/V#)-1
2280    IF I<6 THEN                    !First Controller
2290      OUTPUT Scanner1 USING "DDD";I-1
2300      CLEAR Scanner1
2310    ELSE                           !Second Controller
2320      OUTPUT Scanner2 USING "DDD";(I-5)-1
2330      CLEAR Scanner2
2340    END IF
2350  NEXT I
2360  RETURN
2370  !
```

Figure C2. (Cont.) SCAN Program

```
2380  !
2390  !*****SUBROUTINE:  READ S/V ADDRESS AND POSITION S/V *****
2400 Posit:OUTPUT Controller USING "#,K";V
2410  P0-SPOLL(Controller)
2420  L-BINAND(P0,15)
2430  T-SHIFT(P0,4)
2440  M-BINAND(T,7)
2450  Port_read-10*M+L
2460  CLEAR Controller
2470  IF Port_read=Port_reqd THEN Finish !Exit subroutine if reqd port selected
2480  OUTPUT Scanner USING "DDD";V-1          !Advance S/V to next port
2490  CLEAR Scanner
2500  WAIT .1
2510  GOTO Posit
2520 Finish:RETURN
2530  !
2540  !
2550  !*****SUBROUTINE:  SETS UP DEVICE ADDRESSES*****
2560 Switch:!Sets device addresses to correspond to the proper Scanivalve
2570           !Id is the Scanivalve currently selected (1-10)
2580           !V is the Scanivalve # presented to the controller (1-5)
2590  IF Id<6 THEN
2600    Scanner=Scanner1              !Device set #1 for Scanivalves 1-5
2610    Controller=Controller1
2620    Dvm=Dvm1
2630    V=Id
2640  ELSE
2650    Scanner=Scanner2              !Device set #2 for Scanivalves 6-10
2660    Controller=Controller2
2670    Dvm=Dvm2
2680    V=Id-5
2690  END IF
2700  !Bus reset for when each Device Set is first used:
2710  IF V=1 AND Port_reqd=First_port THEN
2720    CLEAR @Instruments
2730    !Reset Dvms:
2740    OUTPUT @Dvms;"F1R7M3A0H0T3"      !DCV,AutoRange,MathOff,AutoCalOff,
2750    !                                 HiResOff,TriggerManual
2760  END IF
2770  RETURN
2780  !
2790  !
2800  !*****SUBROUTINE:  READ PRESSURE TRANSDUCER*****
2810 Read:!Reads transducer 5 times and averages results.  Result is "P".
2820  CLEAR Scanner
2830  OUTPUT Scanner USING "DDD";V+9   !Makes transducer voltage
2840  Total=0.                         !available to DVM
2850  FOR I=1 TO 5
2860    TRIGGER Dvm
2870    ENTER Dvm;P
2880    Total=Total+P
2890  NEXT I
2900  CLEAR Scanner
2910  P=Total/5.
2920  IF Id=6 OR Id=8 OR Id=9 OR Id=10 THEN P=P*2.  !Range scaling factor for
2930                                                 !100 psid transducers
2940  RETURN
2950  !
2960  !
```

Figure C2. (Cont.) SCAN Program

```
2970  !*****SUBROUTINE:  OUTPUT PRESSURE DATA ON CRT OR PRINTER*****
2980 Write:!
2990  PRINT "SCAN Program Output"
3000  PRINT "Pressure data from File",Filename$,"  Date:",DATE$(TIMEDATE)
3010  PRINT "(File data has been multiplied by 1000.)"
3020  PRINT
3030  PRINT "Atmospheric Pressure =",Atm_psia,"PSIA"
3040  PRINT
3050  PRINT "Gauge pressures:"
3060  PRINT
3070  PRINT "PORT #","        SCANIVALVE NUMBER"
3080  PRINT " "," 1"," 2"," 3"," 4"," 5"," 6"," 7"
3090  PRINT
3100  FOR I=First_port TO Last_port
3110    PRINT I,Pg(1,I),Pg(2,I),Pg(3,I),Pg(4,I),Pg(5,I),Pg(6,I),Pg(7,I)
3120  NEXT I
3130  PRINT
3140  PRINT
3150  PRINT
3160  PRINT "PORT #","        SCANIVALVE NUMBER"
3170  PRINT " "," 8"," 9","10","P2/P1"
3180  PRINT
3190  FOR I=First_port TO Last_port
3200    Pratio=(Pg(9,I)+Atm_psia)/(Pg(8,I)+Atm_psia)
3210    PRINT I,Pg(8,I),Pg(9,I),Pg(10,I),Pratio
3220  NEXT I
3230  RETURN
3240  !
3250  !
3260  !*****SUBROUTINE:  Store Raw Data in an ASCII File*****
3270 Store:PRINT "Storing Data.  Please Wait."
3280  CREATE ASCII Filename$,10
3290  ASSIGN @Path_1 TO Filename$
3300  OUTPUT @Path_1;Atm_psia,Press(*)
3310  ASSIGN @Path_1 TO *
3320  PRINT
3330  PRINT "Raw data is stored in",Filename$
3340  PRINT
3350  PRINT "Run is complete."
3360  PRINT "If more data is to be taken, create a new FILENAME."
3370  RETURN
3380  !
3390  !
3400  !*****END OF SUBROUTINES*****
3410  !
3420  !
3430 Done:LOAD "ACQ_MENU",10        !Return to menu selection screen.
3440  END
```

Figure C2. (Cont.) SCAN Program

APPENDIX D

PRESSURE TAP NUMBERING SCHEME

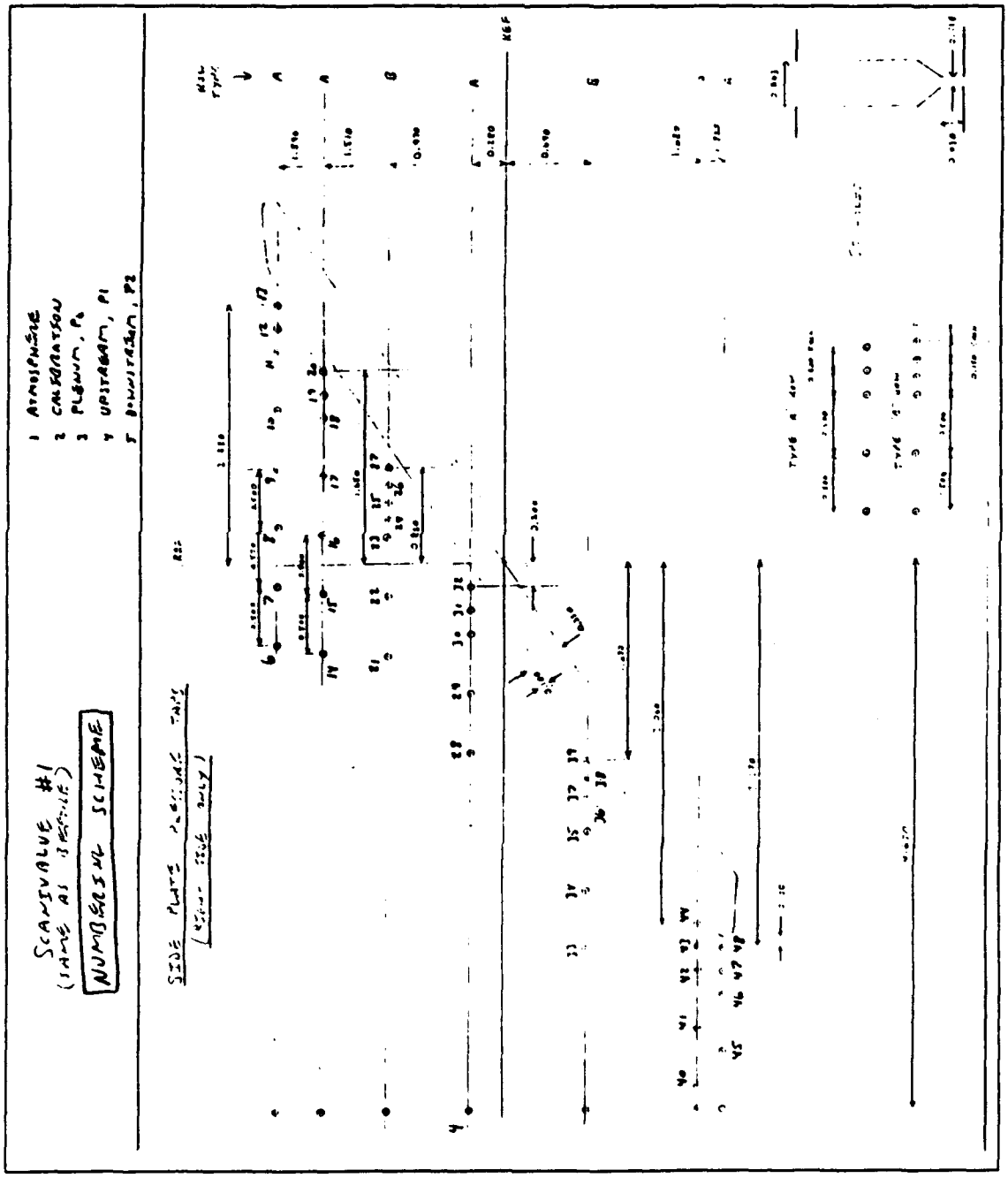

Figure D1. Scanivalve #1 Numbering Scheme

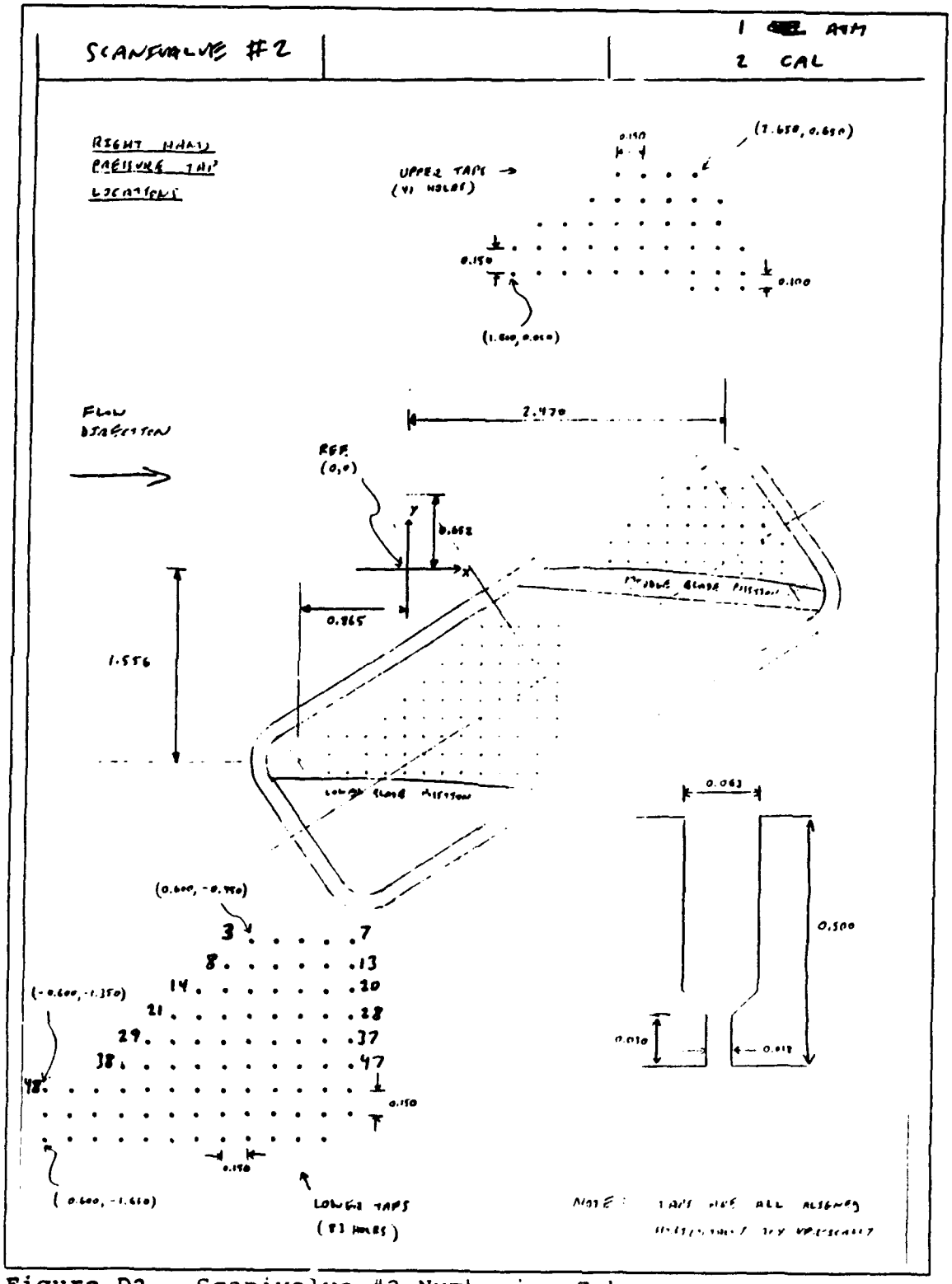

Figure D2. Scanivalve #2 Numbering Scheme

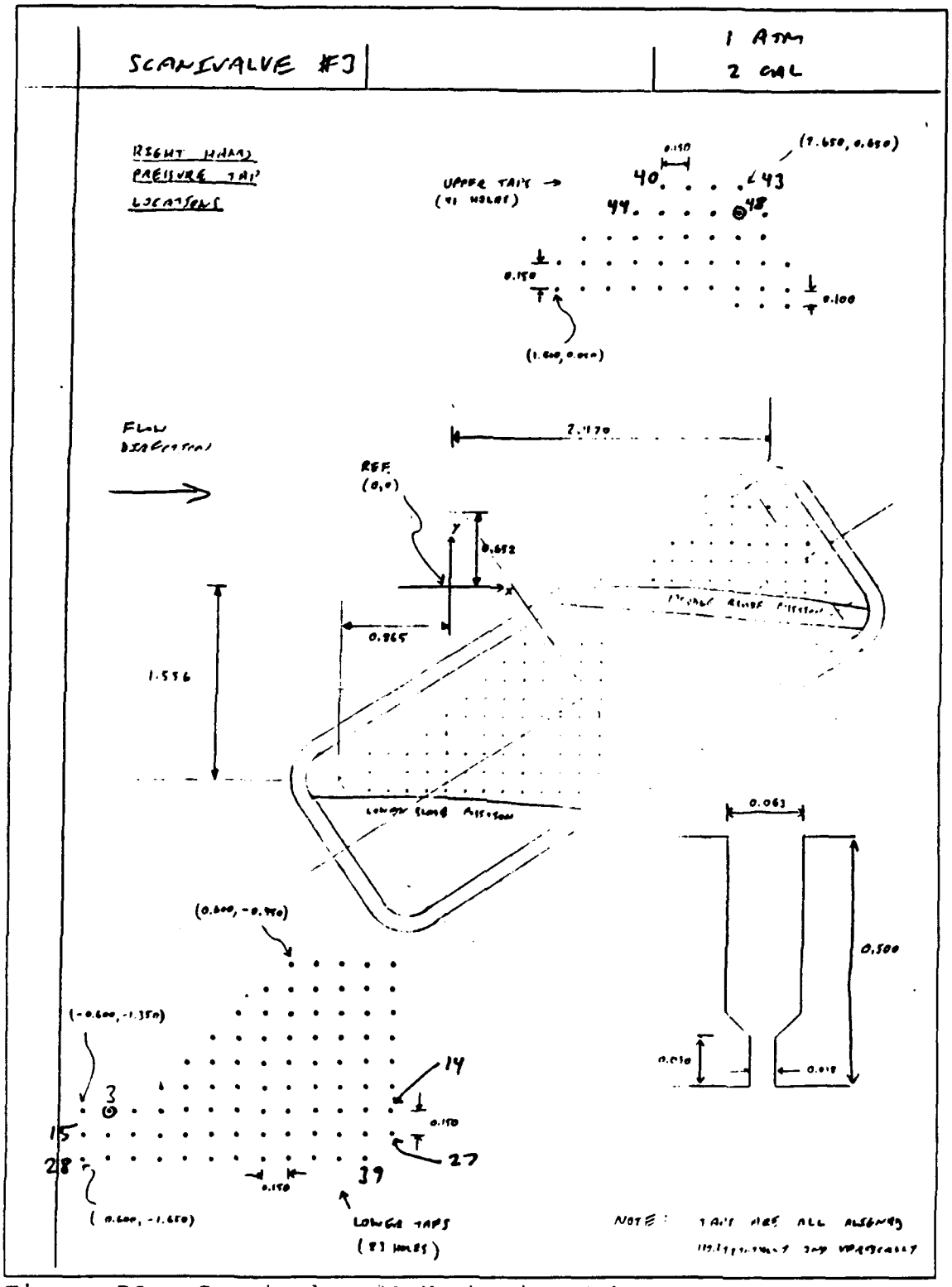

Figure D3. Scanivalve #3 Numbering Scheme

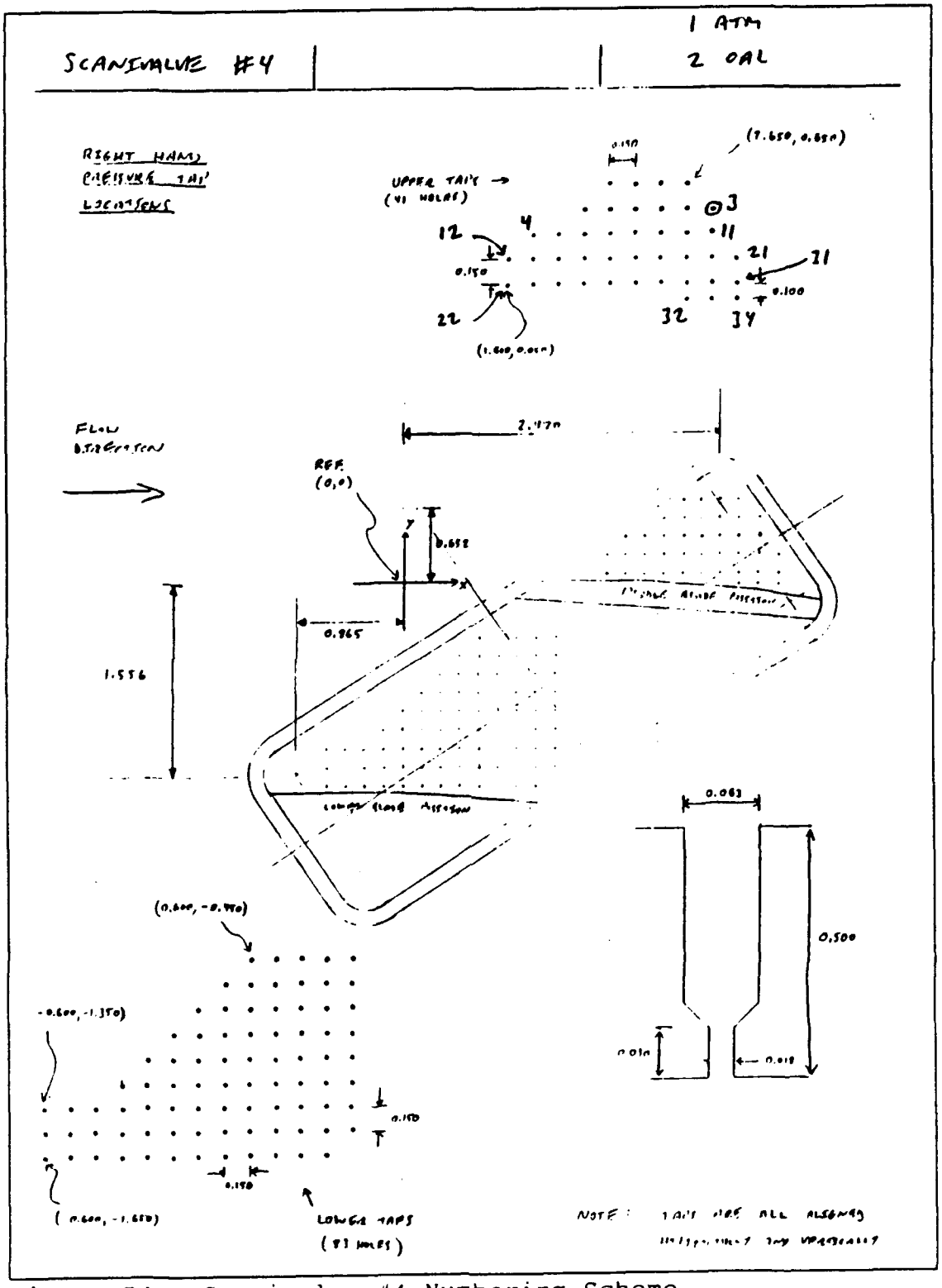

Figure D4. Scanivalve #4 Numbering Scheme

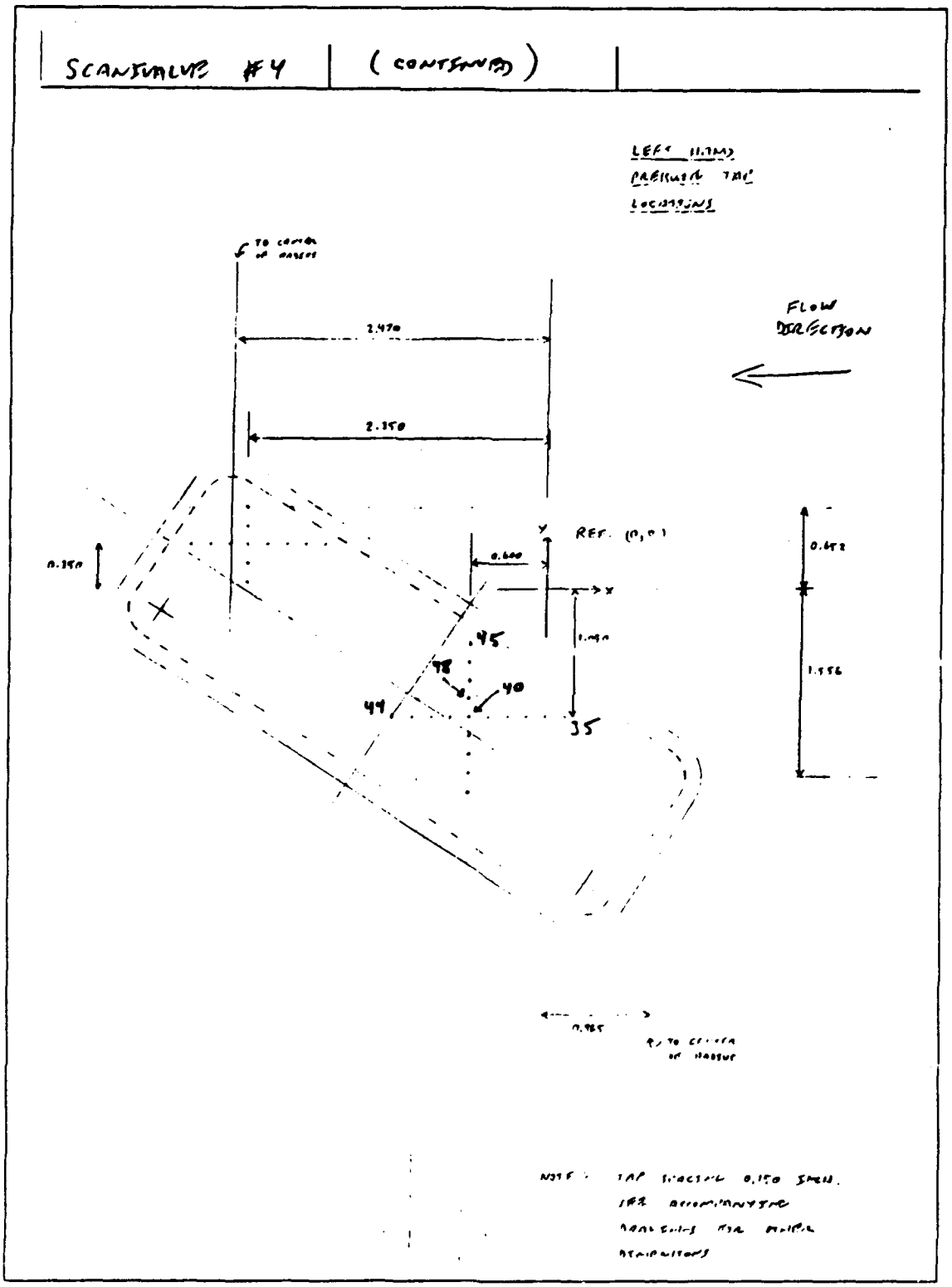

Figure D5. Scanivalve #4 Numbering Scheme (Cont.)

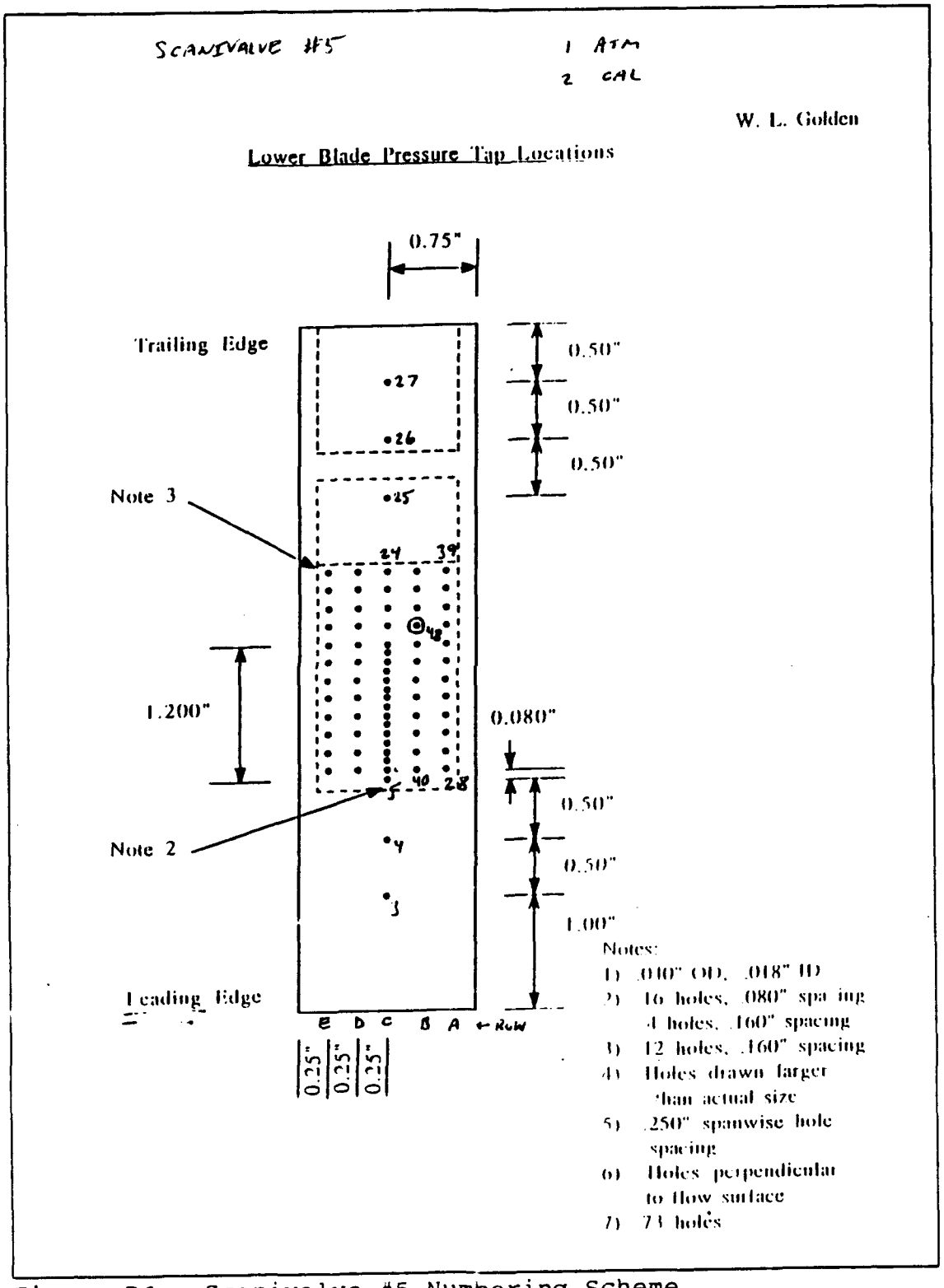

Figure D6. Scanivalve #5 Numbering Scheme

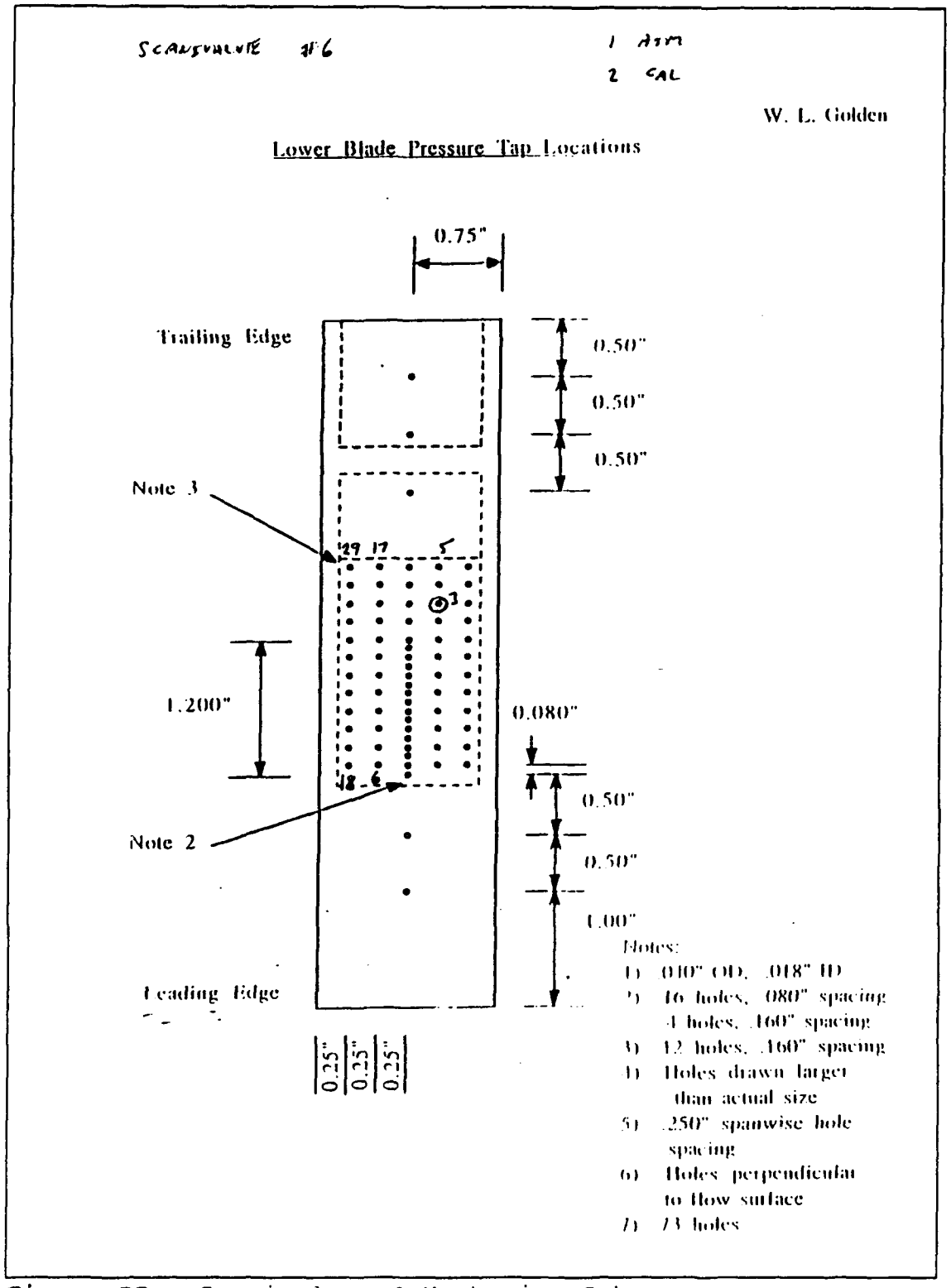

Figure D7. Scanivalve #6 Numbering Scheme

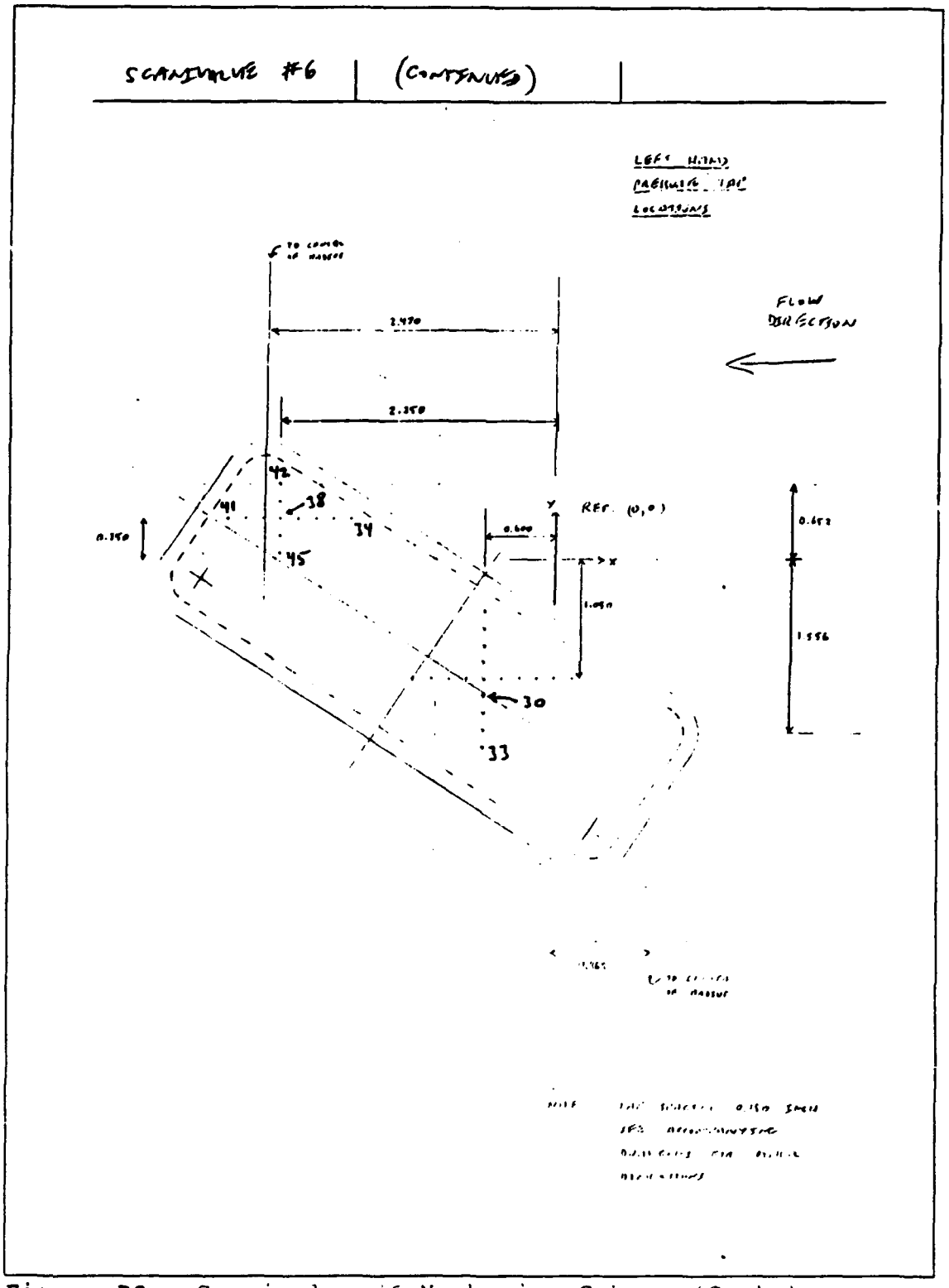

Figure D8. Scanivalve #6 Numbering Scheme (Cont.)

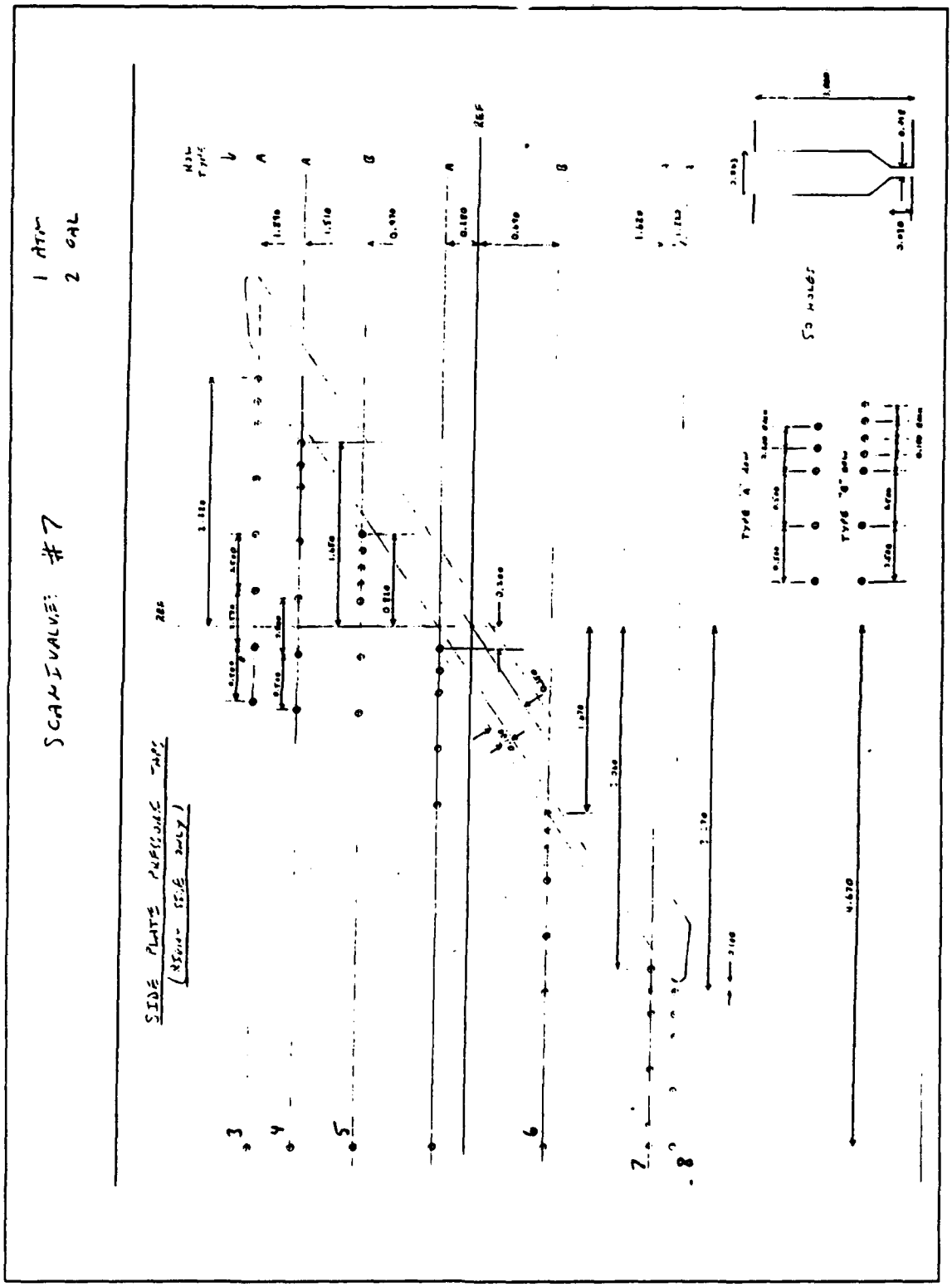

Figure D9. Scanivalve #7 Numbering Scheme

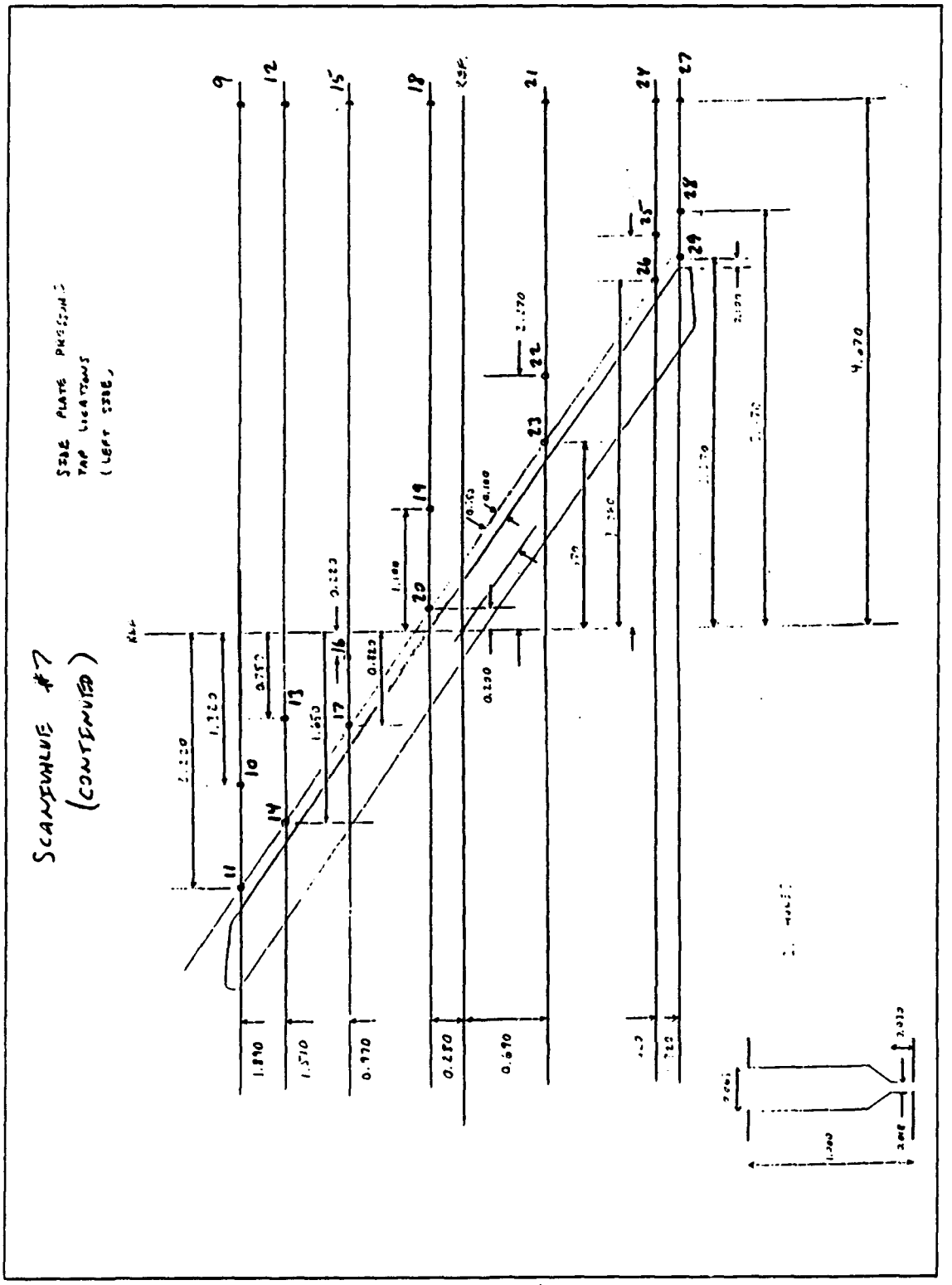

Figure D10. Scanivalve #7 Numbering Scheme (Cont.)

SCANIVALVE #7 (CONTINUED)

ADDITIONAL PORTS: P2 DATA (VERTICAL TAPS, ALIGNED WITH ORIGINAL P2 TAP)

* 43
* 44
* 45
* (S/V #1, PORT #5)
* 47
* 48

Figure D11. Scanivalve #7 Numbering Scheme (Cont.)

APPENDIX E

WALL STATIC PRESSURES

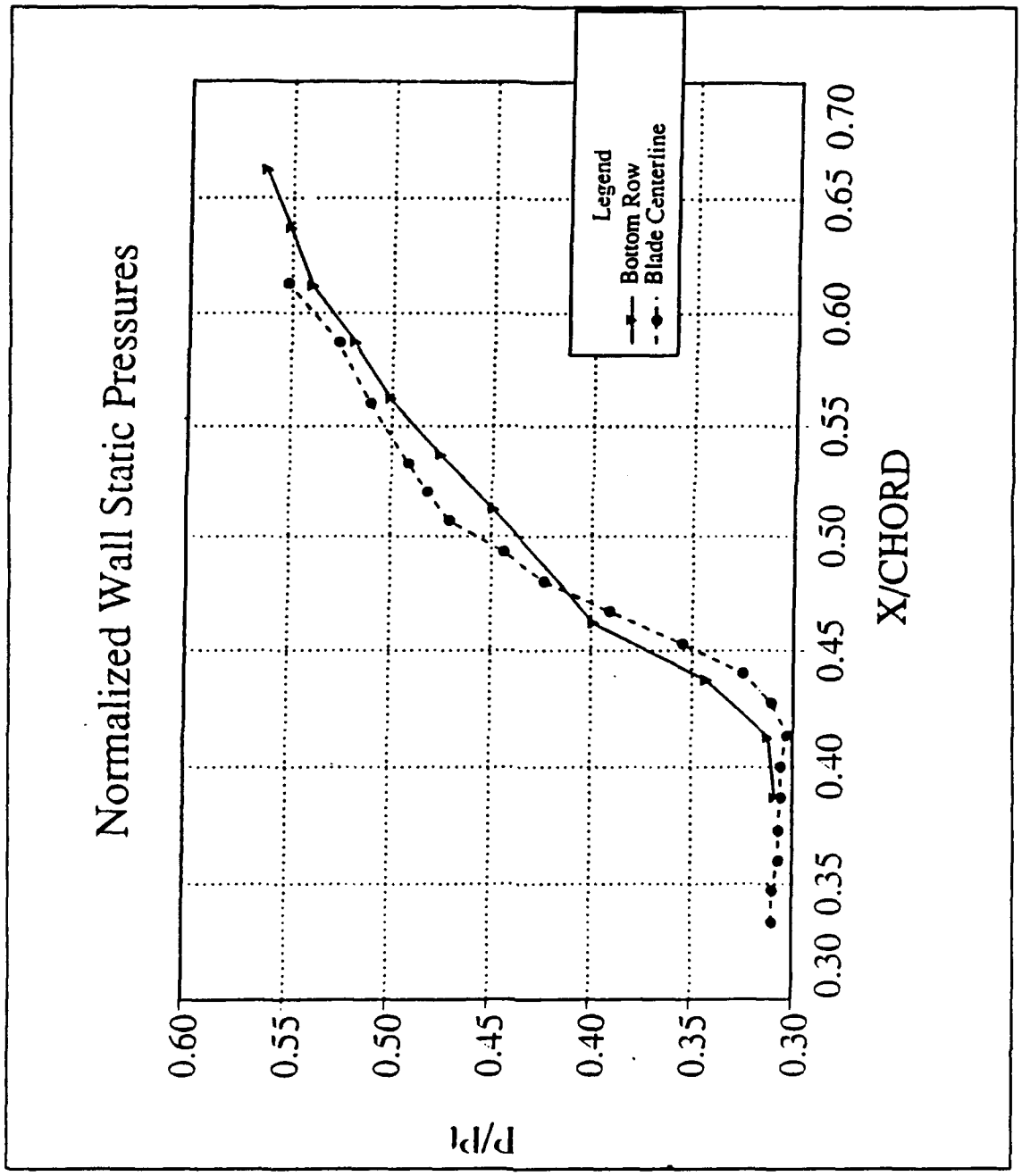

Figure E1. Wall Static Pressures--Bottom Row

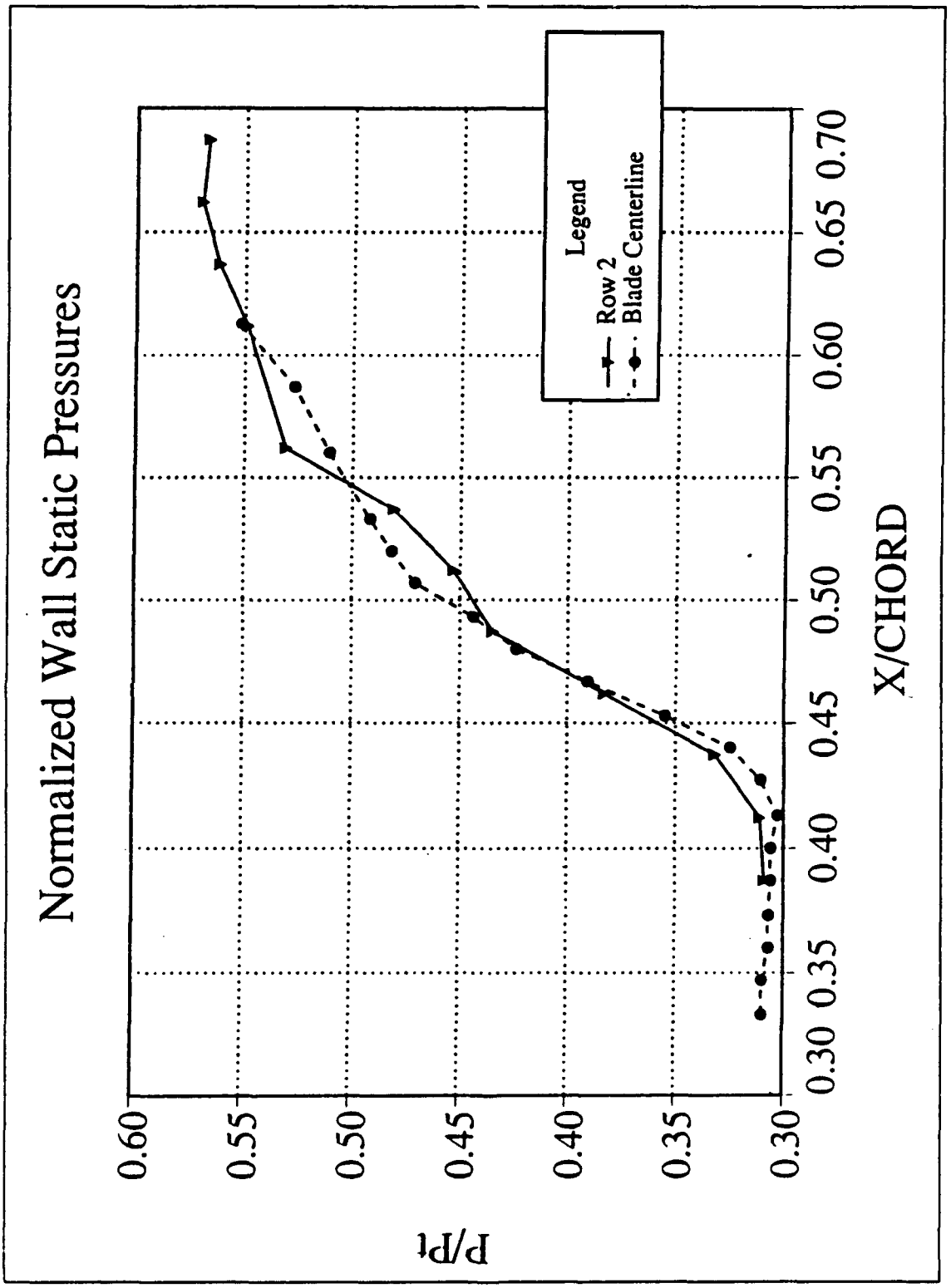

Figure E2. Wall Static Pressures--Row 2

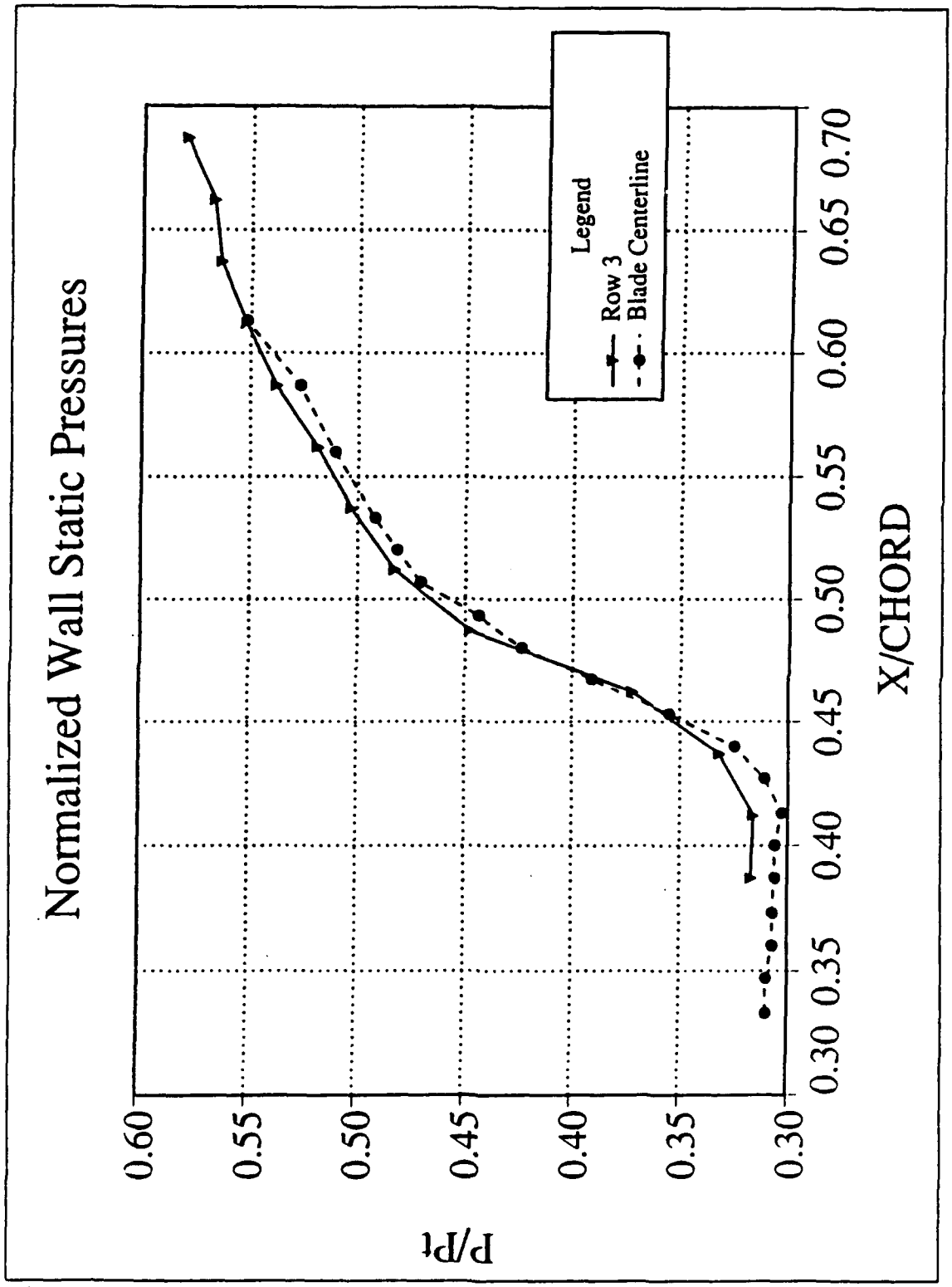

Figure E3. Wall Static Pressures--Row 3

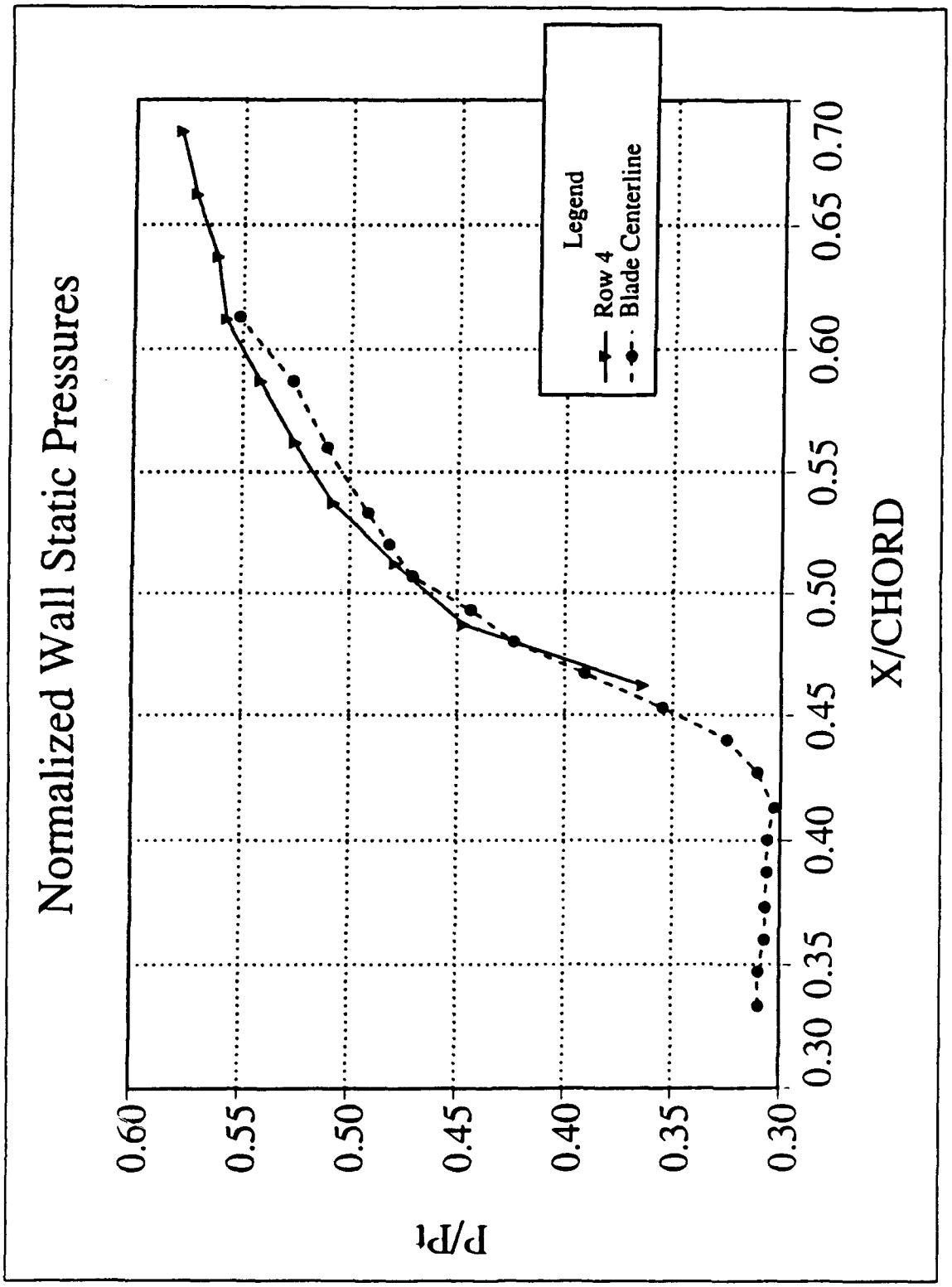

Figure E4. Wall Static Pressures--Row 4

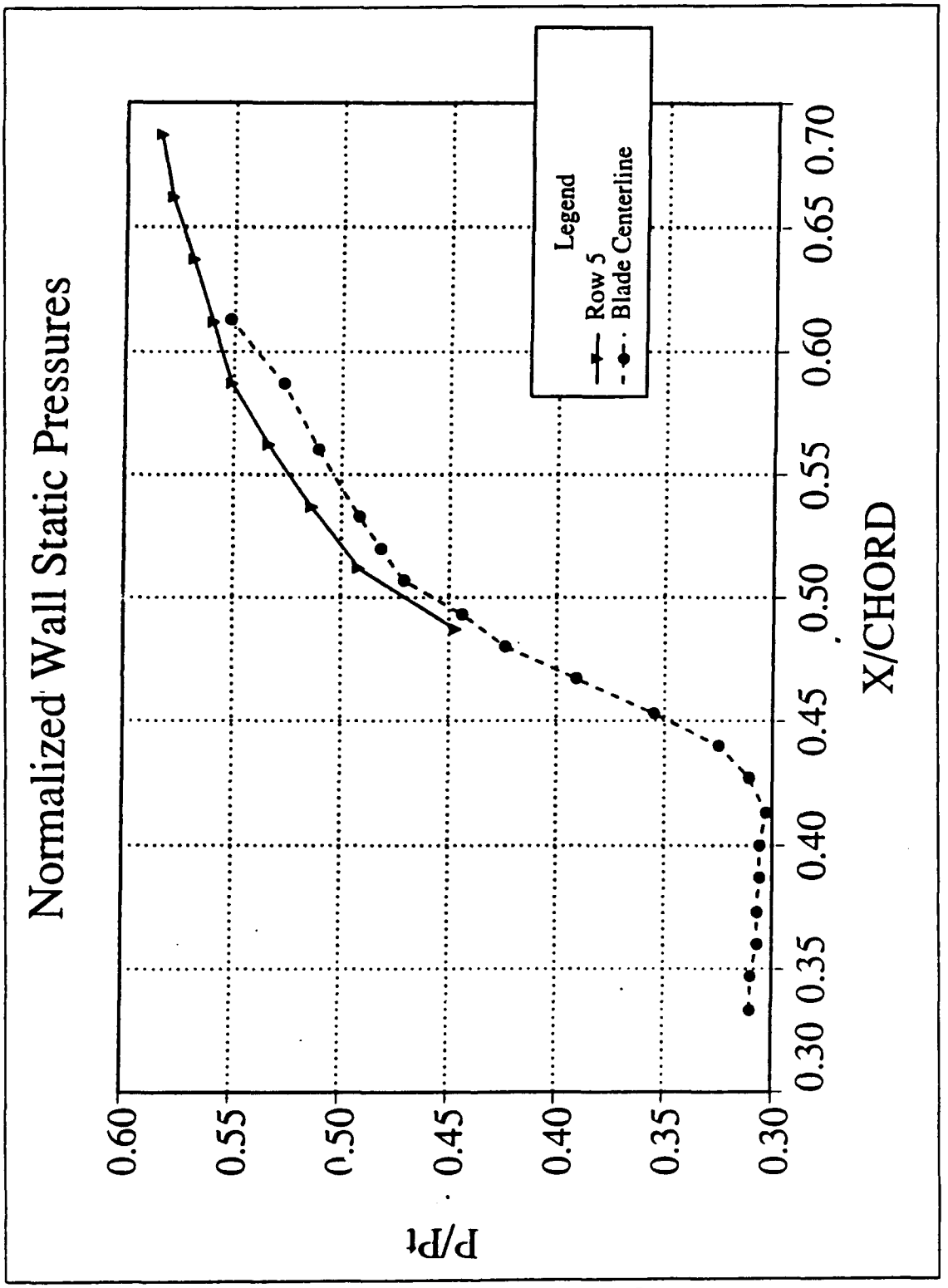

Figure E5. Wall Static Pressures--Row 5

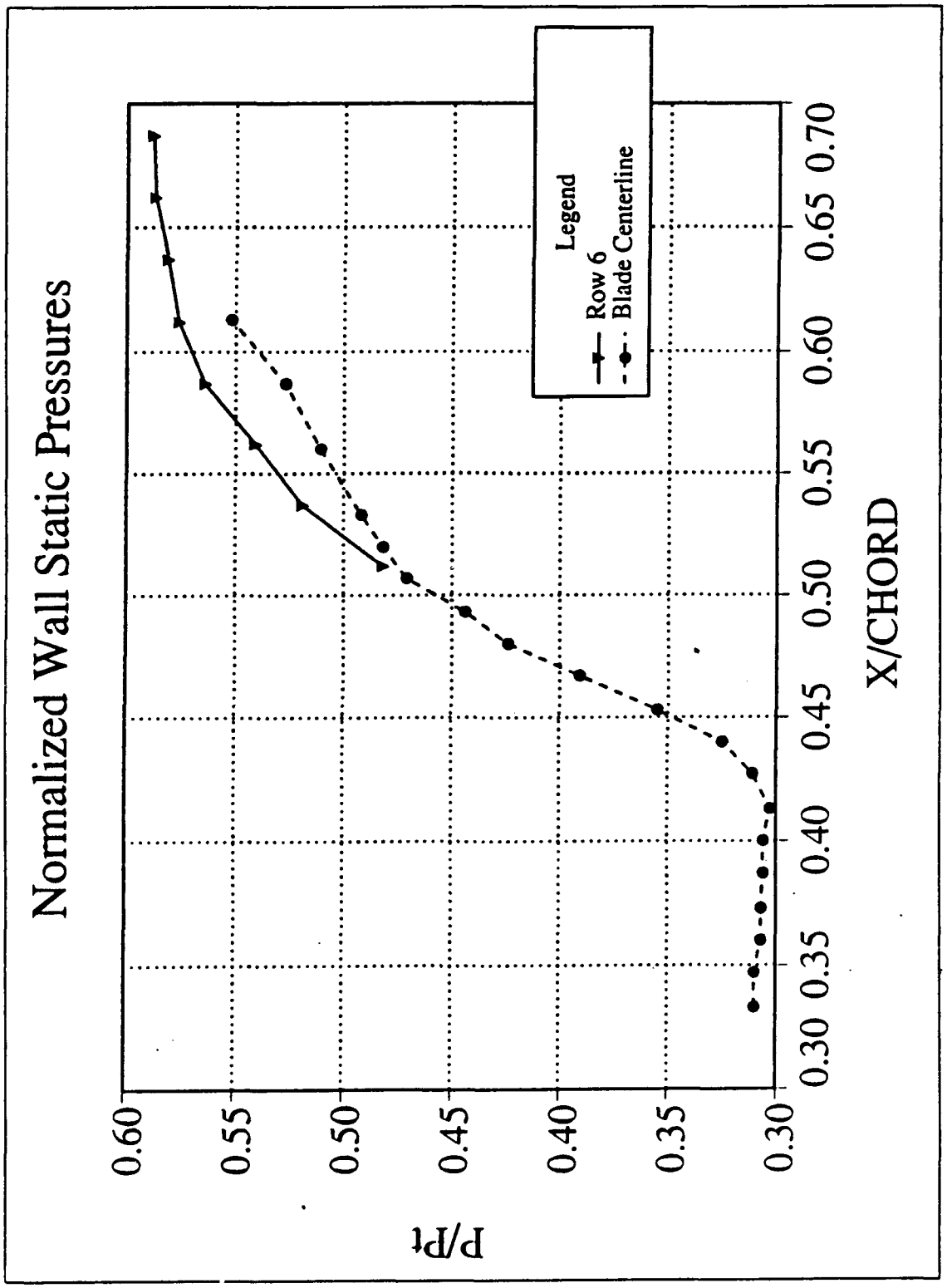

Figure E6. Wall Static Pressures--Row 6

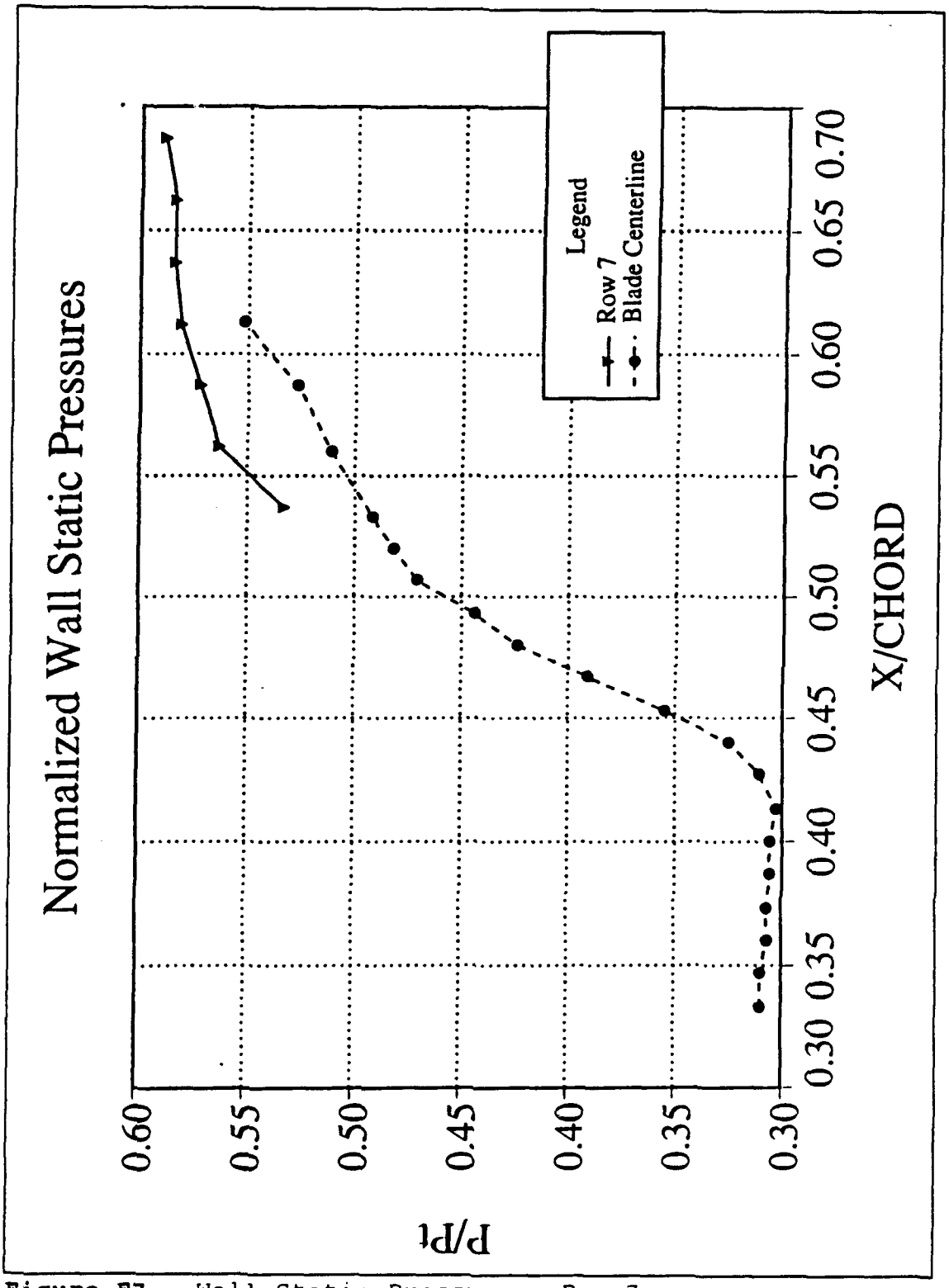

Figure E7. Wall Static Pressures--Row 7

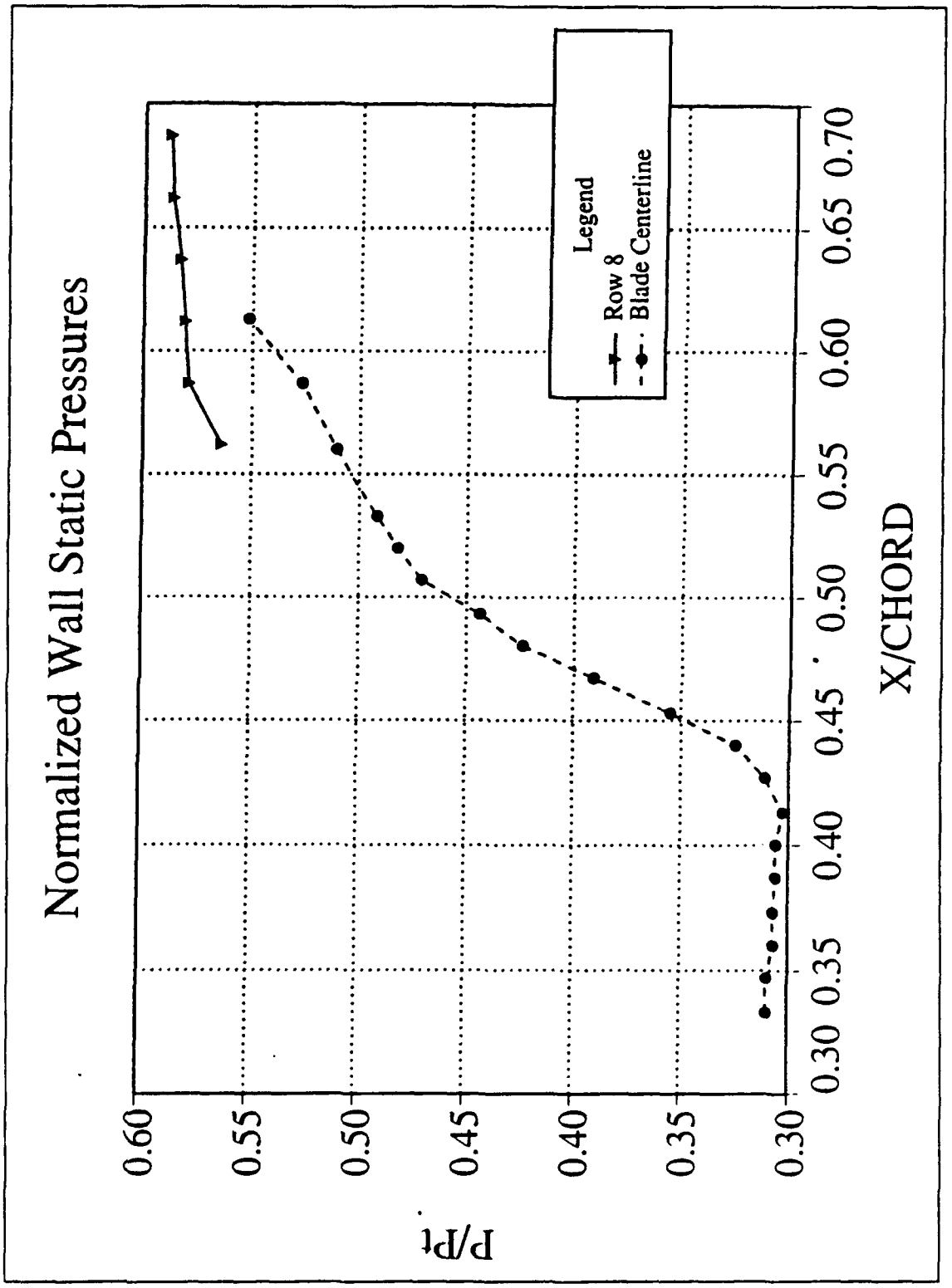

Figure E8. Wall Static Pressures--Row 8

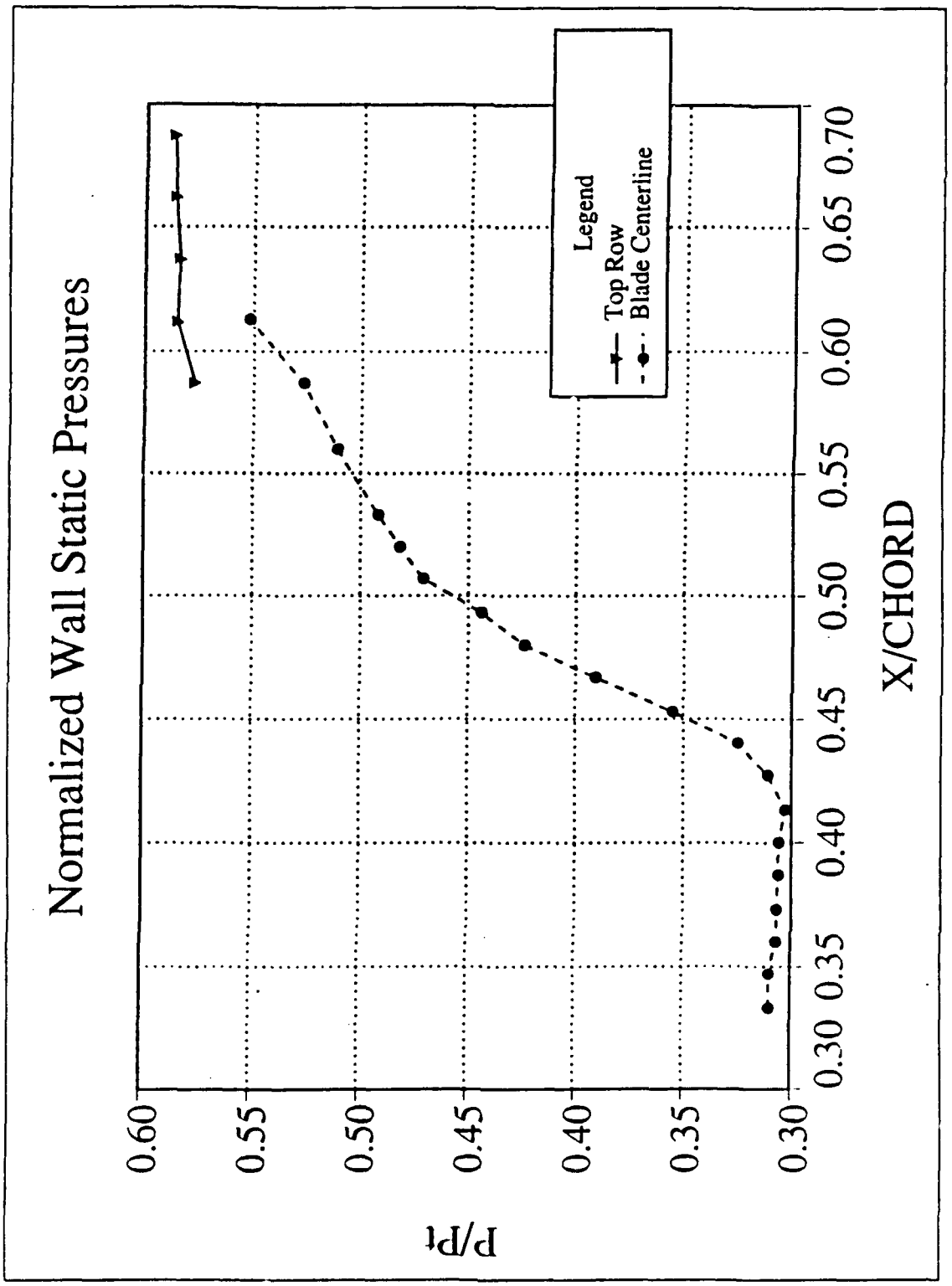

Figure E9. Wall Static Pressures--Row 9

APPENDIX F

COMPARISON OF LEFT AND RIGHT CASCADE DATA

```
10    !Title:        COMPARE
20    !Author:       LT Bill Golden
30    !Date:         05 March 1992
40    !Updated:
50    !Description:  This program examines the differences in pressure data
60    !              acquired from the left and right sides of the Transonic
70    !              Cascade to determine how 2-dimensional the simulation is.
80    !
90    Printer=702
100   REAL Atm_psia
110   DIM P(1:10,1:48)                          !SCAN data array
120   DIM Dside(1:21),Dtop(1:13),Dbottom(1:18) !Pressure differences in PSIA
130   !
140 Start:CALL Getdata(File$,Atm_psia,P(*))
150   MAT P= P*(1000.)                          !Convert to PSIA
160   MAT P= P+(Atm_psia)
170   CALL Difference(P(*),Dside(*),Dtop(*),Dbottom(*))
180 Print:CALL Printout(Dside(*),Dtop(*),Dbottom(*),Printer,File$)
190   INPUT "Type 1 for another copy, 2 to get another data set, 0 to exit:",Ans
200   SELECT Ans
210     CASE 1
220       GOTO Print
230     CASE 2
240       GOTO Start
250   END SELECT
260   END
270   !*************************************************************************
280   SUB Getdata(File$,Atm_psia,P(*))
290   INPUT "Enter ASCII Data Filename:",File$
300   ASSIGN @F_1 TO File$
310   ENTER @F_1;Atm_psia,P(*)
320   ASSIGN @F_1 TO *
330   SUBEND
340   !*************************************************************************
350   !*************************************************************************
360   SUB Difference(P(*),Dside(*),Dtop(*),Dbottom(*))
370   !
380   !Author:       LT Bill Golden
390   !Date:         05 March 1992
400   !Updated:
410   !Description:  Takes the difference between SCAN measurements of the
420   !              right and left sides of the Transonic Cascade to
430   !              examine the 2-dimensionality of the fan simulation.
440   !              Horizontal rows of taps are followed in the streamwise
450   !              direction, vertical columns are from top to bottom.
460   !
470   !Side plate comparison (prior to boundary layer scoops):
480   Dside(1)=P(7,3)-P(7,9)      !Top row
490   Dside(2)=P(1,10)-P(7,10)
500   Dside(3)=P(1,13)-P(7,11)
510   Dside(4)=P(7,4)-P(7,12)     !Second row
520   Dside(5)=P(1,17)-P(7,13)
530   Dside(6)=P(1,20)-P(7,14)
540   Dside(7)=P(7,5)-P(7,15)     !Third row
550   Dside(8)=P(1,23)-P(7,16)
560   Dside(9)=P(1,27)-P(7,17)
570   Dside(10)=P(1,4)-P(7,18)    !Fourth row
580   Dside(11)=P(1,29)-P(7,19)
590   Dside(12)=P(1,32)-P(7,20)
```

Figure F1. COMPARE Program

```
600   Dside(13)=P(7,6)-P(7,21)    !Fifth row
610   Dside(14)=P(1,35)-P(7,22)
620   Dside(15)=P(1,39)-P(7,23)
630   Dside(16)=P(7,7)-P(7,24)      !Sixth row
640   Dside(17)=P(1,42)-P(7,25)
650   Dside(18)=P(1,44)-P(7,26)
660   Dside(19)=P(7,8)-P(7,27)    !Bottom row
670   Dside(20)=P(1,46)-P(7,28)
680   Dside(21)=P(1,48)-P(7,29)
690   !
700   !Top passage (window) comparison:
710   Dtop(1)=P(4,4)-P(6,34)      !Horizontal strip
720   Dtop(2)=P(4,5)-P(6,35)
730   Dtop(3)=P(4,6)-P(6,36)
740   Dtop(4)=P(4,7)-P(6,37)
750   Dtop(5)=P(4,8)-P(6,38)
760   Dtop(6)=P(4,9)-P(6,39)
770   Dtop(7)=P(4,10)-P(6,40)
780   Dtop(8)=P(4,11)-P(6,41)
790   !
800   Dtop(9)=P(3,41)-P(6,42)     !Vertical strip
810   Dtop(10)=P(3,46)-P(6,43)
820   Dtop(11)=P(4,8)-P(6,38)     !Redundant center tap
830   Dtop(12)=P(4,17)-P(6,44)
840   Dtop(13)=P(4,27)-P(6,45)
850   !
860   !Bottom passage (window) comparison:
870   Dbottom(1)=P(2,29)-P(4,36) !Horizontal strip
880   Dbottom(2)=P(2,30)-P(4,37)
890   Dbottom(3)=P(2,31)-P(4,38)
900   Dbottom(4)=P(2,32)-P(4,39)
910   Dbottom(5)=P(2,33)-P(4,40)
920   Dbottom(6)=P(2,34)-P(4,41)
930   Dbottom(7)=P(2,35)-P(4,42)
940   Dbottom(8)=P(2,36)-P(4,43)
950   Dbottom(9)=P(2,37)-P(4,44)
960   !
970   Dbottom(10)=P(2,3)-P(4,45) !Vertical strip
980   Dbottom(11)=P(2,9)-P(4,46)
990   Dbottom(12)=P(2,16)-P(4,47)
1000  Dbottom(13)=P(2,24)-P(4,48)
1010  Dbottom(14)=P(2,33)-P(4,40) !Redundant center tap
1020  Dbottom(15)=P(2,43)-P(6,30)
1030  Dbottom(16)=P(3,10)-P(6,31)
1040  Dbottom(17)=P(3,23)-P(6,32)
1050  Dbottom(18)=P(3,36)-P(6,33)
1060  SUBEND
1070  !*************************************************************************
1080  !*************************************************************************
1090  SUB Printout(Dside(*),Dtop(*),Dbottom(*),Printer,File$)
1100  !
1110  INPUT "Type 1 to send to the CRT, 0 to the PRINTER:",Crt
1120  IF NOT Crt THEN
1130    PRINTER IS Printer
1140  END IF
1150  !
1160  PRINT "Comparison of left and right sides of Transonic Cascade"
1170  PRINT "              (Pressures are in PSIA.)"
1180  PRINT
1190  PRINT "              Data is from file",File$
```

Figure F1. (Cont.) COMPARE Program

```
1200  PRINT
1210  PRINT
1220  PRINT "Side plate data (streamwise left to right):"
1230  PRINT
1240  Count=0
1250  FOR I=1 TO 7
1260    PRINT "Row",I,Dside(Count+1),Dside(Count+2),Dside(Count+3)
1270    Count=Count+3
1280  NEXT I
1290  PRINT
1300  PRINT
1310  PRINT "Top passage data:"
1320  PRINT
1330  PRINT "Horizontal row:"
1340  PRINT Dtop(1),Dtop(2),Dtop(3),Dtop(4),Dtop(5),Dtop(6),Dtop(7),Dtop(8)
1350  PRINT
1360  PRINT "Vertical column:"
1370  PRINT Dtop(9),Dtop(10),Dtop(11),Dtop(12),Dtop(13)
1380  PRINT
1390  PRINT
1400  PRINT "Bottom passage data:"
1410  PRINT
1420  PRINT "Horizontal row:"
1430  PRINT Dbottom(1),Dbottom(2),Dbottom(3),Dbottom(4),Dbottom(5),Dbottom(6),Db
ottom(7),Dbottom(8),Dbottom(9)
1440  PRINT
1450  PRINT "Vertical column:"
1460  PRINT Dbottom(10),Dbottom(11),Dbottom(12),Dbottom(13),Dbottom(14),Dbottom(
15),Dbottom(16),Dbottom(17),Dbottom(18)
1470  PRINTER IS CRT
1480  SUBEND
1490  !*************************************************************************
```

Figure F1. (Cont.) COMPARE Program

Comparison of left and right sides of Transonic Cascade
(Pressures are in PSIA.)

Data is from file RUN26OPEN

Side plate data (streamwise left to right):

Row	1	-.9314	.9674	.244
Row	2	-.439	.1562	.1402
Row	3	-.1368	.8938	.4968
Row	4	-.2146	-.5434	.2922
Row	5	-.7462	1.4084	1528
Row	6	-1.4174	-.4538	-. 26
Row	7	-.2914	-1.0336	.2418

Top passage data:

Horizontal row:

-.778	-.0322	-.3182	.34	.0328	.2168	.9942	1.1846

Vertical column:

1.1894	.6766	.0328	-.4686	-.2404

Bottom passage data:

Horizontal row:

-.2122	.2784	.6512	.2726	1.056	.3828	.3244	.2436
-.1684							

Vertical column:

-.325	.4148	.8844	1.4718	1.056	.6866	1.1754	.4434
1.2828							

Figure F2. Run 26 Left/Right Pressure Differences

Comparison of left and right sides of Transonic Cascade
(Pressures are in PSIA.)

Data is from file RUN27LOWER

Side plate data (streamwise left to right):

Row	1	-.7724	1.0254	.2298
Row	2	-.1538	.1764	.1666
Row	3	.2064	1.0888	.4436
Row	4	-.0702	-.3258	.1466
Row	5	-.5474	1.3414	.1776
Row	6	-1.3464	-.565	-.0942
Row	7	-.2312	-1.0958	.13

Top passage data:

Horizontal row:

-.9054	-.192	-.596	.0284	-.0832	.0636	1.1322	1.4744

Vertical column:

.2036	.452	-.0832	-.4994	.3554

Bottom passage data:

Horizontal row:

.3856	.9086	.62	-.0792	-.142	-.4006	-.0966	.1864
.1978							

Vertical column:

.2888	.5842	.5348	.3934	-.142	-.1358	-.0708	-5.469
-.5296							

Figure F3. Run 27 Left/Right Pressure Differences

Comparison of left and right sides of Transonic Cascade
(Pressures are in PSIA.)

Data is from file RUN28UPPER

Side plate data (streamwise left to right):

Row	1	-.7096	.5404	-.2902
Row	2	-.139	-.0616	-.347
Row	3	.2136	.1656	.101
Row	4	-.0814	-.2978	-1.561
Row	5	-.5324	1.3508	.173
Row	6	-1.3738	-.6238	-.1164
Row	7	-.1986	-1.087	.028

Top passage data:

Horizontal row:

-.3532	-.9324	.6716	1.4114	1.549	1.2496	1.0168	1.0488

Vertical column:

.3794	.3826	1.549	1.7578	1.0108

Bottom passage data:

Horizontal row:

-3.1572	-2.3588	-1.568	-.6478	-.4166	.1492	.1878	.9854
.672							

Vertical column:

.2512	.3244	-.042	.3658	-.4166	-.548	-.5222	-4.7274
-.3012							

Figure F4. Run 28 Left/Right Pressure Differences

APPENDIX G

GRAPE INPUT CODE

```
$GRID1
JMAX=250,KMAX=49,NTETYP=3,NAIRF=5,NIBDST=7,NOBSHP=7,
JAIRF=316,JTEBOT=50,JTETOP=201,NORDA=4,1,MAXITA=200,100,NOUT=4,
DSI=.00010,XLE=0.0,XTE=0.61786,
XLEFT=-0.3089,XRIGHT=1.235,RCORN=0.0333,
JPRT=-1
$END
$GRID2
NOBCAS=0,NLE=22,NTE=10,DSRA=0.5,
DSLE=0.0002,DSTE=0.0003,PITCH=0.50,
YSCL=1.0,XTFRAC=0.8,ROTANG=-51.84,
WAKEP=0.8,DSOBI=0.010
$END
$GRID3
AIRFX=
  0.5000000    0.4999567    0.4999092    0.4998458    0.4997225
  0.4995675    0.4993867    0.4992550    0.4991158    0.4989717
  0.4987500    0.4985000    0.4982250    0.4979225    0.4975900
  0.4972233    0.4968209    0.4963784    0.4958908    0.4953550
  0.4947658    0.4941175    0.4934042    0.4926192    0.4917567
  0.4908067    0.4897625    0.4886142    0.4873500    0.4859600
  0.4844317    0.4827492    0.4808992    0.4788642    0.4766259
  0.4741634    0.4714542    0.4684750    0.4651975    0.4615925
  0.4576267    0.4532642    0.4484658    0.4431875    0.4379633
  0.4327384    0.4275133    0.4222892    0.4170642    0.4118400
  0.4066150    0.4013900    0.3961658    0.3909408    0.3857167
  0.3804917    0.3752667    0.3700425    0.3648175    0.3595934
  0.3543683    0.3491442    0.3439192    0.3386942    0.3334700
  0.3282450    0.3230208    0.3177958    0.3125708    0.3073467
  0.3021217    0.2968975    0.2916725    0.2864484    0.2812234
  0.2759984    0.2707742    0.2655492    0.2603250    0.2551000
  0.2498750    0.2446508    0.2394258    0.2342017    0.2289767
  0.2237525    0.2185275    0.2133025    0.2080783    0.2028534
  0.1976292    0.1924042    0.1871800    0.1819550    0.1767300
  0.1715058    0.1662808    0.1610567    0.1558317    0.1506067
  0.1453825    0.1401575    0.1349333    0.1297083    0.1244842
  0.1192592    0.1140342    0.1088100    0.1035850    9.8360837E-02
  9.3135834E-02    8.7910831E-02    8.2686670E-02    7.7461667E-02
7.2237507E-02
  6.7012504E-02    6.1788335E-02    5.6563333E-02    5.1284164E-02
4.6485834E-02
  4.2123333E-02    3.8157500E-02    3.4550004E-02    3.1275000E-02
2.8295834E-02
  2.5586668E-02    2.3124166E-02    2.0885833E-02    1.8850833E-02
```

Figure G1. GRAPE Input Code (Viscous grid)

```
1.7000834E-02
   1.5319167E-02   1.3790000E-02   1.2400000E-02   1.1135833E-02
9.9875005E-03
   8.9433342E-03   7.9941675E-03   7.1308333E-03   6.3458337E-03
5.6325002E-03
   4.9841669E-03   4.3950002E-03   3.8591668E-03   3.3716669E-03
2.9291667E-03
   2.5266667E-03   2.1600001E-03   1.8275001E-03   1.5250001E-03
1.2500000E-03
   1.1408334E-03   9.2666666E-04   8.2250003E-04   6.2499999E-04
4.4666667E-04
   2.9250002E-04   1.6749999E-04   7.5833334E-05   1.9166668E-05
0.0000000E+00
   1.9166668E-05   7.5833334E-05   1.6749999E-04   2.9250002E-04
4.4666667E-04
   6.2499999E-04   8.2250003E-04   9.2666666E-04   1.1408334E-03
1.4158334E-03
   1.7183333E-03   2.0508333E-03   2.4175001E-03   2.8200001E-03
3.2625000E-03
   3.7500001E-03   4.2858338E-03   4.8750001E-03   5.5233333E-03
6.2358337E-03
   7.0216670E-03   7.8849997E-03   8.8341665E-03   9.8783337E-03
1.1026667E-02
   1.2290834E-02   1.3680833E-02   1.5210001E-02   1.6891668E-02
1.8741667E-02
   2.0776667E-02   2.3239166E-02   2.5948334E-02   2.8927501E-02
3.2205001E-02
   3.5810001E-02   3.9775833E-02   4.4138335E-02   4.8936665E-02
5.4214999E-02
   5.9423335E-02   6.4673334E-02   6.9923334E-02   7.5173333E-02
8.0423340E-02
   8.5423335E-02   9.0923332E-02   9.5923334E-02   0.1011733
0.1064233
   0.1116733   0.1169233   0.1221733   0.1274233   0.1326733
   0.1376733   0.1429233   0.1481733   0.1534233   0.1586733
   0.1639233   0.1691733   0.1744233   0.1796733   0.1849233
   0.1901733   0.1951734   0.2004233   0.2056733   0.2109233
   0.2161733   0.2214233   0.2266733   0.2319233   0.2375000
   0.2434317   0.2494817   0.2544758   0.2597209   0.2649633
   0.2702133   0.2754608   0.2807092   0.2859575   0.2912075
   0.2964567   0.3014575   0.3067075   0.3119575   0.3172067
   0.3224567   0.3277059   0.3329550   0.3382034   0.3434508
   0.3484475   0.3536925   0.3589375   0.3642567   0.3694242
   0.3746650   0.3799050   0.3851425   0.3903792   0.3956134
   0.4008459   0.4060767   0.4113050   0.4165308   0.4217542
   0.4269758   0.4321942   0.4374100   0.4432075   0.4484859
   0.4532875   0.4576467   0.4616125   0.4652184   0.4684958
   0.4714750   0.4740825   0.4766458   0.4788850   0.4809200
   0.4827700   0.4844583   0.4859808   0.4873708   0.4886342
   0.4897833   0.4908275   0.4917767   0.4926400   0.4934242
   0.4941375   0.4947858   0.4953758   0.4959117   0.4963983
   0.4968417   0.4972842   0.4976867   0.4980534   0.4983858
   0.4986883   0.4989633   0.4991083   0.4992475   0.4993800
   0.4995617   0.4996692   0.4998417   0.4999067   0.4999542
```

Figure G1. (Cont.) GRAPE Input Code (Viscous grid)

```
   0.5000000,
 AIRFY=
   1.2500000E-03    9.2416670E-04    7.8333332E-04    6.4916670E-04
4.6416669E-04
   3.0416669E-04    1.7416668E-04    1.0666667E-04    5.5000004E-05
1.9999999E-05
   0.0000000    0.0000000    0.0000000    0.0000000    0.0000000
   0.0000000    0.0000000    0.0000000    0.0000000    0.0000000
   0.0000000    0.0000000    0.0000000    0.0000000    0.0000000
   0.0000000    0.0000000    0.0000000    0.0000000    0.0000000
   0.0000000    0.0000000    0.0000000    0.0000000    0.0000000
   0.0000000    0.0000000    0.0000000    0.0000000    0.0000000
   0.0000000    0.0000000    0.0000000    0.0000000    0.0000000
   0.0000000    0.0000000    0.0000000    0.0000000    0.0000000
   0.0000000    0.0000000    0.0000000    0.0000000    0.0000000
   0.0000000    0.0000000    0.0000000    0.0000000    0.0000000
   0.0000000    0.0000000    0.0000000    0.0000000    0.0000000
   0.0000000    0.0000000    0.0000000    0.0000000    0.0000000
   0.0000000    0.0000000    0.0000000    0.0000000    0.0000000
   0.0000000    0.0000000    0.0000000    0.0000000    0.0000000
   0.0000000    0.0000000    0.0000000    0.0000000    0.0000000
   0.0000000    0.0000000    0.0000000    0.0000000    0.0000000
   0.0000000    0.0000000    0.0000000    0.0000000    0.0000000
   0.0000000    0.0000000    0.0000000    0.0000000    0.0000000
   0.0000000    0.0000000    0.0000000    0.0000000    0.0000000
   0.0000000    0.0000000    0.0000000    0.0000000    0.0000000
   0.0000000    0.0000000    0.0000000    0.0000000    0.0000000
   0.0000000    0.0000000    0.0000000    0.0000000    0.0000000
   0.0000000    0.0000000    0.0000000    0.0000000    0.0000000
   0.0000000    0.0000000    0.0000000    0.0000000    0.0000000
   0.0000000    0.0000000    0.0000000    0.0000000    0.0000000
   0.0000000    0.0000000    0.0000000    0.0000000    0.0000000
   0.0000000    0.0000000    0.0000000    0.0000000    0.0000000
   4.99999999-06    4.2500000E-05    7.5833334E-05    1.6749999E-04
2.9250002E-04
   4.4666667E-04    6.2499999E-04    8.2250003E-04    1.0333334E-03
1.2500000E-03
   1.4675001E-03    1.6775000E-03    1.8750001E-03    2.0533334E-03
2.2000000E-03
   2.3325002E-03    2.4250001E-03    2.4500000E-03    2.4950001E-03
2.5125002E-03
   2.5283333E-03    2.5508334E-03    2.5741667E-03    2.5983334E-03
2.6250002E-03
   2.6550002E-03    2.6874999E-03    2.7266666E-03    2.7633335E-03
2.8033336E-03
   2.8550001E-03    2.9108333E-03    2.9658335E-03    3.0324999E-03
3.1000001E-03
   3.1775001E-03    3.2625000E-03    3.3541666E-03    3.4583332E-03
3.5683333E-03
   3.6966668E-03    3.8433333E-03    4.0116669E-03    4.1950000E-03
4.3933336E-03
   4.6158335E-03    4.8583336E-03    5.1275003E-03    5.4183337E-03
5.7391669E-03
```

Figure G1. (Cont.) GRAPE Input Code (Viscous grid)

```
   6.0608331E-03   6.3816672E-03   6.7025004E-03   7.0233336E-03
7.3450003E-03
   7.6508336E-03   7.9866666E-03   8.2924999E-03   8.6141676E-03
8.9350007E-03
   9.2558339E-03   9.5774997E-03   9.8983338E-03   1.0219167E-02
1.0540834E-02
   1.0846667E-02   1.1167500E-02   1.1488333E-02   1.1810000E-02
1.2130833E-02
   1.2451666E-02   1.2773334E-02   1.3094167E-02   1.3415000E-02
1.3736667E-02
   1.4057500E-02   1.4363334E-02   1.4684167E-02   1.5005833E-02
1.5326667E-02
   1.5647501E-02   1.5969168E-02   1.6290002E-02   1.6610835E-02
1.6951667E-02
   1.7302500E-02   1.7620834E-02   1.7861668E-02   1.8090833E-02
1.8295834E-02
   1.8476667E-02   1.8632501E-02   1.8764168E-02   1.8870834E-02
1.8954167E-02
   1.9011667E-02   1.9045001E-02   1.9055001E-02   1.9041667E-02
1.9003334E-02
   1.8940002E-02   1.8852500E-02   1.8740833E-02   1.8605001E-02
1.8444167E-02
   1.8269166E-02   1.8060833E-02   1.7828334E-02   1.7570835E-02
1.7289167E-02
   1.6983334E-02   1.6653333E-02   1.6298335E-02   1.5919168E-02
1.5515833E-02
   1.5088334E-02   1.4635834E-02   1.4159167E-02   1.3658334E-02
1.3133334E-02
   1.2584168E-02   1.2010000E-02   1.1412500E-02   1.0715834E-02
1.0060834E-02
   9.4400002E-03   8.8583333E-03   8.3141671E-03   7.8058336E-03
7.3349997E-03
   6.8983338E-03   6.5091671E-03   6.1208336E-03   5.7758335E-03
5.4591666E-03
   5.1675001E-03   4.8991665E-03   4.6541668E-03   4.4300002E-03
4.2200000E-03
   4.0341667E-03   3.8616667E-03   3.7033334E-03   3.5591666E-03
3.4274999E-03
   3.3074999E-03   3.1508335E-03   3.0975002E-03   3.0066667E-03
2.9233336E-03
   2.8475001E-03   2.7716667E-03   2.7016667E-03   2.6391668E-03
2.5816667E-03
   2.5291666E-03   2.4816669E-03   2.4475001E-03   2.3966667E-03
2.3300000E-03
   2.2008335E-03   2.0425001E-03   1.8583334E-03   1.7241667E-03
1.5841667E-03
   1.2500000E-03
 $END
```

Figure G1. (Cont.) GRAPE Input Code (Viscous Grid)

APPENDIX H

RVCQ3D INPUT CODE

```
    'nv7.inr  TRANSONIC COMPRESSOR CASCADE'
&NL1 M=250,N=49,MTL=50,MIL=112 &END
&NL2 NSTG=5,IVTSTP=1,IBC=1,IEX=1,MAXTC=4000,AVISC2=1.0,AVISC4=1.0,
     CFL=3.3,EPSCON=1.E-12,IRS=1,EPX=0.50,EPN=0.60 &END
&NL3 IRSTRT=0,IRVC=2,IRE=10,ICRNT=10000,ISIR=10000,IPIR=10000,
     IXRM=0 &END
&NL4 PI=2116.8,TI=518.7,PRAT=1.598639,WLE=1504.50,ALLE=56.49,
     ALTE=58.0,RGAS=1715.87,CEPE=6005.55 &END
&NL5 ILT=2,DYVISI=3.413E-07,XSCL=0.4208139,PRNR=.72,
     TWALL=0.0,CMUTM=14.0,JEDGE=30 &END
&NL6 OMEGA=-1254.44,NBLADE=1,NMN=0 &END
```

Figure H1. RVCQ3D Input Code (Viscous Solution)

LIST OF REFERENCES

1. United Technologies Research Center Report R90-957946, Transonic Fan Shock-Boundary Layer Separation Control, April 1990.

2. McCormick, D. C., "Shock-Boundary Layer Interaction Control with Low-Profile Vortex Generators and Passive Cavity," AIAA Paper 92-0064, January 1992.

3. Wheeler, G. O., *Means for Maintaining Attached Flow of a Flowing Medium*, United States Patent 4,455,045, June 1984.

4. Linn, J. C., Selby, G. V., and Howard, F. G., "Exploratory Study of Vortex-Generating Devices For Turbulent Flow Separation Control," AIAA Paper 91-0042, January 1991.

5. Johnston, J. P., and Nishi, M., "Vortex Generator Jets--Means for Flow Separation Control," *AIAA Journal*, v. 28, pp. 989-994, June 1990.

6. Collins, C. C., *Preliminary Investigation of the Shock-Boundary Layer Interaction in a Simulated Fan Passage*, Master's Thesis, Naval Postgraduate School, Monterey, California, March 1991.

7. Demo, Jr., W. J., *Cascade Wind Tunnel for Transonic Compressor Blading Studies*, Master's Thesis, Naval Postgraduate School, Monterey, California, June 1978.

8. Hegland, M. G., *Investigation of a Mach 1.4 Compressor Cascade with Variable Back Pressure Using Flow Visualization*, Master's Thesis, Naval Postgraduate School, Monterey, California, 1986.

9. NAVORD Report 1488 (Vol. 6), Handbook of Supersonic Aerodynamics, *Wind Tunnel Instrumentation and Operation*, by R. J. Volluz, January 1961.

10. Geopfarth, R. N., *Development of a Device for the Incorporation of Multiple Scanivalves into a Computer-Controlled Data System*, Master's Thesis, Naval Postgraduate School, Monterey, California, March 1979.

11. NASA TM-81198, *A Computer Program to Generate Two-Dimensional Grids About Airfoils and Other Shapes by Use*

of Poisson's Equation, by Sorenson, R. L., 1980.

12. Steger, J. L., and Sorenson, R. L., "Automatic Mesh Point Clustering Near a Boundary in Grid Generation with Elliptic Partial Differential Equations," *Journal of Computational Physics*, v. 33, no. 3, pp. 405-410, December 1979.

13. Chima, R. V., "Revised GRAPE Code Input for Cascades," NASA Lewis Research Center, June 1990.

14. Chima, R. V., "RVCQ3D (Rotor Viscous Code Quasi-3-D) Documentation," NASA Lewis Research Center, August 1990.

15. Chima, R. V., "Explicit Multigrid Algorithm for Quasi-Three-Dimensional Viscous Flows in Turbomachinery," *Journal of Propulsion and Power*, v. 3, no. 5, pp. 397-40[illegible], September-October 1987.

16. NASA TM-88878, *Comparison of Three Explicit Multigrid Methods for the Euler and Navier-Stokes Equations*, by Chima, R. V., Turkel, E., and Schaffer, S., January 1987.

17. Schlichting, H.,*Boundary Layer Theory*, 7th ed., p. 8, McGraw Hill, 1979.

INITIAL DISTRIBUTION LIST

1.	Defense Technical Information Center Cameron Station Alexandria, VA 22304-6145	2
2.	Library, Code 52 Naval Postgraduate School Monterey, CA 93943-5002	2
3.	Turbopropulsion Laboratory, Code 67 Naval Postgraduate School Monterey, CA 93943-5002	10
4.	Commander Naval Air Systems Command Washington, DC 20361 ATTN: AIR 536 T	1
5.	Commanding Officer Naval Air Propulsion Center Trenton, NJ 08628 ATTN: Steve Clauser	1
6.	Office of Naval Research 800 North Quincy Street Arlington, VA 22217 ATTN: Dr. Spiro Lykoudis	1
7.	United Technologies Research Center East Hartford, CT 06108 ATTN: Duane C. McCormick	1
8.	William L. Golden, Jr. 2213 Woodlawn Avenue Virginia Beach, VA 23455	3